

Effects of zinc and cadmium accumulation on the protein expression and chemical form of zinc on the zinc-binding protein in Gynura pseudochina (L.) DC.

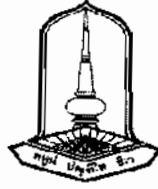
NATTHAWOOT PANITLERTUMPAI

**A thesis submitted in partial fulfillment of the requirements for
the degree of Master of Science in Biology**

Maharakham University

February 2011

Copyright of Maharakham University



The examining committee has unanimously approved this thesis, submitted by Mr.Natthawoot Panitlertumpai, as a partial fulfillment of the requirements for the degree of Master of Science in Biology, Mahasarakham University

Examining Committee

..... <i>Sanong Chomko</i> (Asst.Prof. Sanong Chomko, Ph.D.)	Chairman (Faculty graduate committee)
..... <i>W. Nakh</i> (Woranan Nakbanpote, D.Sc.)	Committee (Advisor)
..... <i>Aphidech Sangdee</i> (Asst.Prof. Aphidech Sangdee, Ph.D.)	Committee (Co-advisor)
..... <i>S. Anguravirutt</i> (Sujint Anguravirutt, Ph.D)	Committee (Faculty graduate committee)
..... <i>Piyada Theerakulpisut</i> (Assoc.Prof. Piyada Theerakulpisut, Ph.D.)	Committee (External expert)

Mahasarakham University has granted approval to accept this thesis as a partial fulfillment of the requirements for the degree of Master of Science in Biology.

.....
La-Orsi Sanoamuang
.....
(Prof. La-Orsi Sanoamuang, Ph.D.)
Dean of the Faculty of Science

.....
Paitool Suksringarm
.....
(Assoc.Prof. Paitool Suksringarm, Ph.D.)
Dean of the Faculty of Graduate Studies
.....*28*.....February.....2011

Acknowledgements

I would like to express my deepest appreciation and sincere gratitude to my advisor, Dr. Woranan Nakbanpote for her invaluable suggestions and assistances throughout my study and research at Mahasarakham University. I wish to thank Asst. Prof. Dr. Aphidech Sangdee, Dr. Sujint Anguravirutt, Assist. Prof. Dr. Sanong Chomko, Faculty of Science, Mahasarakham University, and Assoc. Prof. Dr. Piyada Theerakulpisut, Faculty of Science, Khon kaen University, for their valuable suggestions and comments.

I wish to thank Prof. Dr. Isumi Nakai, Department of Applied Chemistry, Faculty of Science, Tokyo University of Science, Japan, for suggestions and supports a synchrotron radiation X-ray spectroscopy analysis. I would like to thank Dr. Ponlakit Jitto, Faculty of Environmental and Resource Study, Mahasarakham University, for helping and teaching me during research in Japan. I would like to thank Dr. Piyaporn Seansouk for support a tissue culture laboratory. Moreover, I would like to thank High Energy Accelerator Research Organization (KEK), Tsukuba, Japan for research facilities at beamline 12C and 4A, according to proposal number 2008G633, and Synchrotron Light Research Institute (Public Organization), Thailand, for research facilities at beamline 8. I would like to thank all of my friends for their friendship and helps during my study. Finally, I gratefully thank Junior Science Talent Project, National Science and Technology Development Agency, for grand JSTP-06-51-09E.

Natthawoot Panitlertumpai

ชื่อเรื่อง	ผลของการสะสมสังกะสีและแคดเมียมที่มีต่อการแสดงออกของโปรตีนและรูปแบบของสังกะสีที่จับอยู่บนโปรตีนในต้นว่านมหากาฬ
ผู้วิจัย	นายณัฐวุฒิ พานิชย์เลิศอำไพ
ปริญญา	ปริญญาโท สาขาวิชาชีววิทยา
กรรมการควบคุม	อาจารย์ ดร.วรรณันต์ นาคบรรพต และผู้ช่วยศาสตราจารย์ ดร.อภิเดช แสงดี
มหาวิทยาลัย	มหาวิทยาลัยมหาสารคาม ปีที่พิมพ์ 2554

บทคัดย่อ

จากการสำรวจพืชบริเวณเหมืองผาแดง อำเภอแม่สอด จังหวัดตาก ซึ่งมีการถลุงแร่โลหะสังกะสีเพื่อใช้ในอุตสาหกรรมต่างๆ พบต้นว่านมหากาฬสามารถเจริญเติบโตได้บนกองเศษแร่ และมีความสามารถในการสะสมโลหะสังกะสีได้สูง จึงทำการศึกษาประสิทธิภาพของการทนทานและการสะสมโลหะสังกะสี แคดเมียม และโลหะสังกะสีร่วมกับแคดเมียม ศึกษาการแสดงออกของลักษณะโปรตีนเมื่อเกิดการสะสมโลหะดังกล่าวในต้นว่านมหากาฬด้วยเทคนิค SDS-PAGE และศึกษารูปแบบของโลหะสังกะสีในโปรตีนสกัดหยาบด้วยเทคนิค X-ray absorption fine structure (XAFS) และ Fourier transform infrared spectroscopy (FTIR) โดยเฉพาะอย่างยิ่งเนื้อเยื่อต้นว่านมหากาฬเพื่อควบคุมอิทธิพลของสิ่งแวดล้อม ในอาหารสังเคราะห์สูตร MS ที่ผสมฮอร์โมน 1 indole-3-acetic acid (IAA) และ indole-3-butyric acid (IBA) เพาะเลี้ยงให้มีอายุ 1 เดือน ก่อนรดด้วยสารละลายโลหะสังกะสีเข้มข้น 100, 250, 500, 750 และ 1000 มิลลิกรัมต่อลิตร สารละลายแคดเมียมเข้มข้น 5, 20, 50, 100 และ 150 มิลลิกรัมต่อลิตร หรือ สารละลายผสมของโลหะแคดเมียม (50 มิลลิกรัมต่อลิตร) ร่วมกับโลหะสังกะสี (100-1000 มิลลิกรัมต่อลิตร) และเพาะเลี้ยงต่อไปเป็นเวลา 2 สัปดาห์ ผลการศึกษาพบว่าความเข้มข้นของโลหะที่ส่งผลทำให้ต้นว่านมหากาฬแสดงอาการใบเหลืองหรือใบไหม้เกินกว่า 50% คือ สังกะสีเข้มข้น 500 มิลลิกรัมต่อลิตร แคดเมียมเข้มข้น 60 มิลลิกรัมต่อลิตร และโลหะแคดเมียม (50 มิลลิกรัมต่อลิตร) ร่วมกับสังกะสีเข้มข้น 32 มิลลิกรัมต่อลิตร และพบว่านมหากาฬมีการกลไกการขนส่งโลหะจากบริเวณรากไปยังส่วนเหนือพื้นดินโดยมีค่าแฟคเตอร์การขนส่ง (Translocation factor, TF) เมื่อได้รับโลหะสังกะสีระหว่าง 0.61-0.90 และ TF เมื่อได้รับโลหะแคดเมียมมีค่าระหว่าง 0.60-1.52 และเมื่อได้รับโลหะแคดเมียมร่วมกับโลหะสังกะสีพบว่า TF มีค่าลดลงเมื่อเทียบกับการได้รับโลหะเพียงชนิดเดียวโดย TF ของโลหะสังกะสีมีค่า 0.51-0.62 และ TF ของโลหะแคดเมียมมีค่า 0.57-0.66 นอกจากนี้ต้นว่านมหากาฬยังมีการแสดงออกของโปรตีนเมื่อได้รับโลหะสังกะสีที่แถบโปรตีนขนาด 12, 29, 31 และ 55 กิโลดาลตัน และเมื่อได้รับโลหะแคดเมียม

พบการแสดงออกของแถบโปรตีนขนาด 18, 20, 29, 31 และ 55 กิโลดาลตัน โดยผลการศึกษากลไกการทนทานต่อโลหะสังกะสีของโปรตีนสกัดหยาบด้วยเทคนิค XAFS และเปรียบเทียบลักษณะสเปกตรัม X-ray adsorption near-edge structure (XANES) ในช่วง Zn K-edge ของตัวอย่างโปรตีนสกัดหยาบกับสารโลหะสังกะสีมาตรฐาน พบว่าโลหะสังกะสีมีสถานะออกซิเดชัน $2+$ (Zn^{2+}) และมีแนวโน้มจับกับธาตุซัลเฟอร์ ซึ่งการวิเคราะห์โครงสร้าง Extended X-ray adsorption fine structure (EXAFS) พบว่าในชั้นแรกโลหะสังกะสีจะทำพันธะอยู่กับธาตุซัลเฟอร์จำนวน 1.45 อะตอม ที่ระยะห่าง 2.30 อังสตรอม ซึ่งผลการศึกษา XANES สเปกตรัม ในช่วง S K edge พบว่าสเปกตรัมของซัลเฟอร์ในโปรตีนสกัดหยาบมีแนวโน้มเป็นซัลเฟอร์ของอะมิโนซิสเทอีน (cysteine) ที่จับอยู่กับโลหะสังกะสี และผลจากการศึกษาโปรตีนสกัดหยาบด้วยเทคนิค FTIR พบว่าโลหะสังกะสีมีผลต่อการเปลี่ยนแปลงของหมู่ฟังก์ชัน Amide I และ Amide II และเปลี่ยนแปลงโครงสร้างทุติยภูมิของโปรตีนให้มีโครงสร้าง β -sheet เพิ่มมากขึ้น

คำสำคัญ : ว่านมหากาฬ; กลไกการทนทานโลหะ; โปรตีน; EXAFS; FTIR

TITLE Effects of zinc and cadmium accumulation on the protein expression and chemical form of zinc on the zinc-binding protein in *Gynura pseudochina* (L.) DC.

CANDIDATE Mr. Natthawoot Panitlertumpai

DEGREE degree of Master of Science in Biology

ADVISORS Dr. Woranan Nakbanpote, D.Sc.,
Asst. Prof. Dr. Aphidech Sangdee, Ph.D.

UNIVERSITY Mahasarakham University **YEAR** 2011

ABSTRACT

The exploration of metal hyper-accumulative plants in a zinc mine area (Padaeng-Industry Co., Mae Sod district, Tak province, Thailand) found that *Gynura pseudochina* (L.) DC. could survive in the mine tailing area and has a potential as a zinc hyperaccumulator. Therefore, the aim of this research was to study the tolerance and accumulation of zinc and cadmium under separate and dual treatments with zinc and/or cadmium. The expression of proteins associated with zinc and/or cadmium accumulation was studied by SDS-PAGE techniques. In addition, the chemical form of zinc on the crude protein was investigated by X-ray absorption fine structure (XAFS) and Fourier transform infrared spectroscopy (FTIR). This research was carried out in a tissue culture system to control environmental effects. The healthy plants were grown on a MS medium containing 1 indole-3-acetic acid (IAA) and indole-3-butyric acid (IBA). One month old healthy plants were exposed to 2 ml each of various zinc concentrations (100, 250, 500, 750 and 1000 mg l⁻¹), various cadmium concentrations (5, 20, 50, 100 and 150 mg l⁻¹), and a combination of cadmium (50 mg l⁻¹) mixed with various zinc concentrations (100-1,000 mg l⁻¹). After 2 weeks of treatment, the symptom on plants' leaves (yellowish leaves or chlorosis of leaves) was investigated. Calculated from the experiments 50% phytotoxicity levels were shown to be 500 mg l⁻¹ for zinc, 60 mg l⁻¹ for cadmium and for the combination of 50 mg l⁻¹ of cadmium plus 32.50 mg l⁻¹ for zinc. Quantitative analysis of the zinc and/or cadmium accumulated in the plants indicated the transportation of the metals from root to shoot. Translocation factors (TF) of zinc were 0.61-0.90, and TFs of cadmium were 0.60-1.52. After

exposure to the combination of zinc and cadmium, TFs decreased when compared with the treatment as separate metals, as the TFs of zinc were 0.51-0.62 and TFs of cadmium were 0.57-0.66. In addition, zinc induced changes in the expression of proteins with MWs of 12, 29, 31 and 55 kDa and cadmium with 18, 20, 29, 31 and 55 kDa. The X-ray absorption fine structure (XAFS) techniques were used for studying the mechanism of zinc tolerance and accumulation on crude protein. The X-ray adsorption near-edge structure (XANES) with Zn K-edge XANES spectrums showed that the chemistry of zinc on protein extracted was dominated by 2^+ (Zn^{2+}) oxidation state and might be coordinated with sulfur. The extended X-ray adsorption fine structure (EXAFS) analysis showed the first Zn-S coordination shell was 1.45 (N) and 2.30 \AA (R), respectively. In addition, the X-ray adsorption near-edge structure (XANES) with S K-edge XANES spectrums showed the sulfur of the protein extract corresponded to the sulfur spectra of cysteine adsorbed zinc. Moreover, FTIR analysis on protein extract indicated that zinc induced changes in amide I and amide II function groups and the protein secondary structure by increasing expressive β -sheet structure on the protein extract.

Key Words : *Gynura pseudochina* (L.) DC.; Phytoremediation; Protein; EXAFS; FTIR

CONTENTS

	Page
Acknowledgement	i
Abstract in Thai	ii
Abstract in Eng	iv
Chapter 1 Introduction	1
1.1 Background	1
1.2 Objectives	3
1.3 Hypotheses of the study	3
1.4 Advantages of the study	4
1.5 Scope of research work	4
1.6 Planning	7
Chapter 2 Literature Review	8
2.1 <i>Gynura pseudochina</i> (L.) DC.	8
2.2 Zinc	9
2.3 Cadmium	10
2.4 Phytoremediation	11
2.5 Electrophoresis	15
2.6 Applications of X-ray absorption spectroscopy to Phytoremediation	18
2.7 FT-IR analysis of protein structure	19
2.8 Literature reviews	22
Chapter 3 Methodology	25
3.1 Research diagram	26
3.2 Equipments and materials	27
3.3 Chemical reagents	27
3.4 Methods	29
Chapter 4 Results and Discussion	34
4.1 Propagation of <i>Gynura pseudochina</i> (L.) DC. in tissue culture system	34
4.2 Effect of zinc and/or cadmium on plant growth	35

	Page
4.3 Zinc and cadmium accumulation in plant	39
4.4 Distribution of zinc and cadmium in plant tissue	42
4.5 Effect of zinc and/or cadmium on protein patterns	43
4.6 The speciation of zinc on crude protein extract	46
4.7 Effect of zinc on the secondary structure of protein	50
Chapter 5 Conclusion	55
5.1 Conclusions	55
5.2 Suggestions	56
References	57
Appendices	67
Appendix A Plant growth	68
Appendix B Metals accumulation in plant	71
Appendix C SPSS	75
Appendix D SDS-PAGE	85
Appendix E X-ray absorption spectroscopy	91
Biography	100

List of Tables

			Page
Table	3.1	Experimental conditions for XAFS analysis at BL-8, SLRI	32
Table	3.2	Experimental conditions for XAFS analysis at BL-12C, PF, KEK	33
Table	4.1	Percent phytotoxicity of <i>Gynura pseudochina</i> (L.) DC.	38
Table	4.2	EXAFS fitting of the samples and references compounds	49
Table	4.3	The relative percentages of the component structure in the crude proteins extracted from the leaves	54
Table	A-1	Percent dry weight of <i>Gynura pseudochina</i> (L.) DC. exposed to difference concentrations of zinc for 2 weeks.	69
Table	A-2	Percent dry weight of <i>Gynura pseudochina</i> (L.) DC. exposed to different concentrations of cadmium for 2 weeks.	69
Table	A-3	Percent dry weight of <i>Gynura pseudochina</i> (L.) DC. exposed to difference concentrations of cadmium and zinc combination for 2 weeks.	70
Table	A-4	Percent survival of <i>Gynura pseudochina</i> (L.) DC. exposed to difference concentrations of zinc and cadmium alone and the combination of cadmium and zinc for 2 weeks.	70
Table	B-1	Concentration of metals in leaves of plants	72
Table	B-2	Zinc and cadmium accumulation (averages \pm SD; n=5) in <i>Gynura pseudochina</i> (L.) DC. exposed to difference concentrations of zinc and cadmium and translocation factors (n=5).	73
Table	B-3	Zinc and cadmium accumulation (averages \pm SD; n=5) in <i>Gynura pseudochina</i> (L.) DC. exposed to difference concentrations of cadmium and zinc combination and translocation factors (n=5).	74
Table	C-1	Percent dry weight of <i>Gynura pseudochina</i> (L.) DC. exposed to difference concentrations of zinc.	76

	Page
Table C-2 Percent dry weight of <i>Gynura pseudochina</i> (L.) DC. exposed to difference concentrations of cadmium.	76
Table C-3 Percent dry weight of <i>Gynura pseudochina</i> (L.) DC. exposed to difference concentrations of cadmium and zinc combination.	76
Table C-4 Translocation factor of <i>Gynura pseudochina</i> (L.) DC. exposed to difference concentrations of zinc.	76
Table C-5 Translocation factor of <i>Gynura pseudochina</i> (L.) DC. exposed to difference concentrations of cadmium.	77
Table C-6 Translocation factor of <i>Gynura pseudochina</i> (L.) DC. exposed to difference concentrations of cadmium and zinc combination for zinc.	77
Table C-7 Translocation factor of <i>Gynura pseudochina</i> (L.) DC. exposed to difference concentrations of cadmium and zinc combination for cadmium.	77
Table C-8 Comparing a percent dry weight of <i>Gynura pseudochina</i> (L.) DC. exposed to difference concentrations of zinc.	78
Table C-9 Comparing a percent dry weight of <i>Gynura pseudochina</i> (L.) DC. exposed to difference concentrations of cadmium.	79
Table C-10 Comparing a percent dry weight of <i>Gynura pseudochina</i> (L.) DC. exposed to difference concentrations of cadmium and zinc combination.	80
Table C-11 Comparing translocation factor of <i>Gynura pseudochina</i> (L.) DC. exposed to difference concentrations of zinc.	81
Table C-12 Comparing a percent dry weight of <i>Gynura pseudochina</i> (L.) DC. exposed to difference concentrations of cadmium.	82
Table C-13 Comparing a translocation factor of <i>Gynura pseudochina</i> (L.) DC. exposed to difference concentrations of cadmium and zinc combination for zinc.	83

	Page
Table C-14 Comparing a Translocation factor of <i>Gynura pseudochina</i> (L.) DC. exposed to difference concentrations of cadmium and zinc combination for cadmium.	84
Table E-1 EXAFS fitting of the model compounds showing the bond, coordination number (N), atomic radius $R(\text{\AA})$, and the Debye-Waller factor is represented by σ^2 for protein control.	92
Table E-2 EXAFS fitting of the model compounds showing the bond, coordination number (N), atomic radius $R(\text{\AA})$, and the Debye-Waller factor is represented by σ^2 for protein zinc.	93
Table E-3 EXAFS fitting of the model compounds showing the bond, coordination number (N), atomic radius $R(\text{\AA})$, and the Debye-Waller factor is represented by σ^2 for zinc cysteine model	94
Table E-4 EXAFS fitting of the model compounds showing the bond, coordination number (N), atomic radius $R(\text{\AA})$, and the Debye-Waller factor is represented by σ^2 for zinc cellulose model.	95
Table E-5 EXAFS fitting of the model compounds showing the bond, coordination number (N), atomic radius $R(\text{\AA})$, and the Debye-Waller factor is represented by σ^2 for zinc oxide model	96
Table E-6 EXAFS fitting of the model compounds showing the bond, coordination number (N), atomic radius $R(\text{\AA})$, and the Debye-Waller factor is represented by σ^2 for zinc sulfide model.	97
Table E-7 EXAFS fitting of the model compounds showing the bond, coordination number (N), atomic radius $R(\text{\AA})$, and the Debye-Waller factor is represented by σ^2 for zinc sulfate model.	98
Table E-8 EXAFS fitting of the model compounds showing the bond, coordination number (N), atomic radius $R(\text{\AA})$, and the Debye-Waller factor is represented by σ^2 for zinc nitrate model.	99

List of Figures

		Page
Figure 2.1	<i>Gynura pseudochina</i> (L.) DC.	9
Figure 2.2	Pathway of metal/nutrient uptake in plants	12
Figure 2.3	Some metal binding ligands in plants	13
Figure 2.4	Chemical structure of phytochelatin	14
Figure 2.5	The structure of Histidine and Crystal structure of Ni ^{II} (His) ₂	15
Figure 2.6	The molecular weight of protein is difference a concentration of acrylamide of SDS-gel	16
Figure 2.7	Structure of Sodium dodecyl sulfate (SDS)	17
Figure 2.8	Denaturing proteins by detergent Sodium dodecyl sulfate (SDS)	17
Figure 2.9	The entire XAS spectra	19
Figure 2.10	The structure of an amino acid and the Amide I and Amide II bands	20
Figure 2.11	Segments of an α -helix and segments of β -sheet.	21
Figure 2.12	FTIR spectrum of Amide I and Amide II bands	21
Figure 3.1	Research diagram	26
Figure 4.1	The growth of <i>Gynura pseudochina</i> (L.) DC. for 4 week in MS medium presented hormone and absence	35
Figure 4.2	The dry weight of <i>Gynura pseudochina</i> (L.) DC	37
Figure 4.3	Fifty percent phytotoxicity of <i>Gynura pseudochina</i> (L.) DC.	38
Figure 4.4	Translocation of <i>Gynura pseudochina</i> (L.) DC.	41
Figure 4.5	μ -XRF imaging for zinc and cadmium distribution in <i>G. pseudochina</i> (L.) DC.'s tissues of stem and leaf.	43
Figure 4.6	Electrophoresis on SDS polyacrylamide gel (12% w/v) of protein extracts from the leaves of <i>G. pseudochina</i> (L.) DC	45
Figure 4.7	Zn K-edge XANES spectra of the protein extract and the Zn K-edge of zinc reference materials	48
Figure 4.8	Sulfur K-edge XANES spectra of the protein extract And zinc compound (Zn-cysteine Zn-Glutathione and ZnS)	50

	Page
Figure 4.9 FTIR spectra of the crude proteins extracted from the leaves	52
Figure 4.10 Derivatives FTIR spectra and integral areas of the crude proteins extracted from the leaves	53
Figure 4.11 Curve-fitted and secondary structure determination of the crude proteins extracted from the leaves	54
Figure D-1 Compared the efficiency of extraction buffers during HEPES buffer (H), modified HEPES buffer (M-H) and phenol buffer (PH) by separating on SDS polyacrylamide gel (12% w/v) of 1 μ g of soluble proteins from leaves	86
Figure D-2 Intensity of band on SDS-PAGE was determined by Quantity One version 4 (Bio-Rad) for identification the expression protein.	87
Figure D-3 Identification molecular weight of protein expressions were determined by Quantity One version 4 (Bio-Rad)	88
Figure D-4 Identification molecular weight of protein expressions were determined by Quantity One version 4 (Bio-Rad)	89
Figure D-5 μ -XRF spectra of SDS-PAGE gel; (A) experiment condition in room temperature and (B) Relative content of metals in protein bands.	90
Figure E-1 Radial-distribution-function (leaf) Inverse-FOURIER-Transform (right) for protein control	92
Figure E-2 Radial-distribution-function (leaf) Inverse-FOURIER-Transform (right) for protein zinc	93
Figure E-3 Radial-distribution-function (leaf) Inverse-FOURIER-Transform (right) for zinc cysteine model	94
Figure E-4 Radial-distribution-function (leaf) Inverse-FOURIER-Transform (right) for zinc cellulose model	95
Figure E-5 Radial-distribution-function (leaf) Inverse-FOURIER-Transform (right) for zinc oxide model	96
Figure E-6 Radial-distribution-function (leaf) Inverse-FOURIER-Transform (right) for zinc sulfide model	97

	Page
Figure E-7 Radial-distribution-function (leaf) Inverse-FOURIER-Transform (right) for zinc sulfate model	98
Figure E-8 Radial-distribution-function (leaf) Inverse-FOURIER-Transform (right) for zinc nitrate model	99

List of Abbreviations

SDS-PAGE	Sodium dodecyl sulfate polyacrylamide gel electrophoresis
FTIR	Fourier transform infrared spectroscopy
ATR	Attenuated total reflectance infrared spectroscopy
XAFS	X-ray absorption fine structure
XANES	X-ray absorption near edge structure
EXAFS	Extended X-ray absorption fine structure
AAS	Atomic absorption spectrophotometer
DMRT	Duncan's new multiple range test
MS medium	Murashige and Skoog medium
IAA	Indole-3-acetic acid
IBA	Indole-3-butyric acid
TF	Translocation factor
kDa	Kilogram Dalton
<i>N</i>	Coordination number
<i>R</i>	Inter atomic distance
σ^2	Debye-Waller factor
rpm	Revolution per minute
cm	Centimeter
°C	Degree Celcius
μ l	Microliter
mA	Milliampere
ml	Milliliter
g l ⁻¹	Gram per liter
mg l ⁻¹	Milligram per liter
mg g ⁻¹	Milligram per gram
mM	Millimolar
min	Minute

CHAPTER 1

Introduction

1.1 Background

Heavy metals are discharged in to the environment from industrial activities, such as metalliferous mines (Yadav *et al.*, 2009). Due to the increasing demand for the economic resources in Thailand, the Thai government has promoted zinc mining. That has led to increasing volumes of mine tailing waste. Phatat Phadaeng sub-district, Mae Sot, Tak province, Thailand is a source of zinc mineralization. Metal mine tailings (such as zinc and cadmium) are important sources of heavy metals that are dispersed in and enrichment the environment. The heavy metals accumulate throughout the food chain and so pose a serious threat to animal and human health (Antiochia *et al.*, 2007). Although zinc is an essential element of the diet, for healthy growth, a high concentration of zinc can cause illness due to abnormalities in the amount of proteins and enzymes produced (Daniels *et al.*, 2004). Therefore, phytoremediation is an efficient, *in situ* process suitable for cleaning up heavy metals contaminating the environment. This process takes advantages of an environmental friendly process, low cost, and it requires little equipment or labor (Raskin *et al.*, 1997).

Our exploration of metal hyper-accumulative plants in a zinc mining area, Tak province, Thailand found that *Gynura pseudochina* (L.) DC. was a zinc hyperaccumulator and had a potential for phytoremediation. Moreover, the plant can survive in the mine tailing area all year round, both dry and rainy seasons (Natthawoot *et al.*, 2003). Phaenark *et al.* (2009) also reported that *G. pseudochina* was a zinc and cadmium hyperaccumulative plant, which could survive on soil contaminated with 20,673 mg-Zn/kg and 596 mg-Cd/kg, of zinc and cadmium respectively. However, the mechanism of zinc accumulation, the tolerance to zinc and cadmium, and the effect of cadmium on zinc uptake of *G. pseudochina* (L.) DC. have not been studied.

The general processes of metals accumulation in plants are the uptake of metals from soil, sequestration within the root, efficiency of xylem loading and transport, and storage in leaf cells. The primary mechanism, at the cellular level, is the induction of

proteins, which function by preventing to damage the cell and resistance the heavy metal effects (Yang *et al.*, 2005; Hall, 2002). Plants are also involved in the chelating of metals by peptide and metalloproteins (Callahan *et al.*, 2006). The proteins could detoxify contaminated soil and establish greater uptake and accumulation in the plant (Cobbett and Goldsbrough, 2002), for example, phytochelatin (PCs) and metallothioneins (MTs) (Memon *et al.*, 2001). These proteins used oxygen and sulfur groups of amino acids to bind metals (De La Rosa *et al.*, 2004; Hall, 2002). In order to understand the structure and function of these biological components and the relationship of the metals with the proteins, a technique with high-resolution for protein separation and high sensitivity for metal analysis is required. Sodium dodecyl sulfate-polyacrylamide gel electrophoresis (SDS-PAGE) is a technique most widely used to understand the structures and functions of proteins (Bollag *et al.*, 1996). It has been applied to investigate protein detoxification of metals (Yoshida, *et al.*, 2006; Sobkowiak and Deckert, 2006). In addition, the fundamental data of the physiochemical properties of zinc complexes could be provided by Fourier-transform infrared (FT-IR) spectroscopy. Moreover, X-ray absorption fine structure (XAFS) is one of the premier tools for investigating the local structural environment of metal ions. It consists of two complimentary techniques X-ray absorption near edge structure (XANES) and extended X-ray absorption fine structure (EXAFS), which provide invaluable chemical information (Gardea-Torresdey *et al.*, 2005). XAFS has provided the nature of heavy metal complexes accumulated in metal tolerant and hyperaccumulating plant species previously (Kelly *et al.*, 2002).

Therefore, this research aimed to study the accumulation of zinc and/or cadmium by *G. pseudochina* (L.) DC., and investigate resistance mechanisms to zinc and/or cadmium, focusing on protein expression. The tissue culture technique was used in this experiment in order to control the effects of the environment, nutrients and growth factors that control the cell's state of growth and differentiation. The distributions of zinc and cadmium were also studied by micro X-ray fluorescence imaging (μ -XRF imaging). The protein expression of *G. pseudochina* (L.) DC., grown under zinc and/or cadmium induction, was investigated by separation with SDS-PAGE techniques. The chemical forms of zinc and sulfur on the crude protein extracts were studied by synchrotron based X-ray adsorption spectroscopy (SR-XAS), and the

changing protein structures were studied by an attenuated total reflection using infrared Fourier transform (ATR-FTIR) spectroscopy.

1.2 Objectives

This research aims to:

- 1.2.1 Study the accumulation and tolerance of *in vitro* grown *G. pseudochina* (L.) DC. in zinc and/or cadmium treatment.
- 1.2.2 Study the distributions of zinc and cadmium accumulated in *in vitro* grown *G. pseudochina* (L.) DC. by micro X-ray fluorescence imaging (μ -XRF imaging).
- 1.2.3 Study the protein expression of *in vitro* grown *G. pseudochina* (L.) DC., growing under zinc and/or cadmium induction, by SDS-PAGE techniques.
- 1.2.4 Study the chemical form of zinc and sulfur on the crude proteins extracted from the leaves of *in vitro* grown *G. pseudochina* (L.) DC. by synchrotron based X-ray adsorption spectroscopy (SR-XAS).
- 1.2.5 Study the structure of the protein extracts by an attenuated total reflection using infrared Fourier transform (ATR-FTIR) spectroscopy.

1.3 Hypotheses of the study

- 1.3.1 *G. pseudochina* (L.) DC. has the ability to accumulate and tolerate zinc and cadmium.
- 1.3.2 *G. pseudochina* (L.) DC. can transport zinc and cadmium from roots to leaves via the transportation system.
- 1.3.3 *G. pseudochina* (L.) DC.'s leaves induced with zinc and/or cadmium have differences in protein expression.
- 1.3.4 Phytochelatin is the main protein relating to zinc and cadmium accumulation and tolerance.
- 1.3.5 Sulfur (S) in the structure of cysteine and/or methionine in the first shell coordinated with zinc in the crude protein extracted from the Zn/Cd treated *G. pseudochina* (L.) DC.

1.4 Advantages of the study

1.4.1 The results could explain the accumulation and tolerance of *G. pseudochina* (L.) DC. in zinc and cadmium

1.4.2 The results could provide evidence to support the phytoremediation of zinc and cadmium by *G. pseudochina* (L.) DC., especially its application for zinc mine tailing.

1.4.3 The experimental design could be applied for the study of other hyperaccumulative plants, especially *Gynura* species and tuber-plants.

1.5 Scope of research work

1.5.1 Scope of the study:

1.5.1.1 *G. pseudochina* (L.) DC. was cultured on MS medium supplemented with the indol-3-acetic acid (IAA) and indol-3-butyric acid (IBA), at 25°C under 1000 lux of light intensity and a 12 hour photoperiod.

1.5.1.2 Zn^{2+} and Cd^{2+} ions were prepared from $ZnSO_4 \cdot 7H_2O$ and $3CdSO_4 \cdot 8H_2O$.

1.5.1.3 The characterization of protein expression was carried out by SDS-PAGE.

1.5.1.4 Micro X-ray fluorescence imaging (μ -XRF imaging) was used to investigate the distribution of zinc and cadmium in the tissues of *G. pseudochina* (L.) DC.

1.5.1.5 Synchrotron based X-ray adsorption spectroscopy (SR-XAS) was used for studying the chemical form of zinc and sulfur in the crude protein extracts.

1.5.1.6 Attenuated total reflection using infrared Fourier transform (ATR-FTIR) spectroscopy was used to study the structure and functional groups of the crude protein extracts.

1.5.2 Variance in the study:

1.5.2.1 Tolerance of *G. pseudochina* (L.) DC. to zinc and/or cadmium

Independent variable: *G. pseudochina* (L.) DC. treated with zinc, cadmium, and combination of cadmium and zinc for 2 weeks.

Dependent variable: Dry weight of *G. pseudochina* (L.) DC., amount of leaves, and the number of leaves showing necrotic spots and chlorosis (yellowish colour).

Control variable: Exposure to 2 ml of various concentrations of zinc solutions, cadmium solutions and mixed solutions of cadmium and zinc.

1.5.2.2 Accumulation of zinc and/or cadmium in *G. pseudochina* (L.) DC.

Independent variable: *G. pseudochina* (L.) DC. treated with various zinc concentrations of 0, 100, 250, 500, 750 and 1,000 mg l⁻¹, cadmium concentrations of 0, 5, 20, 50, 100 and 150 mg l⁻¹, and solutions of 50 mg l⁻¹ cadmium combined with various zinc concentrations of 50/0, 50/100, 50/250, 50/500, 50/750 and 50/1,000 mg l⁻¹.

Dependent variable: Zinc and cadmium accumulated in root, stem including petiole, and leaves.

Control variable: Exposure to 2 ml of zinc solutions, cadmium solutions and mixed solutions of zinc and cadmium for 2 weeks.

1.5.2.3 The protein expression of *G. pseudochina* (L.) DC. induced with zinc and/or cadmium solutions.

Independent variable: Protein patterns in the crude-protein extracts separated by SDS-PAGE from the leaves of *G. pseudochina* (L.) DC..

Dependent variable: Differences between the protein patterns of the control plants and the plants treated with zinc and/or cadmium.

Control variable: 0.1 g of leaf sample extracted with 400 µl of phenol extraction buffer, and separated by SDS-PAGE techniques.

1.5.2.4 Distributions of zinc and cadmium accumulated in the *in vitro* grown *G. pseudochina* (L.) DC.

Independent variable: Distributions of zinc and cadmium accumulated in each part of *G. pseudochina* (L.) DC.

Dependent variable: Difference of zinc and cadmium accumulated in each part of the control plant and the plant treated with zinc and/or cadmium.

Control variable: Thickness of plant samples for study by μ -XRF imaging.

1.5.2.5 Chemical form of zinc accumulated in the crude protein extracts.

Independent variable: Structure of protein extracted from the leaves induced by zinc solution.

Dependent variable: The first shell of zinc coordinated with an element in the protein structure.

Control variable: Protein extracted from leaves by phenol extraction buffer.

1.6 Planning

Framework researches	Time table for research 2008-2010														
	2008			2009				2010							
	May-Jun	Jul-Aug	Sep-Oct	Nov-Dec	Jan-Feb	Mar-Apr	May-Jun	Jul-Aug	Sep-Oct	Nov-Dec	Jan-Feb	Mar-Apr	May-Jun	Jul-Aug	Sep-Oct
Study a condition of tissue culture	↕		↕												
Cultivate of <i>G. pseudochina</i> (L.) DC.		↕													↕
Treat <i>G. pseudochina</i> (L.) DC. metals solution.		↕		↕	↕										
Analyse concentration of zinc and/or cadmium in plant.				↕	↕										
Study a condition for extraction and separation proteins.				↕	↕										
Analyse effect of metals on the protein patterns by SDS-PAGE.							↕								
Analyse crude protein by XANES. *										↕				↕	
Analyse crude protein by XANES and EXAFS. **													↕		
Analyse distribution of metals on the protein separating by μ -XRF imaging and μ -XANES. **															↕
Analyse crude protein by FT-IR. *															↕
Prepare final report and manuscript.															↕

Note: *Analyse samples at SLRI, Thailand, **Analyse samples at KEK, Japan

CHAPTER 2

Theoretical and Literature Reviews

2.1 *Gynura pseudochina* (L.) DC.

Gynura pseudochina extends from Sierra Leone eastwards through the Central African Republic and Ethiopia to Somalia and south to Malawi, Zambia and Angola. It also occurs in Sri Lanka, India, Bhutan, China, Myanmar, Thailand, Vietnam and Australia. It is cultivated in Java (Indonesia) and on the Malaysian Peninsular.

Kingdom: Plantae

Division: Spermatophyta

Class: Dicotyledoneae

Order: Asterales

Family: Asteraceae

Genus: *Gynura*

Species: *Gynura pseudochina*

Pictures of *G. psuedochina* (L.) DC. are showed in figure 2.1. The botany of the plants is perennial herb, 0.4–1 m high with an unpleasant musky smell. The root is tuberous, 10 cm long and up to 5 cm across. Leaves are slightly fleshy, green or purplish, the basal leaves ovate or spatulate, 4–22 cm long and 2.5–11 cm wide. Flower orange or yellow, corolla 9–12.5 mm long, expanded in upper part, lobes 0.9–1.7 mm long. Achenes are 3 mm long.

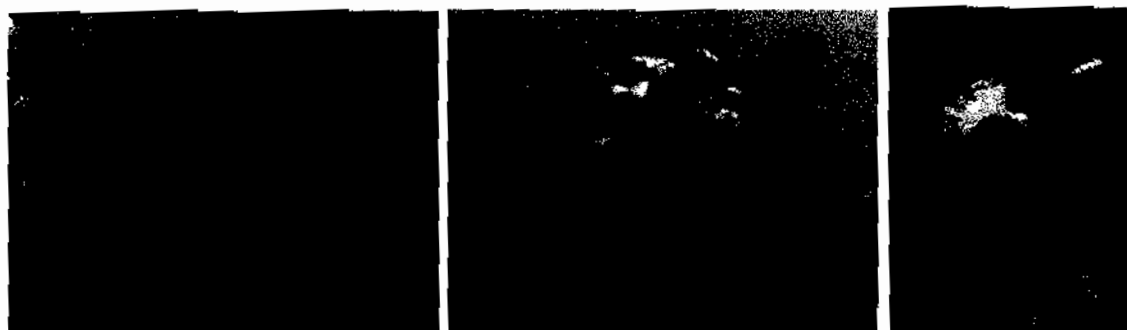


Figure 2.1 *Gynura pseudochina* (L.) DC. (Photograph by Nakbanpote, W.)

2.2 Zinc

2.2.1 Properties of zinc

Zinc is a bluish-white, lustrous, diamagnetic metal, though most common commercial grades of the metal have a dull finish. It is somewhat less dense than iron and has a hexagonal crystal structure. The metal is hard and brittle at most temperatures but becomes malleable between 100 and 150°C. Above 210 C, the metal becomes brittle again and can be pulverized by beating. Zinc is a fair conductor of electricity. For a metal, zinc has relatively low melting (420°C) and boiling points (900°C). Its melting point is the lowest of all the transition metals aside from mercury and cadmium (David, 2006).

2.2.2 Toxicity of zinc to humans

The mineral zinc is present in every part of the body and has a wide range of functions. It helps with the healing of wounds and is a vital component of many enzyme reactions. Zinc is vital for the healthy working of many of the body's systems. It is particularly important for healthy skin and is essential for a healthy immune system and resistance to infection. However, excess zinc is toxic. Too much zinc will interfere with the metabolism of other minerals in the body, particularly iron and copper. Symptoms of zinc toxicity occur after ingestion of 2 or more grams. The presenting symptoms include nausea and vomiting, epigastria pain, abdominal cramps, and diarrhea (frequently bloody) (Fosmire, 1990).

2.2.3 Toxic effects of zinc on plants

Zinc toxicity occurs in soils contaminated by mining and smelting activities, and in agricultural soils treated with sewage sludge especially in low-pH soils (Broadley *et al.*, 2007). A general guide for zinc concentration in mature leaf tissue is as follows: deficient less than 20 ppm, sufficient 25 to 150 ppm, excessive or toxic over 150 ppm (Kabata-Pendias and Pendias, 1992). Toxicity symptoms usually become visible, such as reduced yields and stunted growth, Fe-deficiency-induced chlorosis through reduction in chlorophyll synthesis and chloroplast degradation, and interference with P (and Mg and Mn) uptake (Broadley *et al.*, 2007; Kabata-Pendias and Pendias, 1992).

2.3 Cadmium

2.3.1 Properties of cadmium

Cadmium is a chemical element with the symbol Cd and atomic number 48. The soft, bluish-white transition metal is chemically similar to zinc and mercury. The most common oxidation state of cadmium is similar to zinc, with an oxidation state of +2, though rare examples of +1 can be found. It has a low melting point for a transition metal, similar to mercury. Cadmium burns in air to form brown amorphous cadmium oxide (CdO). The crystalline form of the same compound is dark red and changes colour when heated, similar to zinc oxide. Cadmium is a relatively abundant element. Cadmium occurs as a minor component in most zinc ores and therefore is a by-product of zinc production (Holleman *et al.*, 1985).

2.3.2 Toxicity of cadmium to human

Cadmium is absorbed more efficiently by the lungs (30 to 60%) than by the gastrointestinal tract, the latter being a saturable process (Nordberg *et al.*, 1985). It is transported in the blood and widely distributed in the body but accumulates primarily in the liver and kidneys. Moreover, cadmium burden (especially in the kidneys and liver) tends to increase in a linear fashion up to about 50 or 60 years of age after which the body burden remains somewhat constant. Metabolic transformations of cadmium are limited to its binding to protein and nonprotein sulfhydryl groups, and various macromolecules, such as metallothionein, which is especially important in the kidneys

and liver (ATSDR, 1989). Cadmium is excreted primarily in the urine. Acute oral exposure to 20-30 g has caused fatalities in humans (Young, 1991).

2.3.3 Toxic effects of cadmium on plants

In general, cadmium is a non-essential element that negatively affects plant growth and development. Overt symptoms induced by cadmium contents of plants are growth retardation and root damage, chlorosis of leaves, and red-brown coloration of leaf margins or veins (Kabata-Pendias and Pendias, 1992). In addition, it has inhibitory effects on photosynthesis, disturbs transpiration and CO₂ fixation, and alters the permeability of cell membranes (Prasad, 1995).

2.4 Phytoremediation

Plants have constitutive and adaptive mechanisms for accumulating or tolerating high contaminant concentrations in their rhizospheres. The use of such plants to cleanup soils and water contaminated with pollutants, a technique known as phytoremediation, is emerging as a new tool for *in situ* remediation. To date, phytoremediation efforts have focused on the use of plants to accelerate degradation of organic contaminants, usually in concert with the root rhizosphere microorganisms, or remove hazardous heavy metals from soils or water. Phytoremediation of contaminated sites is appealing because it is relatively inexpensive and aesthetically pleasing to the public compared to alternative remediation strategies involving excavation/removal or chemical *in situ* stabilization/conversion. Five aspects of phytoremediation are phytoextraction, phytodegradation, rhizofiltration, phytostabilization, and phytovolatilization (Peer *et al.*, 2006; Salt *et al.*, 1998) as following:

1. phytoextraction: the use of pollutant-accumulating plants to remove metals or organics from soil by concentrating them in the harvestable parts of the plant
2. phytodegradation: the use of plants and associated microorganisms to degrade organic pollutants
3. rhizofiltration: the use of plant roots to absorb and adsorb pollutants, mainly metals, from water and the aqueous waste streams
4. phytostabilization: the use of plants to reduce the bioavailability of pollutants in the environment

5. phytovolatilization: the use of plants to volatilize pollutants and the use of plants to remove pollutants from air

2.4.1 Metal uptake and transport strategies

Plant ligands play a role in the sequestration of metals from soils, transport to the above-ground tissue and finally storage (Figure 2.2). The first stage of metal uptake in plants is the interaction with the soil. In order to solubilize metals for absorption, plants need to interact with the soil in the rhizosphere (soil zone immediately surrounding the root). Presence of microbes, a decrease in pH, a change in the redox potential and/or the exudation of ligands are factors that can increase the metal uptake. In addition, two strategies have been identified for explanation of metal uptake and transport in plants. In the first, the plants (dicotyledons and non-grass monocotyledons) solubilize Fe (III) by reduction to the more soluble Fe(II) and decrease pH by H^+ excretion. In the second, the plants (graminaceous monocotyledons) produce specific ligands (phytosiderophores, PS) from the mugineic acid family (Figure 2.3) (Callahan *et al.*, 2006).

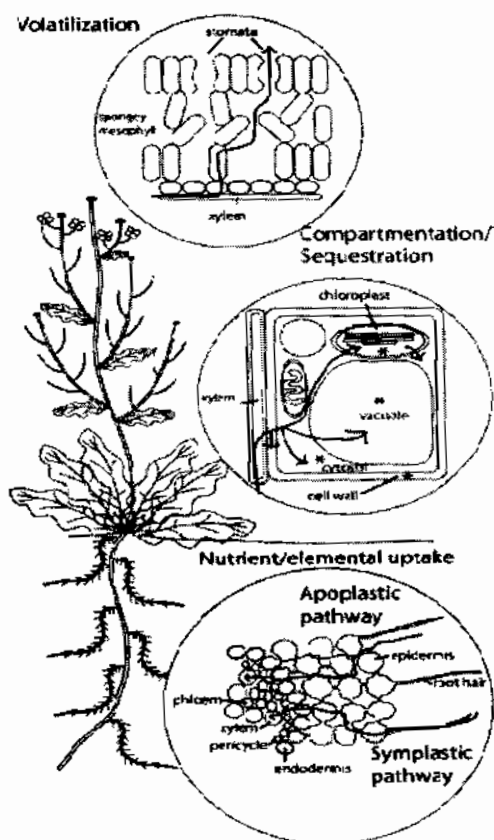


Figure 2.2 Pathway of metal/nutrient uptake in plants (Peer *et al.*, 2006)

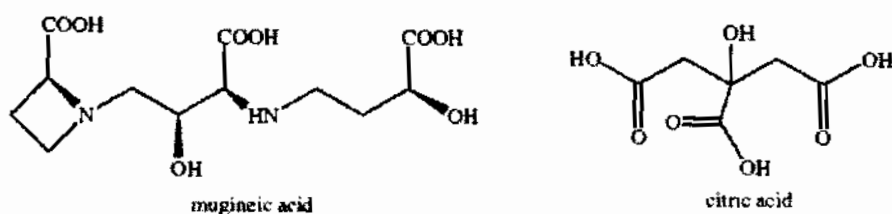


Figure 2.3 Two metal binding ligands in plants (Callahan *et al.*, 2006)

2.4.2 Role of heavy metal detoxification in plants

Some heavy metals, particularly copper and zinc are essential micronutrients for a range of plant physiological processes via the action of Cu- and Zn-dependent enzymes. These and other nonessential heavy metal ions, such as cadmium, lead, and mercury, are highly reactive and consequently can be toxic to living cells. Thus plants, like all living organisms, have evolved a suite of mechanisms that control and respond to the uptake and accumulation of both essential and nonessential heavy metals. These mechanisms include the chelation and sequestration of heavy metals by particular ligands such as organic acids, amino acids, peptides and proteins. The two best-characterized heavy metal-binding ligands in plant cells are the phytochelatins (PCs) and metallothioneins (MTs) (Cobbett and Goldbrough, 2002).

2.4.2.1 Phytochelatins

Phytochelatins form a family of peptides that consists of repetitions of the γ -Glu-Cys dipeptide followed by a terminal Gly, the basic structure being $(\gamma$ -Glu-Cys) $_n$ -Gly[(PC) $_n$] (Figure 2.4), where n is generally in the range of two to five. Phytochelatins are synthesized enzymatically from glutathione (GSH) in response to many metals (Memon *et al.*, 2001; Rauser, 1990). A number of other structural variants of PCs, such as $(\gamma$ -Glu-Cys) $_n$ -b-Ala, $(\gamma$ -Glu-Cys) $_n$ -Ser) and $(\gamma$ -Glu-Cys) $_n$ -Glu, have been identified in some plant species (Memon *et al.*, 2001; Rauser, 1990). Phytochelatins (PC) synthase has an isoelectric point near pH 4.8 and has optimum temperature of 35°C and pH 7.9. The molecular weight of the enzyme is around 95 kDa and seems to be composed of four subunits. The occurrence of PC-synthase in different higher plants has been confirmed (Clemens *et al.*, 1999). The vacuole is the ultimate storage site for those heavy metal ions that happen to enter the cytosol of a given plant

cell. These ions will activate PC-synthase, which synthesizes at the expense of GSH, and PC molecules of varying chain lengths thus chelate the metal. The metal-PC complex is subsequently actively transported from the cytosol to the vacuole (Memon *et al.*, 2001). Thomine *et al.* (2000) reported that heavy metal ions such as Cd^{2+} enter the plant cell by transporters for essential cations such as Fe^{2+} .

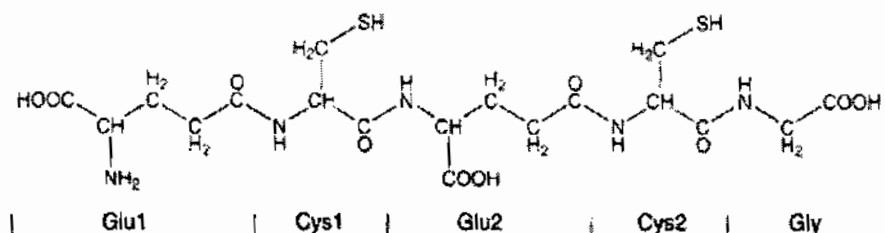


Figure 2.4 Chemical structure of phytochelatin. (n=2) (Kobayashi and Yoshimura, 2006)

2.4.2.2 Metallothioneins

Metallothioneins (MT) are the other low molecular weight proteins which bind heavy metals and are found throughout the animal and plant kingdoms. These proteins also play an important role in detoxification by sequestering metals in plant cells. Plants have been found to contain a number of genes encoding MT-like proteins having sequence similarity to animal MT proteins. They are subdivided into two types, MT1 and MT2, on the basis of arrangements of cysteine residues. In 1997, Murphy *et al.* identified and purified protein products of MT1 and MT2 genes from *Arabidopsis*, and therefore the list of plant MTs was enlarged with those proteins (Memon *et al.*, 2001).

2.4.2.3 Amino acids and organic acids

2.4.2.3.1 Histidine

Nitrogen-donor ligands and especially free amino acids are assumed to play a role in hyperaccumulators (Krämer *et al.*, 1996). Among them, histidine (His) is considered to be the most important free amino acid involved in metal hyperaccumulation. It can act as a tridentate ligand via its carboxylate, amine and imidazole functions (Callahan *et al.*, 2006). For example, $\text{Ni}^{\text{II}}(\text{His})_2$ (Figure 2.5) (Fraser, 1965).

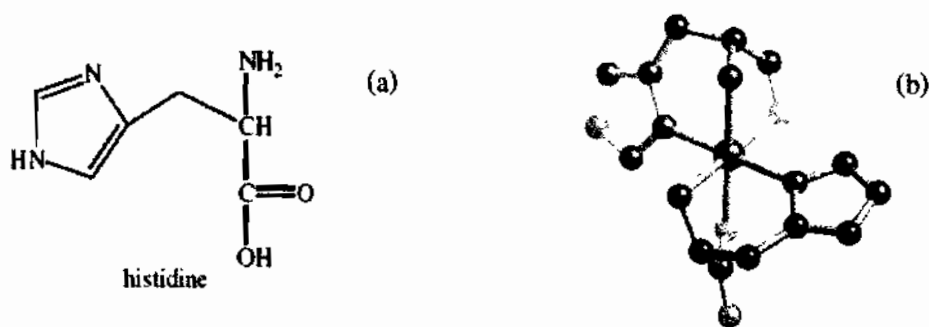


Figure 2.5 The structure of Histidine (a) (Callahan *et al.*, 2006) and Crystal structure of $\text{Ni}^{\text{II}}(\text{His})_2$ (b) (Ni in pink, C in black, N in blue, O in red) (Fraser, 1965)

2.4.2.3.2 Organic acid

Plants have carboxylic acids, which are present in high concentrations in the cell vacuoles of photosynthetic tissues (Callahan *et al.*, 2006). These include citric, isocitric, oxalic, tartaric, malic, aconitic and malonic. Many studies have implied that these acids play a role in hyperaccumulation (Callahan *et al.*, 2006). Zhao *et al.* (2000) reported the roots of *Arabidopsis halleri* (L.) increased the levels of organic acids in response to increasing Zn levels in the soil.

2.5 Electrophoresis

2.5.1 Principle of electrophoresis

Electrophoresis is the movement of an electrically charged substance under the influence of an electric field. This movement is due to the Lorentz force, which may be related to fundamental electrical properties of the body under study and the ambient electrical conditions (Amersham, 2001).

2.5.2 Gel electrophoresis

Gel electrophoresis is a technique in which charged moleculars, such as proteins or DNA, are separated according to physical properties as they are forced through a gel by electrical current. This method is limited to special applications; instead gels of polyacrylamide are commonly used. The pore size of these gels can be adjusted by the polyacrylamide concentration (Figure 2.6). If very large pores are required, agarose or starch gels are used instead (Buxbaum, 2007).

SDS-PAGE or Sodium dodecyl sulfate polyacrylamide gel electrophoresis is a method that separates based on the mass of the molecular. Sodium dodecyl sulfate (SDS) (Figure 2.7) is a detergent that breaks up the interactions between proteins. The proteins are dissolved in SDS and reducing agents such as dithiothreitol (DTT) and mercaptoethanol, are used to remove the remaining tertiary and quaternary structure by reducing disulfide bonds (Figure 2.8). The SDS denatured and reduced proteins are flexible rods with uniform negative charge per unit length. Thus, molecular weight is essentially a linear function of peptide chain length, in a sieving gel the proteins separate by molecular weight.

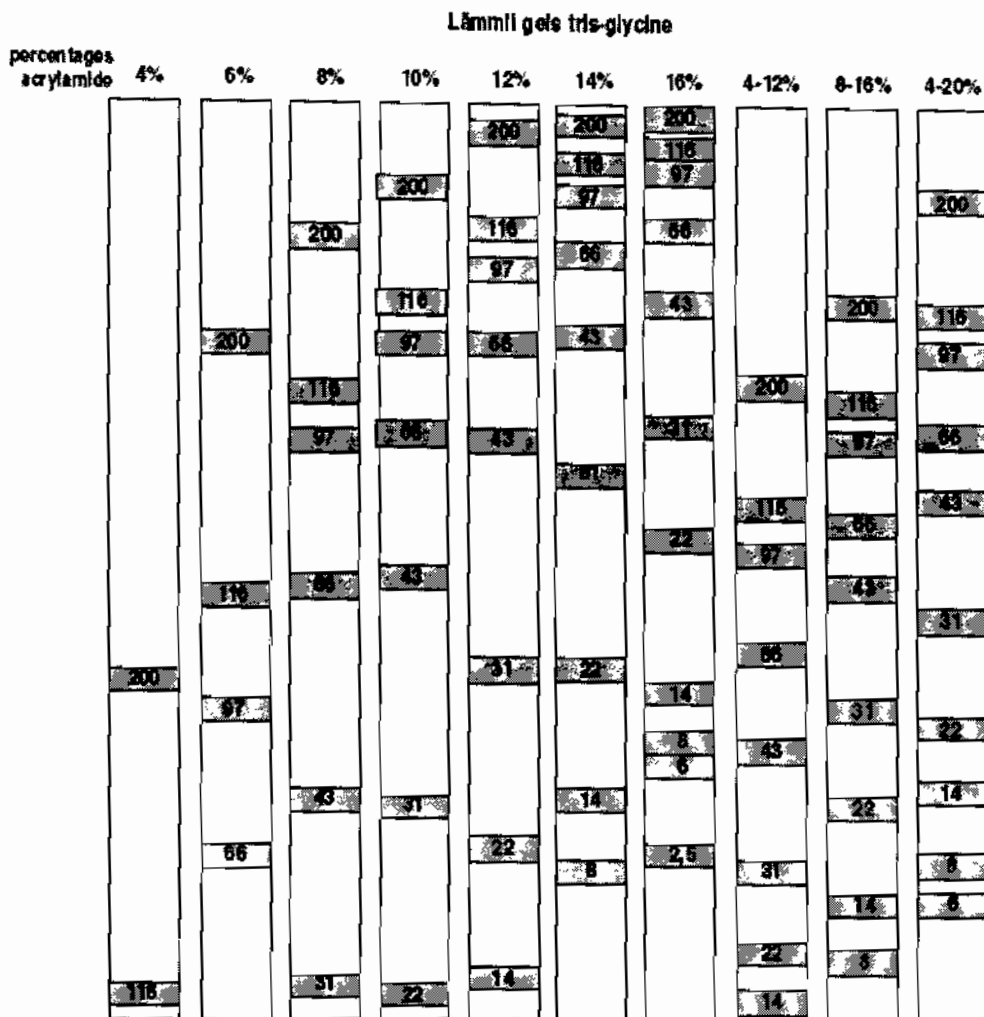


Figure 2.6 The relative movements of proteins of different molecular weights on SDS-gels made with different acrylamide concentrations (Rehm, 2006).

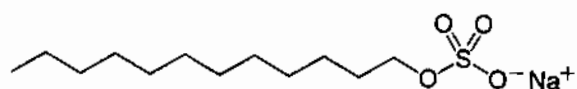


Figure 2.7 Structure of Sodium dodecyl sulfate (SDS)
 (http://en.wikipedia.org/wiki/Sodium_dodecyl_sulfate)

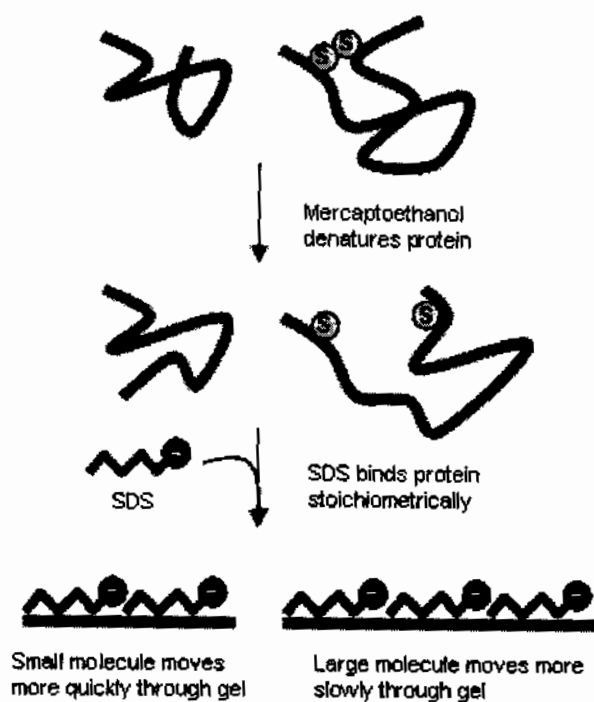


Figure 2.8 Denaturing of proteins by detergent Sodium dodecyl sulfate (SDS)
 (http://www.gibthai.com/services/technical_detail.php?ID=20)

2.6 Applications of X-ray absorption spectroscopy to phytoremediation

X-rays have sufficient energy to eject one or more core electrons from an atom. Each core electron has a well-defined binding energy, and when the energy of the incident X-ray is scanned across one of these energies, there is an abrupt increase in the absorption coefficient. This is the so-called “absorption edge” of the element (Pener-Hahn, 2005). The absorption coefficient near an edge typically shows fine structure that is divided, somewhat arbitrarily into XANES and EXAFS regions (Natoli *et al.*, 2003). The physical basis of both EXAFS and XANES is the scattering of the X-ray excited photoelectron by the surrounding atoms (Figure 2.9). Therefore, X-ray absorption spectroscopy (XAS) is one of the premier tools for investigating the local structural environment of metal ions, which can be divided into X-ray absorption near edge structure (XANES), which provides information primarily about geometry and oxidation state, and extended X-ray absorption fine structure (EXAFS), which provides information about metal site ligation (Pener-Hahn, 2005). Many reports have been used XAS to study different aspects of the coordination chemistry in many diverse phytoremediation systems. The uptake and coordination of Cr, Ni, Cu, As, Au, and Se by mesquite, *Thalpi goesingense*, *Larrea tridentata*, *Pteris vittata*, *Medicago sativa*, and *Astragalus bisulcatus*, respectively, are only a few examples of phytoremediation systems studied using X-ray absorption spectroscopy. The application of XAS to phytoremediation studies presents a series of advantages over other techniques. The main advantage of XAS would be the fact that there is no sample pretreatment. The basic samples as liquids, solids, or gases are run on XAS (Gardea-Torresdey *et al.*, 2005).

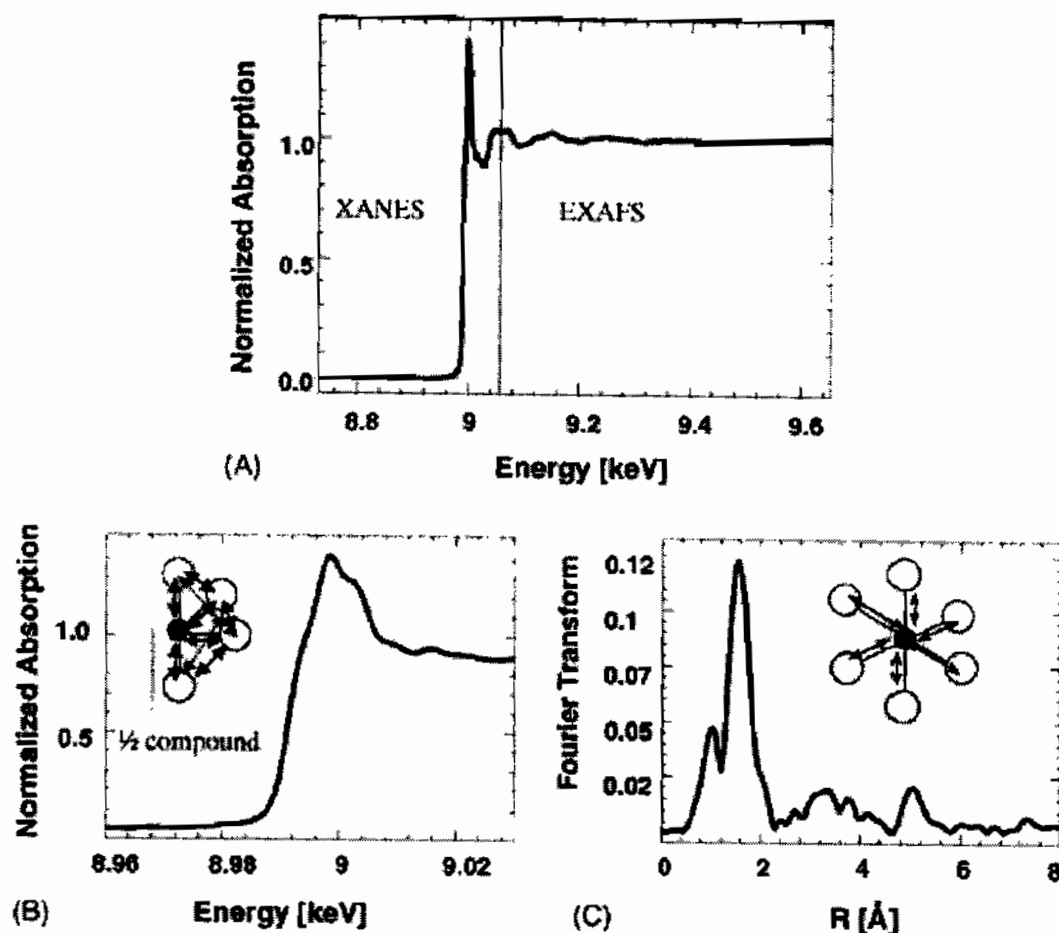


Figure 2.9 (A) The entire XAS spectra. The line indicates the separation between the XANES and EXAFS spectra. (B) The XANES spectra obtained for a metal compound with an octahedral geometry. (C) The Fourier transformed EXAFS of a metal compound with an octahedral geometry (Gardea-Torresdey *et al.*, 2005).

2.7 FT-IR analysis of protein structure

In recent years, FTIR spectroscopy with its self-deconvolution and derivative methods has been widely used to determine protein secondary structure, unlike X-ray crystallography and NMR spectroscopy which provide information about the tertiary structure. This technique is also being applied to determine the secondary structural variations, even in more complex proteins such as photosystems I and II reaction centers (Nahar and Tajmir-Riahi, 1995). FTIR spectroscopy works by shining infrared

radiation on a sample and seeing which wavelengths of radiation in the infrared region of the spectrum are absorbed by the sample. Every compound has a characteristic set of absorption bands in its infrared spectrum, such as proteins and polypeptides including amide I and amide II (Gallagher, 2011). These arise from the amide bonds that link the amino acids. The absorption associated with the amide I band leads to stretching vibrations of the C=O bond of the amide, absorption associated with the amide II band leads primarily to bending vibrations of the N-H bond (Figure 2.10). Both the C=O and the N-H bonds are involved in the hydrogen bonding that takes place between the different elements of secondary structure, the locations of both the Amide I and Amide II bands are sensitive to the secondary structure content of a protein. The type of protein secondary structure includes the α -helices and β -sheets, which allow the amides to hydrogen bond, very efficiently, with one another. Both are periodic structures. In an α -helix the polypeptide backbone is coiled in a right-handed helix where the hydrogen bonding occurs between successive turns of the helix (Figure 2.11). In β -sheets, the strands of polypeptide are stretched out and lay either parallel or antiparallel to one another. The hydrogen bonds form between the strands (Figure 2.11). Structures of proteins have been used to correlate, systematically, the shape of the amide I. This band is small compared to the intrinsic width of the band (Figure 2.12). Instead of a series of nicely resolved peaks for each type of secondary structure, one broad lumpy peak is observed.

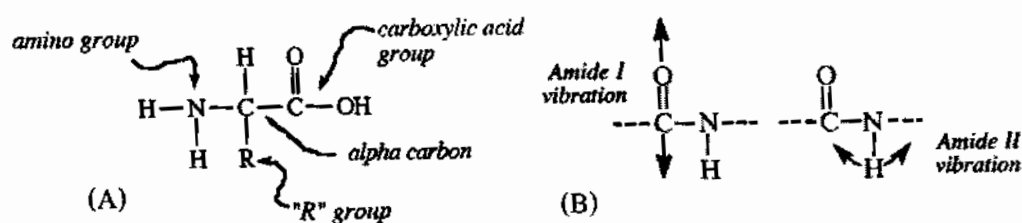


Figure 2.10 (A) the structure of an amino acid and (B) the Amide I and Amide II bands (Gallagher, 2011).

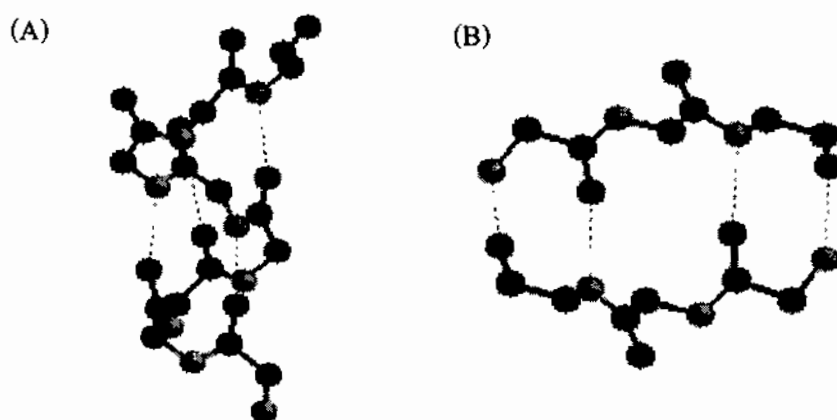


Figure 2.11 (A) Segments of an α -helix and (B) segments of β -sheet (Gallagher, 2011).

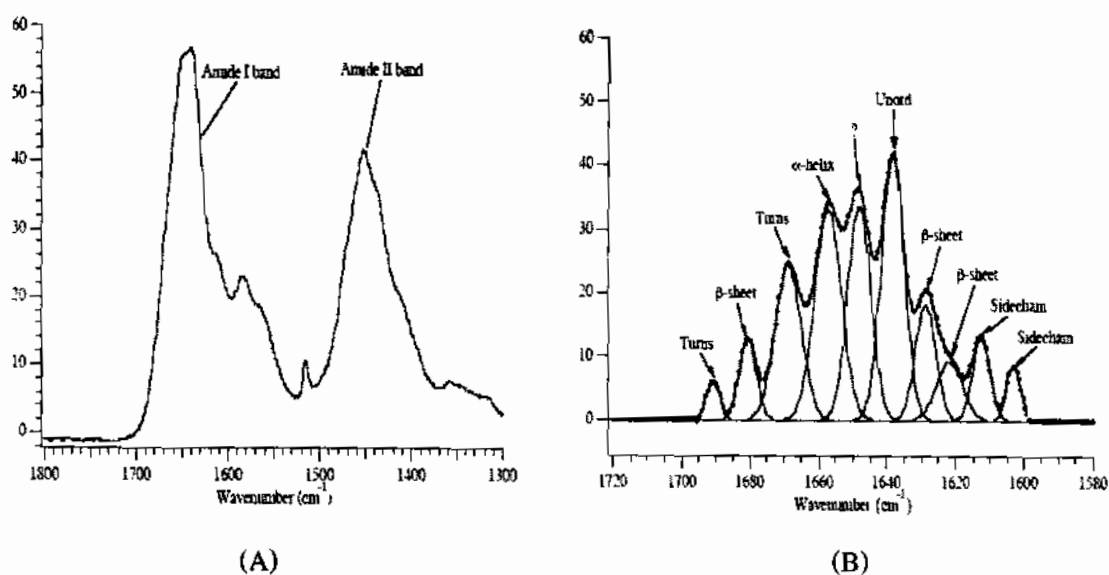


Figure 2.12 (A) FTIR spectrum of Amide I and Amide II bands and (B) result of a Fourier self-deconvolution analysis on the Amide I band (Gallagher, 2011).

2.8 Literature review

Van Keulen *et al.* (2008) reported that *Helianthus annuus*, dwarf sunflower, growing in 30 mg l^{-1} each of Cd, Cr, and Ni for 17-days showed variable amounts of the metals in roots, leaves, and stems. The concentration of metals was the highest in roots and the lowest in leaves. Proteins extracted from the leaves of sunflowers exposed to arsenic alone or in combination with other metals were size-fractionated by SDS-PAGE. Proteins with molecular masses ranging from less than 10 to over 45 kDa appeared in arsenic stress. One polypeptide with approximately 32 kDa was induced strongly. The peptide was identified by LC-MS/MS as a class III chitinase, whose gene appeared to be induced by As at the transcription level.

Yu *et al.* (2008) cloned *KT111* from *Saccharomyces cerevisiae* S288C into a pET-28a(+) expression vector (Novagen) and rebuilt *Escherichia coli* BL21 (DE3) Gold (Stratagene) host cells. The bacteria was cultured with M9 medium containing 1 mM IPTG and $20 \mu\text{M ZnSO}_4$ at 16°C for 20 h. The expression protein was purified by a Nickel-Chelating Sepharose Fast Flow and filtered in a HiLoad 16/60 Superdex 75 with an HPLC system. SDS-PAGE supported the purity of the protein and a bicinchoninic acid (BCA) protein assays was used to measure the sample concentration by X-ray absorption near-edge spectroscopy (XANES). MXAN software was applied to obtain chemical and stereo structural information around the Zn ion in Kti11p. The results showed that the high-spatial resolution technique confirmed the formation of a stable Zn tetrahedral configuration with four sulfur ligands on KT111, and returned extremely accurate bond angle information between ligands.

Weseloh *et al.* (2004) combined SDS-PAGE with SRXRF to analyze metal-loaded apoazurin (non-covalently bound metals) and selenoproteins in rat testis homogenate (as an example for a covalently-bound trace element). The apoazurin sample was incubated together with $2 \text{ m mol l}^{-1} \text{ ZnCl}$ in order to replace the Cu(II) ion in the molecule by Zn(II)-ion, and the selenoprotein sample was appropriately prepared. All samples were separated by SDS-PAGE, blotted onto a PVDF-membrane, and stained with Coomassie-blue. The selenoprotein distribution determined by SRXRF was compared to that of 75Se -labeled selenoproteins from rat testis. The distribution of several elements along the separation lane was determined in a zinc-loaded apoazurin

sample. Zinc and chlorine were found to be present in the protein band, while iron, tin and calcium were detected along the lane.

Krüger *et al.* (2002) showed the phloem-mediated transport of micronutrients during the germination of castor bean seedlings and identified an iron transport protein (ITP) for *Ricinus*. The results demonstrated that essentially all ^{55}Fe fed to the seedlings was associated with the protein fraction of phloem exudates. ITP bonded to Fe^{3+} but not to Fe^{2+} and also formed complexes with Cu^{2+} , Zn^{2+} , and Mn^{2+} . In addition, a protein of 96 amino acids showed high similarity to the stress-related family of late embryogenesis abundant proteins. Therefore, the RNA expression pattern was consistent with a function in metal ion binding. In addition, the ITP from *Ricinus* provided the first identified micronutrient binding partner for phloem-mediated long distance transport in plants.

Gao *et al.* (2003) proposed a more suitable approach to separation and detection of metalloproteins in human liver cytosol. The procedure included gel filtration chromatography and isoelectric focusing separation of proteins, a step of gel drying and a SRXRF analysis of trace elements in the protein bands. The results showed that there were at least two Zn, two Cu and about eleven Fe-containing protein bands present in human liver cytosol.

Verbi *et al.* (2005) investigated protein bands from *in vitro* embryogenic calluses using micro-RXRF after SDS-PAGE separation. The protein bands ranged from 14 to 86 kDa, and each band was scanned using synchrotron radiation. Two protein bands (81 and 14 kDa) presented a heterogeneous iron distribution through the protein clusters, suggesting that different proteins could be linked to this metal. The 53 kDa protein measured presented iron, calcium, copper, potassium and zinc. Once again, heterogeneity of metals distributed along the protein band was observed. Metal-binding protein quantification was done, after microwave oven decomposition of a gel protein band, by synchrotron radiation total reflection X-ray fluorescence (SR-TXRF), FAAS and Flame Atomic Emission Spectrometry (FAES). Ca, Cu, K, Fe and Zn were determined by SR-TXRF, Ca and Mg by FAAS, and Na by FAES. The quantitative and qualitative results were in agreement, besides good precision between SR-TXRF and FAAS results. Another interesting result was obtained for Fe and Mg. They were only quantified in two protein bands (81 and 14 kDa for Fe and 86 and 27 kDa bands for

Mg), indicating that both metals played an important role in the biochemical events where these proteins participate.

De la Rosa *et al.* (2004) investigated the uptake and translocation of Cd in *Salsola kali*. XAS spectra of whole plant parts (roots, stems, and leaves) indicated that Cd in the plants remained in the (II) oxidation state. The EXAFS data showed that Cd was bound to O, S, and Cd. The Cd transportation from roots to the aerial part might occur through complexation with small organic acids. In addition, the presence and coordination of Cd S in stems and leaves of the plant suggested the formation of Cd-phytochelatin complexes.

Salt *et al.* (1995) studied the uptake of Cd, its mobility, and accumulation in Indian mustard, as well as the types of Cd-complexes formed within the plant. The EXAFS of the whole root tissue indicated that Cd was bound into a phytochelatin complex containing four S ligands. However, in the xylem sap the Cd was found to be coordinated to 6 O/N ligands.

Barone *et al.* (2007) studied protein-transition metal ion networks by mixture between divalent metal ions and protein of feather keratin, egg albumin, and wheat gluten. FTIR was used to investigate binding reactions occurring between protein chains. The results showed that the direct valence of the transition metals was primarily binding at glycerol and amide sites and secondarily carbonyl sites on the protein.

Si *et al.* (2009) reported the bioaccumulation and transformation of Cd by *Phaeodactylum tricornutum* in the presence of ethylenediamine tetra acetic acid (EDTA) and cysteine (Cys). A considerable body of evidence and the prediction of the Free Ion Activity Model (FIAM), which was developed to explain the core-relation between the concentration of free ions and the observed biological effects, suggested that metal toxicity and bioavailability were a function of free ion activity. FTIR and XAS indicated that the ligand formed a complex with Cd. The Cd interacted with -Si-OH, -C-OH and -NH₂(CO)-OH on the cell wall. In addition, PCs, oxidized-PCs and Cd-PC₂ provided the evidence for deactivation of Cd by the PCs and reduction of Cd-toxicity.

CHAPTER 3

Methodology

This research was designed to investigate the effect of zinc and cadmium on plant growth and detoxification mechanism in *Gynura pseudochina* (L.) DC. through the observation of metal-binding proteins. *G. pseudochina* (L.) DC. was grown in MS medium (supplemented with 2 mg l⁻¹ indole-3-acetic acid (IAA) and 2 mg l⁻¹ indole-3-butyric acid (IBA) contaminated with zinc and/or cadmium. FAAS was used to analyze zinc and cadmium accumulated in the treated plant. Crude proteins from *in vitro* grown *G. pseudochina* (L.) DC. were extracted with phenol extraction buffer and separated by SDS-PAGE. A mechanism for detoxification of zinc and/or cadmium, focusing on protein was studied by micro X-ray fluorescence (μ XRF) imaging and X-ray absorption fine structure (XAFS); X-ray absorption near edge structure (XANES) and X-ray absorption fine structure (EXAFS), using synchrotron based radiation. The secondary structure of protein was also investigated by an attenuated total reflection using infrared Fourier transform (ATR-FTIR) spectroscopy.

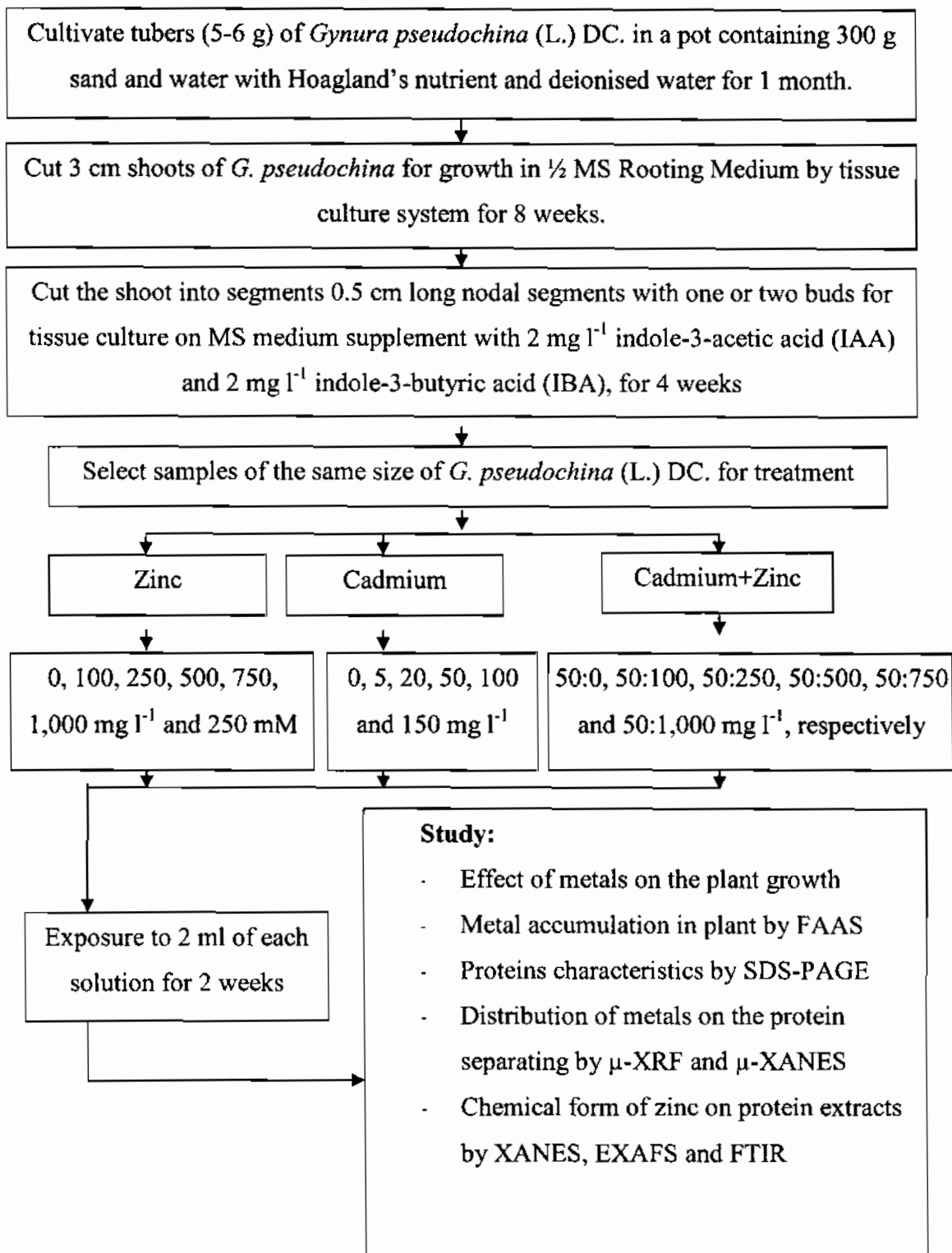
3.1 Research diagram

3.2 Materials and equipment

3.3 Chemical reagents

3.4 Materials and Methods

3.1 Research diagram



3.2 Materials and equipment

1. High speed refrigerated micro centrifuge MX-301 (TOMY, Japan)
2. Spectrophotometer (Spectronic[®]20-GENESYS[™], USA)
3. UV-visible spectrometer (Agilent 8453 UV-Vis, USA)
4. Scanning electron microscopy combined with energy dispersive X-ray analysis (JEOL Jsm-7000 FSHL, Japan)
5. Vertical electrophoresis (miniVE, Amersham Bioscience, USA)
6. Atomic Absorption/Flame Emission Spectrophotometer (AAS) (Shimadzu AA-680, Japan)
7. Vortex mixer FINEVORTEX (FINEPCR, Korea)
7. Autoclave ES-315 (Tomy, Japan)
8. pH meter HI 9321 (HANNA, Mauritius)
9. Ultrasonic Cleaner TRU-SWEEP (CREST, America)
10. Power supply EC250-90 (Thermo EC., USA.)
11. Lyophilizer (Labconco Co. Lyph-Lock 6 Liter Freeze-Dry System Model 77530)
12. Synchrotron radiation X-ray absorption spectroscopy on beam line 8 (BL-8) at Synchrotron Light Research Institute (Public Organization), Thailand
13. Synchrotron radiation X-ray absorption spectroscopy on beam line 4A and 12C at Photon Factory (PF), KEK, Tsukuba, Japan
14. Fourier transform infrared (FTIR) spectroscopy (TENSOR 27 FT-IR Spectrometer, Bruker Optics, German), at Synchrotron Light Research Institute (Public Organization), Thailand

3.3 Chemical reagents

All chemicals used in experiments were analytical grade.

1. Zinc sulfate ($\text{ZnSO}_4 \cdot 7\text{H}_2\text{O}$) (MERCK, German)
2. Cadmium Sulphate ($3\text{CdSO}_4 \cdot 8\text{H}_2\text{O}$) (Ajax Finechem, Australia)
3. Hoagland solution, followed Hoagland and Arnon (1950)
4. MS medium solution, followed Murashige *et al.*, (1962)

5. Indole-3-acetic acid (IAA) (Sigma, German)
6. Indole-3-butyric acid (IBA) (Sigma, German)
7. Ethanol (MERCK, German)
8. Methanol (MERCK, German)
9. Phosphoric acid (VWR, England)
10. Acetone (VWR, England)
11. Tris base (AMRESCO, America)
12. Glycine (AMRESCO, America)
13. HEPES buffer (Sigma, German)
14. Bovine serum albumin (BSA) (Fluka, Switzerland)
15. EDTA (Ajax Finechem, Australia)
16. EGTA (Fluka, Switzerland)
17. TEMED (Fluka, Switzerland)
18. Ammonium persulfate (AMRESCO, America)
19. Ammonium acetate (Ajax Finechem, Australia)
20. Sodium dodecyl sulfate (AMRESCO, America)
21. Acrylamide buffer 40% (AMRESCO, America)
22. Potassium chloride (Ajax Finechem, Australia)
23. 2-Mercaptoethanol (Sigma, German)
24. Coomassie Brilliant Blue R 250 (Panreac, England)
25. Coomassie Brilliant Blue G 250 (Fluka, Switzerland)
26. Dithiothreitol (DTT) (Promega, USA)
27. Phenylmethanesulfonylfluoride (PMSF) (Promega, USA)
28. L-Cysteine (Himedia, India)
29. L-Methionine (Himedia, India)
30. L-Glutathione reduced (Sigma, German)

3.4 Methods

3.4.1 Plant material

Tubers of *G. pseudochina* (L.) DC. collected from a non-contaminated site in Thailand were cleaned and cut into 5-6 g pieces. Each tuber was grown in a pot containing 300 g sterilised sand. Plants were treated with Hoagland's nutrient solution (Hoagland and Arnon, 1950) and deionised water in a soil less cultivation system. Plants were grown for one month in a glass house (20-40°C, humidity 70-75% and light intensity greater than 10,000 lux at noon)

3.4.2 *In vitro* establishment and culture conditions

Shoot tips of *G. pseudochina* (L.) DC. were soaked with soap and washed with tap water. The cleaned shoot tips were cut into 3 cm long pieces before being soaked in 70% (v/v) alcohol for 10 minutes, and sterilized with 15% (v/v) of Clorox containing 1% (v/v) Tween 20 for 15 minutes, then rinsed three times with sterile distilled water. The apical bud tissues were cut into 1 cm long pieces and cultured on 20 ml $\frac{1}{2}$ MS Rooting Medium (Murashige *et al.*, 1962). The pH was adjusted to 5.7 with 0.1 M KOH before adding agar to obtain 7.0 g l⁻¹ and autoclaving at 121°C for 15 min. The apical bud explants were cultured at 25°C under 1,500 lux of light intensity and a 12 hour photoperiod. After 2 months, cuttings nodal segments 0.5 cm long from *in vitro* shoot of *G. pseudochina* (L.) DC. with one or two buds were transferred to 20 ml of the MS medium with additives of 2 mg l⁻¹ indole-3-acetic acid (IAA) plus 2 mg l⁻¹ indole-3-butyric acid (IBA) (Cuenca *et al.*, 1999) and cultured for 4 weeks.

3.4.3 Metal tolerance and accumulation

The healthy plants were selected for Zn and/or Cd treatment under the tissue culture system. The plant samples were separately treated with 2 ml each of zinc solutions of 0 (control), 100, 250, 500, 750 and 1000 mg l⁻¹, or treated with 2 ml each of cadmium solutions of 0 (control), 5, 20, 50, 100 and 150 mg l⁻¹. The dual treatment of zinc and cadmium was carried out with various zinc concentrations containing 50 mg l⁻¹ of cadmium for 2 weeks. The zinc and cadmium solutions were prepared from ZnSO₄·7H₂O (Ajax Finechem, Australia) and CdSO₄·8H₂O (Ajax Finechem, Australia), respectively.

The toxicity of high metal concentration was related to the appearance of symptoms on leaves, of the adverse effects, and the phytotoxicity was evaluated by determination of the amount of the plant with necrotic spots and/or chlorosis of leaves (yellowish colour). The plant samples were washed with an excess of deionised water before being carefully blotted dried with clean soft paper. A whole plant was weighted for the wet weight and then separated into root, stem and leaves.

Other separated samples were dried at 80°C for 24 hour. A 0.05 g sample of each was digested following the modified method of Miller (1998); soaked with 3 ml of 65% v/v HNO₃ for 24 hours, then heating at 150°C for 1 hour, before adding 1 ml of 70% (v/v) HClO₄ and heating at 215°C for 2 hours, then adding 3 ml of deionised water and boiling at 90°C for 1 hour. The digestion was analysed for zinc and cadmium concentration by an Atomic Absorption Spectrophotometer (AAS) (Shimadzu AA-680, Japan). The data was analyzed by one-way analysis of variation (ANOVA) in a completely randomized design (CRD) and randomized complete block design (RCBD). The variance and means separation were performed using the Duncan's new multiple range test (DMRT) at $p < 0.01$. Statistical analysis was performed using SPSS Version 13.0, software program.

3.4.4 Protein extraction for SDS-PAGE

For extraction of total soluble protein, *in vitro* plants were harvested and washed with deionised water before being separated into root, shoot, and leaves. In the first method, a sample of 100 mg was homogenized in 400 µl phenol saturated buffer (80% (v/v) Tris-HCl, pH 8.0 saturated phenol, 0.01% (v/v) 2-mercaptoethanol in 120 mM Tris-HCl, pH 6.8, 50 mM EDTA, pH 8.0, 100 mM potassium chloride). The homogenate was transferred to 1.5 ml microcentrifuge tube and briefly centrifuged at 13,000 rev min⁻¹ for 5 min. The phenol and aqueous phases were transferred into a new microcentrifuge tube. The total proteins were precipitated by adding 5 volume of 100 mM ammonium acetate in methanol and incubated at -20°C for 30 min. The protein pellet was centrifuged at 13,000 rev min⁻¹ for 20 min, washed with acetone buffer and resuspended in 250 µl of protein sample buffer (63mM Tris-HCl, pH 6.8, 2%(v/v) SDS, 5%(v/v) mercaptoethanol, 20%(v/v) glycine). The protein sample was stored at -20°C (Sangdee *et al.*, 2003). In the second and third method, sample was homogenized and extracted with 300 µl HEPES buffer (100 mM HEPES-KOH pH 7.1), and modified

HEPES buffer (100 mM HEPES pH 7.1, 250 mM sorbitol, 10 mM MgCl₂, 10 mM KCl, 1 mM EDTA, 1 mM EGTA, 2 mM DTT, and 1 mM PMSF), respectively. The samples were then centrifuged for 20 min at 15,000 g at 4°C (Heiss *et al.*, 2003). The supernatant was collected and kept at -20°C. The protein concentration was measured using the Bradford assay and characterised by SDS-PAGE.

3.4.5 Determination of protein concentration

The Bradford assay was used for determination of protein concentration using bovine serum albumin (BSA) as a protein standard (Bradford, 1976). The total volume of modified assay was 3.06 ml containing 60 µl of protein sample and 3 ml of the Bradford working solution (dissolving 100 mg of Coomassie Blue G-250 in 50 ml of 95% ethanol, 100 ml of 85% phosphoric acid and made up to 1 l with distilled water) after mixing well. The reaction mixture was incubated at room temperature for 5-60 min. The absorbance for each sample was measured at 595 nm (Becker, 1996).

3.4.6 SDS-PAGE

The concentration of proteins (20 mg) were fractionated on a 12% acrylamide gel electrophoresis (2.375 ml of distillation water, 3.125 ml of 30% acrylamide, 1.9 ml of 1.5 M Tris-HCl pH 8.8, 75 µl of 10% SDS, 15 µl of 30% APS and 15 µl of TEMED) and a 5% stacking gel (2.77 ml of distillation water, 0.83 ml of 30% acrylamide, 1.26 ml of 1.0 M Tris-HCl pH 6.8, 50 µl of 10% SDS, 15 µl of 30% APS and 15 µl of TEMED.) for 3 h at 20 mA/gel. The gels were stained with coomassie brilliant blue R-250 staining buffer (0.1% (w/v) coomassie brilliant blue R-250, 40% methanol and 10% acetic acid) for 24 h and destained with 40% methanol and 10% acetic acid. The molecular weight of the protein band was measured based on the molecular weight of two broad range protein markers of 7.1 kDa to 209 kDa (precision plus protein dual color standards, Bio-Rad, USA) and 10 kDa to 250 kDa (prestained SDS-PAGE standard, broad range, Bio-Rad, USA). The expression of proteins in SDS-PAGE was analyzed by Quantity One 1-D analysis software program (Bio-Rad, USA). The protein patterns were kept using a cellulose membrane by fixing on cellulose membrane and drying at room temperature.

3.4.7 X-ray absorption fine structure (XAFS)

Two month old plants growing in the tissue culture system were e⁻ 2 ml of sterile 250 mM of Zn solution (pH 5.5 ± 0.5) prepared from ZnSO₄

cultivated for 4 days before harvesting. Control plants were untreated. The plant samples were washed with an excess of deionised water before being carefully blotted dried. A crude protein sample was obtained from a whole plant. The protein extract was freeze dried by a freeze dryer (Labconco freezezone 4.5, USA) before being ground and pressed into a pellet. The protein pellet was wrapped with Mylar[®] film on the 4x4 cm² acrylic sample board.

The Zn K-edge XAFS were performed at beamline 12C, Photon Factory (PF), KEK, Japan. Sulfur K-edge XANES spectra were performed at beam line 8, Synchrotron Light Research Institute (Public Organization), Thailand. The experimental conditions for XAFS analysis is summarized in Table 3.1 - 3.2. The XAFS analysis data was analyzed by Rigaku Rex2000 Version 2.3.2 and Athena under IEFIT version 1.2.9. The reference materials were Zn(NO₃)₂, ZnS, ZnSO₄·7H₂O, ZnCl₂ and ZnO (analytical chemicals) Zn-cellulose (prepared by absorption system), Zn-cysteine (prepared by absorption system) and Zn-glutathione (prepared by absorption system).

Table 3.1 Experimental conditions for XAFS analysis at BL-8, SLRI

Method	XAFS
Monochromator	Double crystal Si(111) monochromator
Focusing mirror	Bending magnet
Beam size	10 mm (h) x 1 mm (v)
Incident X-ray detector	10-cm-long ion chamber (I ₀) filled with a gas mixture of Ar (24 mbar) and He (989 mbar) 40-cm-long ion chamber (I ₁) filled with gas mixture of Ar (133 mbar) and He (880 mbar)
Fluorescence X-ray detector	13-channel Germanium detector (GeD)
Atmosphere in sample chamber	Air
Temperature	Room temperature

Table 3.2 Experimental conditions for XAFS analysis at BL-12C, PF, KEK

Method	XAFS
Monochromator	Si(111) double crystal
Focusing mirror	Bent cylindrical mirror
Beam size	ca. 1 mm x 1 mm
Incident X-ray detector	Ionization chamber
Fluorescence X-ray detector	19-element Ge solid-state detector
Atmosphere in sample chamber	Air
Temperature	Room temperature

3.4.8 Fourier transform infrared spectroscopy (FTIR) analysis.

The crude protein was extracted from the leaves of plants treated with 1,000 mg l⁻¹ of zinc solution for 2 weeks. The crude protein extracts were freeze dried by a freeze dryer before being ground to a homogenized powder. FT-IR Spectra were obtained using TENSOR Series FT-IR Spectrometer (Bruker optic, German) equipped with diamond crystal Platinum ATR accessory. FT-IR analysis was conducted at Synchrotron Light Research Institute (Public Organization), Thailand. All spectra were acquired between 4000 and 700 cm⁻¹ with 64 accumulations and a spectral resolution of 4 cm⁻¹. The spectra were recorded in attenuated single reflection and corrected by the ATR correction of the OPUSTM software. The first and second derivatives of the absorbance spectra were used to evaluate the spectra. Pretreated spectrums were statistically analyzed by multivariate data analysis (principle component analysis; PCA) and the Unscramble 9.7, CAMO software.

CHAPTER 4

Results and discussion

4.1 Propagation of *Gynura pseudochina* (L.) DC. in tissue culture system

Auxins are often used to promote initiation of adventitious roots, they are essential for cell growth, promote axial elongation (in shoots as well) and lateral expansion (as in root swelling). Indole-3-acetic acid (IAA) and indole-3-butyric acid (IBA) are auxins that have the ability to induce formation in explants (Minorsky, 2005). In addition, Cuenca *et al.* (1998) showed MS medium containing IAA and IBA was the best for micropropagation of *Centaurea paui* Loscos ex Willk, a plant in the family Compositae. *G. pseudochina* (L.) DC. is also in the family Compositae, therefore, the initial nodal segments from *in vitro* shoots of *G. pseudochina* (L.) DC. with one or two buds were cultured in a modified MS medium in the absence or presence of 2 mg l^{-1} each of IAA and IBA for 4 weeks. The comparison of plant growth in MS medium with and without the hormone are shown in figure 4.1. Figures 4.1 (a) and (b) clearly show that the plants growing in MS medium supplemented with the combination of both IAA and IBA looked healthier as the number of leaves and roots was greater. Therefore, MS medium with IAA and IBA was used for germination and propagation of *G. pseudochina* (L.) DC.

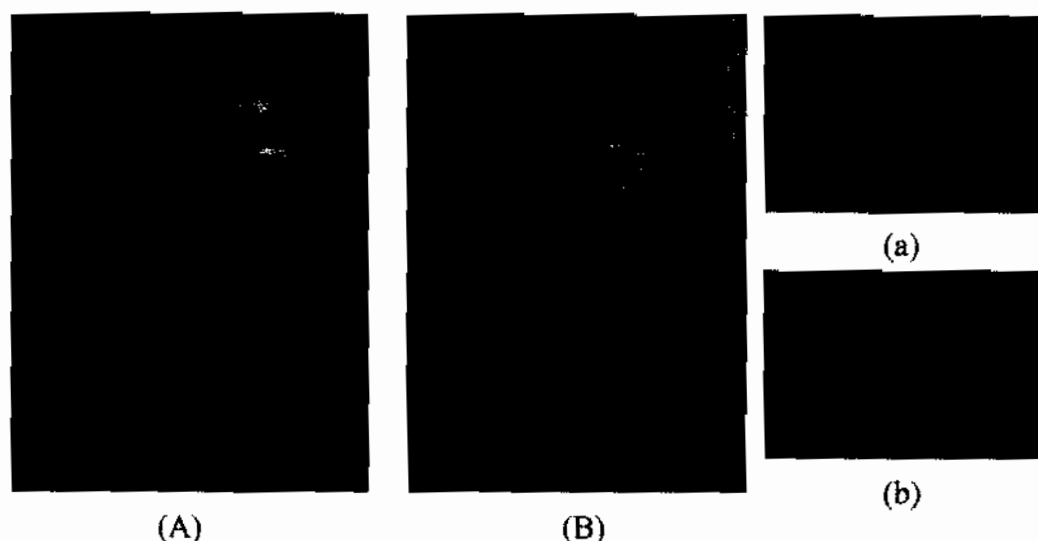


Figure 4.1 Growth of *Gynura pseudochina* (L.) DC. after 4 week in (A, a) MS medium; and (B, b) MS medium containing 2 mg l^{-1} each of IAA and IBA hormones.

4.2 Effect of zinc and/or cadmium on plant growth

The effects of zinc and/or cadmium on the growth of *G. pseudochina* (L.) DC. after 2 weeks were determined by percentage of dry weight and phytotoxicity. Figures 4.2 (a)-(c) shows that the % dry weight of plants separately treated with various zinc and cadmium concentrations were significantly different when compared with the control plants ($p < 0.01$). Figure 4.2 (a) shows the increase in zinc concentrations from 100 to 500 mg l^{-1} tended to promote plant growth, whereas higher zinc concentrations of 750 and $1,000 \text{ mg l}^{-1}$ resulted in a slightly lower % dry weight. However, the growth of plants at each zinc concentration were similar to the growth of the control plants. On the other hand, the growth of plants in the MS media containing cadmium at 5 mg l^{-1} was not significantly different from the controls (Figure 4.2 (b)). Although the plants survived in the higher cadmium concentrations of 20, 50, 100 and 150 mg l^{-1} , they showed a gradual decrease in the percentage of dry weight when treated with higher concentrations. The 50 mg l^{-1} of cadmium, which started to affect the plant growth, was chosen for dual treatments with various zinc concentrations of (100-1,000 mg l^{-1}). The plants dually treated with various zinc concentrations and 50 mg l^{-1} of cadmium (Figure

4.2 (c)) showed a smaller effect of cadmium on the % dry weight when compared with the cadmium treatment alone (50 mg l^{-1}).

The metal toxicity symptoms usually expresses in leaves. The toxicity of metals caused necrotic spots and/or chlorosis of leaves (yellowish colour) as shown in Table 4.1. The level of 50% phytotoxicity, as estimated from the graphs, was 500 mg l^{-1} of zinc alone (Figure 4.3 (a)), 60 mg l^{-1} of cadmium alone (Figure 4.3 (b)), and for the dual treatment of cadmium and zinc it was 50 mg l^{-1} of cadmium and 32.5 mg l^{-1} of zinc (Figure 4.3 (c)). The growth of *G. pseudochina* (L.) DC. in high concentrations of zinc and/or cadmium might be due to mechanisms for metals detoxification. In addition, the nutritional additives in MS medium could reduce the heavy metals toxicity to the plants (Yadav *et al.*, 2009). Nakbanpote *et al.* (2010) reported that *G. pseudochina* (L.) DC. still photosynthesised under the zinc treatment as starch grains and plastoglobules showed in the TEM images. However, the yellow leaves of the plants treated with the higher zinc concentration of 500 mg l^{-1} might be badly affected by zinc induction of Fe deficiency resulting in chlorophyll degradation (Kabata-Pendias and Pendias, 1992).

Cadmium is a non-essential trace metal for plant growth and it is highly toxic to plants; however, there was no effect on the plant dry weight when grown in the lowest cadmium concentration of 5 mg l^{-1} . Calabrese and Blain (2009) suggested that cadmium might be a hormesis, a dose-response phenomenon is characterized by low-dose stimulation and high dose inhibition. The high cadmium concentrations of 20-150 mg l^{-1} resulted in decreased plant growth, because cadmium could inhibit cell division (Prasad, 1995) and reduce photosynthesis by chlorophyll degradation (Benavides *et al.*, 2005). On the other hand, the interaction of zinc and cadmium showed the overcoming of cadmium toxicity as the dry weight of the Zn-Cd combination treatment were higher than the dry weights from the individual cadmium treatment (Figures 4.2 (c)-(d)). The interaction of zinc and cadmium overcoming the toxicity of cadmium was found in the *in vitro* cultures of *Linum usitatissimum* (linseed) (Chakravarty and Srivastava, 1997). However, the phytotoxicity of zinc was induced by 50 mg l^{-1} of cadmium as the level of 50% phytotoxicity of zinc decreasing from 500 mg l^{-1} for zinc alone to 32.5 mg l^{-1} for zinc in the combination treatment.

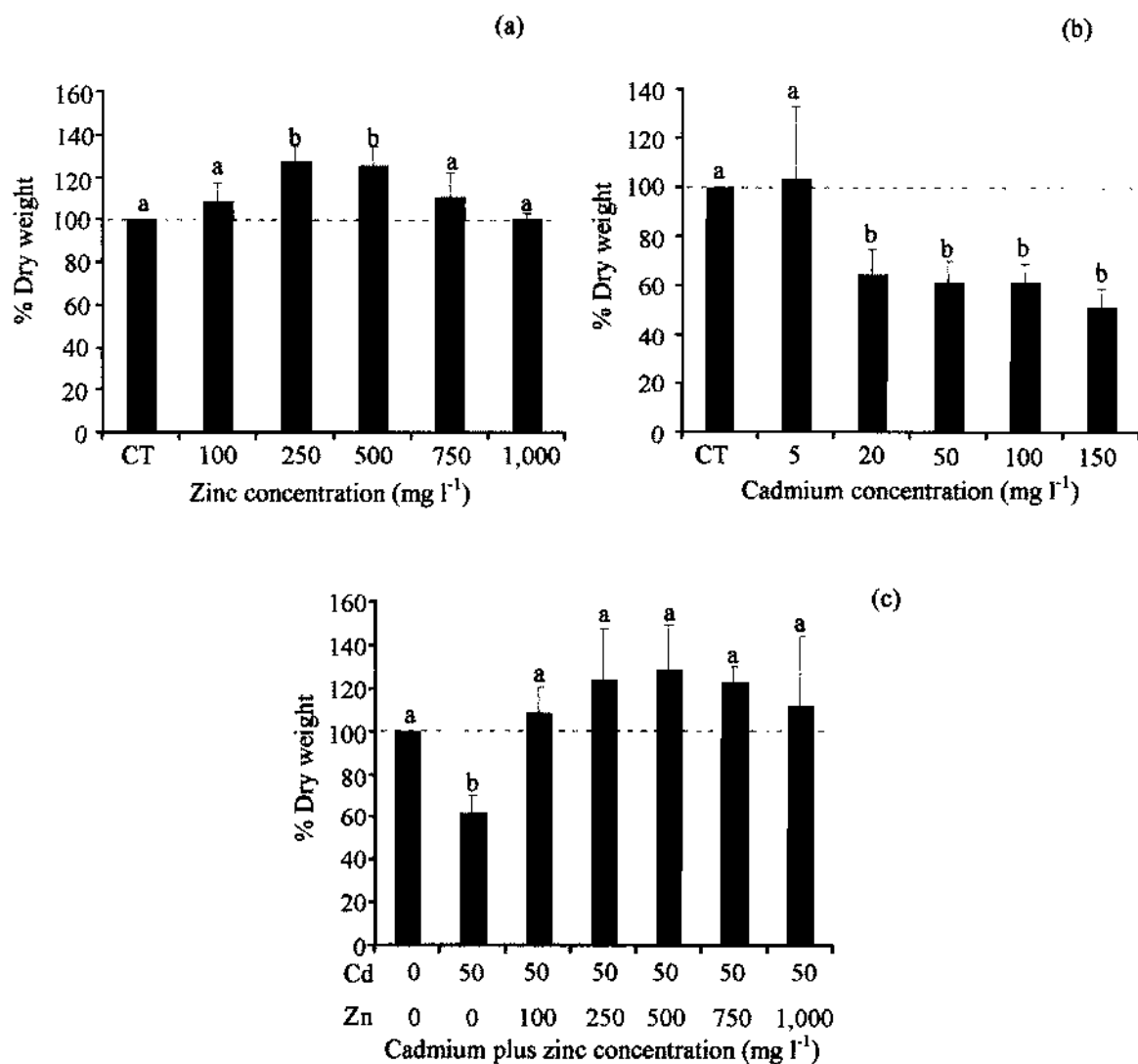


Figure 4.2 The dry weight of *Gynura pseudochina* (L.) DC. as a percentage, after 2 weeks treated with (a) various zinc concentrations, (b) various cadmium concentrations, and (c) dually treated with cadmium (50 mg l⁻¹) and various zinc concentrations. Vertical bar for each point represents the standard deviation for 5 replicates.

Table 4.1 Phytotoxicity percentages of *Gynura pseudochina* (L.) DC. under treatment with zinc and/or cadmium

Zinc		Cadmium		Cadmium plus zinc	
Conc.	% Phytotoxicity	Conc.	% Phytotoxicity	Conc.	% Phytotoxicity
0	0	0	0	50+0	38
100	0	5	0	50+100	63
250	0	20	25	50+250	75
500	50	50	38	50+500	100
750	63	100	100	50+750	100
1,000	100	150	100	50+1,000	100

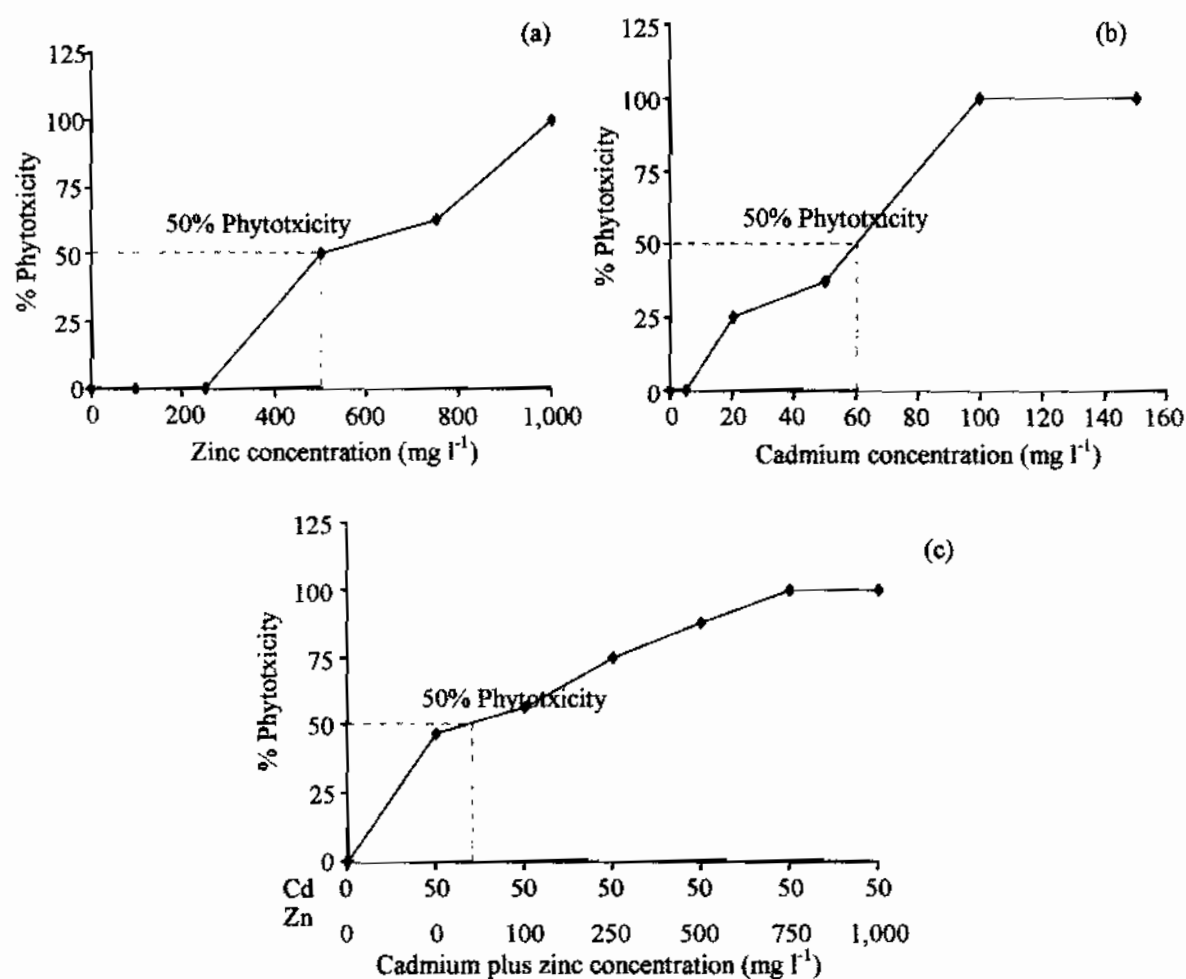


Figure 4.3 Phytotoxicity percentages of *Gynura pseudochina* (L.) DC., after 2 weeks treated with (a) various zinc concentrations, (b) various cadmium concentrations, and (c) dually treated with cadmium (50 mg l⁻¹) and various zinc concentrations.

4.3 Zinc and cadmium accumulation

The metals accumulated in the roots and shoots of *G. pseudochina* (L.) DC. were determined in term of translocation factor (TF). TF is the relationship between the metal concentration in the root and the shoot (Eq.1), which is an important phytoremediation parameter that can be used to evaluate the capacity of each accession to translocate metal from root to shoot (Barrutia *et al.*, 2009). McGrath and Zhao (2003) determined that the criterion for a hyperaccumulator should be the translocation factor (TF) > 1.

$$\text{Translocation Factor (TF)} = \frac{\text{Metal content in shoot (mg g}^{-1}\text{)}}{\text{Metal content in root (mg g}^{-1}\text{)}} \quad (1)$$

The translocation factor (TF) of the separate treatments of zinc and cadmium are shown in figures 4.4 (a) and (b), respectively. The results showed that TF of zinc increase from 0.61-0.90 when zinc concentrations were increased from 100 to 1000 mg l⁻¹ (Figure 4.4 (a)). The increase of zinc transportation from root to leaf (TF) might affect the percentage of phytotoxicity (Figure 4.3). While TF of cadmium decreased from 1.52-0.60 when the cadmium concentrations were increased (Figure 4.4 (b)). The plants had TF of ~1 when treated with a lower cadmium concentration of 50 mg l⁻¹, which was the concentration point of 50% phytotoxicity. In addition, TF of cadmium decreased to TF<1 when treated with high cadmium concentrations (100 and 150 mg l⁻¹) obtaining 100% phytotoxicity.

The TF of the combined zinc and cadmium treatment are shown in figures 4.4 (c) and (d). The result indicated that cadmium affected the zinc translocation factor. TF of zinc under dual treatment with cadmium were in the range of 0.56-0.62. The TF of cadmium under the dual treatment were 0.57-0.66, which was lower than the cadmium treatment alone at 50 mg l⁻¹. TF of zinc was lower than the critical hyperaccumulator (TF >1) due to the conditions of the tissue culture system and the short period of this study (An *et al.*, 2006). However, the increase of TF at a higher zinc concentration indicated that the plant prevents the zinc becoming toxic to the root by increasing the transportation of zinc to the shoot and storage into leaf cells (Santa-Maria and Cogliatt, 1998). Kabata-Pendias and Pendias (1992) also showed that plants growing in high

levels of zinc in soil trended to translocate zinc from the roots and accumulated it in the top part of shoot. The decreased TF of cadmium at the higher concentrations might have been affected by cadmium toxicity, and the plant tried to decrease the cadmium toxicity for cadmium tolerance by reducing the translocation of cadmium from root to shoot. Many researchers also found that cadmium ions were mainly retained in the root and only small amounts were transported to the above-ground portion of the plant (Benavides *et al.*, 2005; Cataldo *et al.*, 1983; Arnetoli *et al.*, 2008). Likewise, Nishizono *et al.* (1989) and Sridhar *et al.* (2005) showed that the strategy for avoiding cadmium toxicity of plants was mainly by the accumulation of such metals at the cell wall of the root, then followed by the leaves and the stem. On the other hand, the decreasing TF of both cadmium and zinc under the dual treatment might have been due to competition between zinc and cadmium to transfer into the cells (Hart *et al.*, 2002; de la Rosa *et al.*, 2004; Bunluesin *et al.*, 2007).

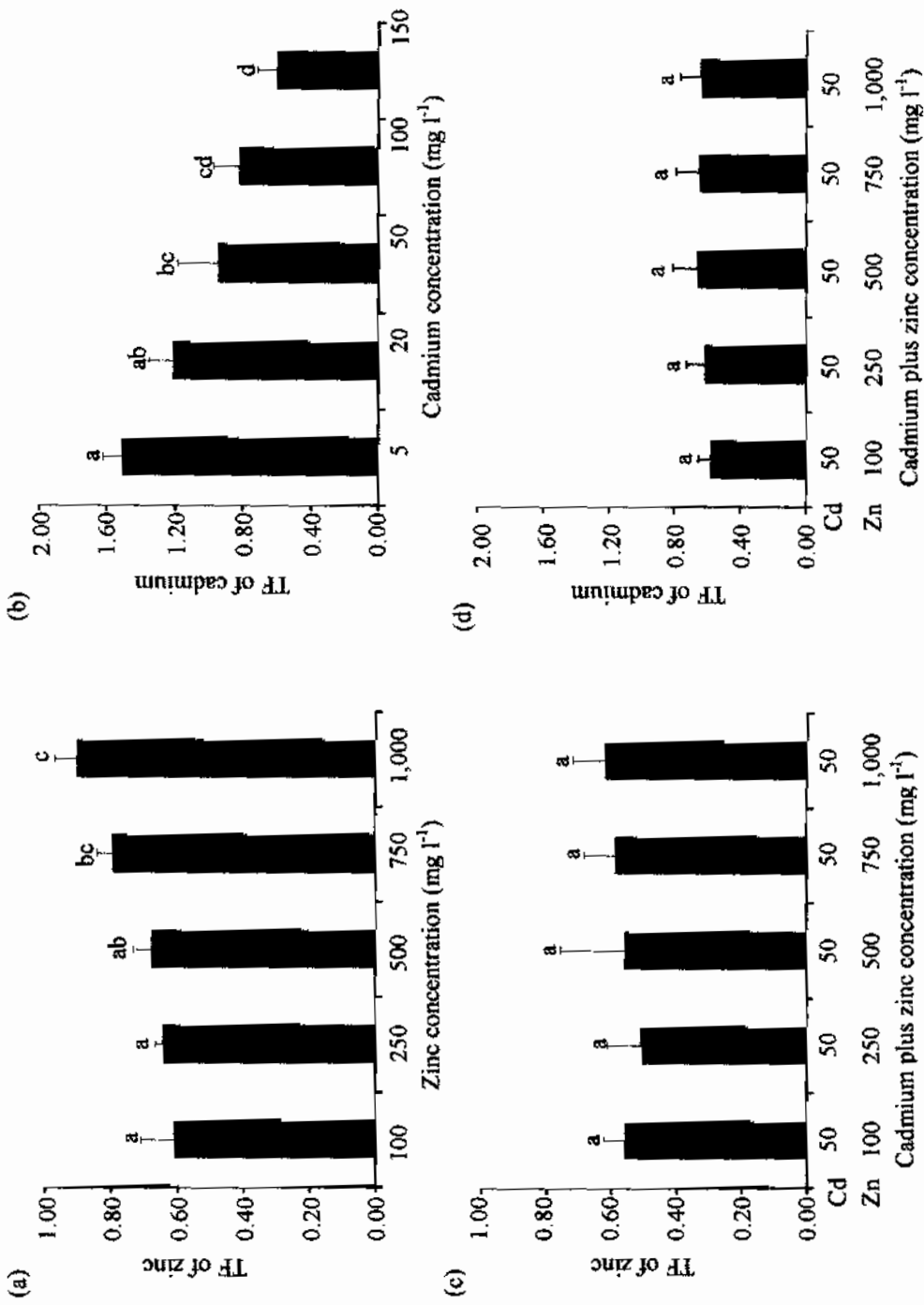


Figure 4.4 Translocation factor (TF) of *Gynura pseudochina* (L.) DC., (a) TF of zinc for zinc treatment, (b) TF of cadmium for cadmium treatment, (c) TF of zinc for cadmium and zinc treatment and (d) TF of cadmium for cadmium and zinc treatment.

4.4 Distribution of zinc and cadmium in plant tissues

The distributions of zinc and cadmium in the shoot (stem and leaves) of *G. pseudochina* (L.) DC. were examined by synchrotron base micro-XRF imaging. Figure 4.5 shows the distributions of zinc and cadmium in the cross sections of tissues from the stem and leaves. The XRF intensity normalized by the incident X-rays, that are by color scaled from red (highest intensity) to blue (lowest intensity). The micro-XRF imaging showed that zinc and cadmium were transported from root to stem and leaves. The combination of the apoplast and symplast systems probably explained the distribution of zinc and cadmium (Karley *et al.*, 2000). Figure 4.5 (a) indicated that zinc and cadmium was mostly accumulated in the cortex of the stem, especially the purple colour of the parenchyma cell containing anthocyanin. In addition, the zinc and cadmium signal in the leaf cross section (Figure 4.5 (b)) confirmed the transportation of zinc and cadmium from stem to leaves via xylem and vein; and the accumulation in the vascular bundle and epidermis. Vogel-Mikus *et al.* (2008) also reported that zinc and cadmium was accumulated in the upper and lower epidermises of the leaves for *Thlaspi praecox*. Once inside the organism, zinc and cadmium might react with several biological ligands, such as phytochelatins (PCs) (Kobayashi and Yoshimura, 2006).

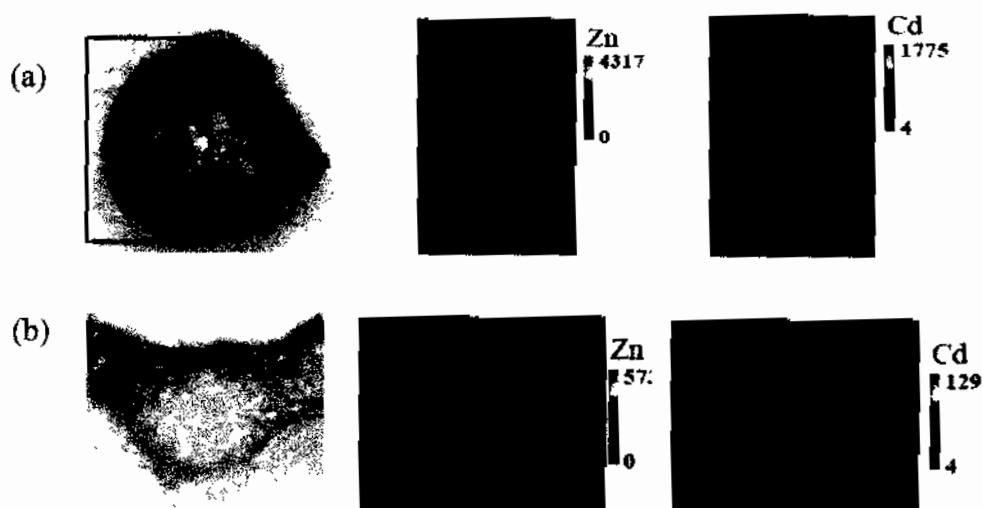


Figure 4.5 μ -XRF imaging for zinc and cadmium distribution in *Gynura pseudochina* (L.) DC.'s tissues of (a) stem, and (b) leaf. The red colour depicting elemental concentrations in each map are scaled to the maximum value for that map.

4.5 Effect of zinc and/or cadmium on protein patterns

The highest metal concentrations of $1,000 \text{ mg l}^{-1}$ for zinc, 150 mg l^{-1} for cadmium and $50/1,000 \text{ mg l}^{-1}$ for cadmium plus zinc, which resulted to 100% phytotoxicity of yellowish leaves and/or chlorosis of leaves, were used to study the effect of zinc and/or cadmium on protein expression. The protein patterns of crude protein extracted from the leaves of treated plants were separated on a 12% SDS-PAGE as shown in figure 4.6. The different protein patterns and the graphs showing average density of bands were determined by Quantity One version 4 (Bio-Rad). The intensity of the protein band at 55 kDa of the control plant gradually decreased following the cadmium and zinc combined treatment, zinc treatment, and cadmium treatment, respectively. The 31 kDa polypeptide was induced and the 29 kDa of polypeptide was decreased when the plants were separately treated with zinc or cadmium, but not in the case of combined cadmium and zinc treatment. On the other hand, the 20 kDa polypeptide and 18 kDa polypeptide were up-regulated by the cadmium treatment, whereas, the plants treated with zinc showed a slight increasing in the 12 kDa polypeptide.

The 55 kDa protein of *G. pseudochina* (L.) DC. was a similar size to Rubisco protein (55-56 kDa) that is localized in the soluble fraction of chloroplast (Demirevska *et al.*, 2008). Therefore, the toxic level of zinc and/or cadmium might cause a decrease in the level of the 55 kDa polypeptide. The 29 kDa polypeptide might be the chloroplast envelope membrane protein of the triose-P translocator (TPT), which was central for the communication between chloroplasts (Riesmeier *et al.*, 1993). The protein might be destroyed by the toxicity of the zinc and cadmium. However, the plants might increase the 31 kDa for supporting photosynthesis for plant growth. Hayden *et al.* (1986) showed that a 31 kDa polypeptide was present in the purified fraction of light-harvesting chlorophyll protein complex (LHC II), and the protein was functional in association with photosystem II. In addition, plants have responded to stress from heavy metals by up-regulating proteins (Gwozdz *et al.*, 1997). The proteins in the molecular weight range of 10 to 70 kDa were induced by cadmium stress (Prasad, 1995). The 20 kDa and 18 kDa proteins were induced when plants were treated with cadmium. Moreover, many reports have shown that metal detoxification was an important role of metalloproteins, such as heat shock protein (HSPs), metallothioneins (MTs) and phytochelatins (PCs) (Callahan *et al.*, 2006). Therefore, the protein expression pattern of *G.pseudochina* (L.) DC. under zinc and/or cadmium treatments might be due to metal detoxification proteins. The difference between protein expressions also indicated that there were different mechanisms involving protein expression for resistance to zinc and cadmium toxicity.

In addition, the distribution of metals on the specific proteins from SDS-PAGE was carried out by μ -XRF imaging to finding protein binding metals (Figures shown in the appendix). However, the distribution of the zinc bound to a protein band on the SDS-PAGE was not indicated by μ -XRF imaging, because there were many steps for protein preparation, which provoked loss of bound metals, and so there were less metal bound to the proteins. Verbi *et al.* (2005) and Laursen *et al.* (2008) reported that the zinc concentration on the proteins separated with SDS-PAGE should be more than 3 mg of zinc per 1 g of protein using μ SR-XRF and/or more than 0.1 ppm of zinc for XRF. Therefore, the result indicated that the methodologies for protein preparation in Chapter 3 might be not suitable for studying the distribution of metals on the specific proteins by μ -XRF imaging.

Consequently, the results indicated that the patterns of protein extracts from the control *G.pseudochina* (L.) DC.'s leaves were changed by induction with zinc and/or cadmium.

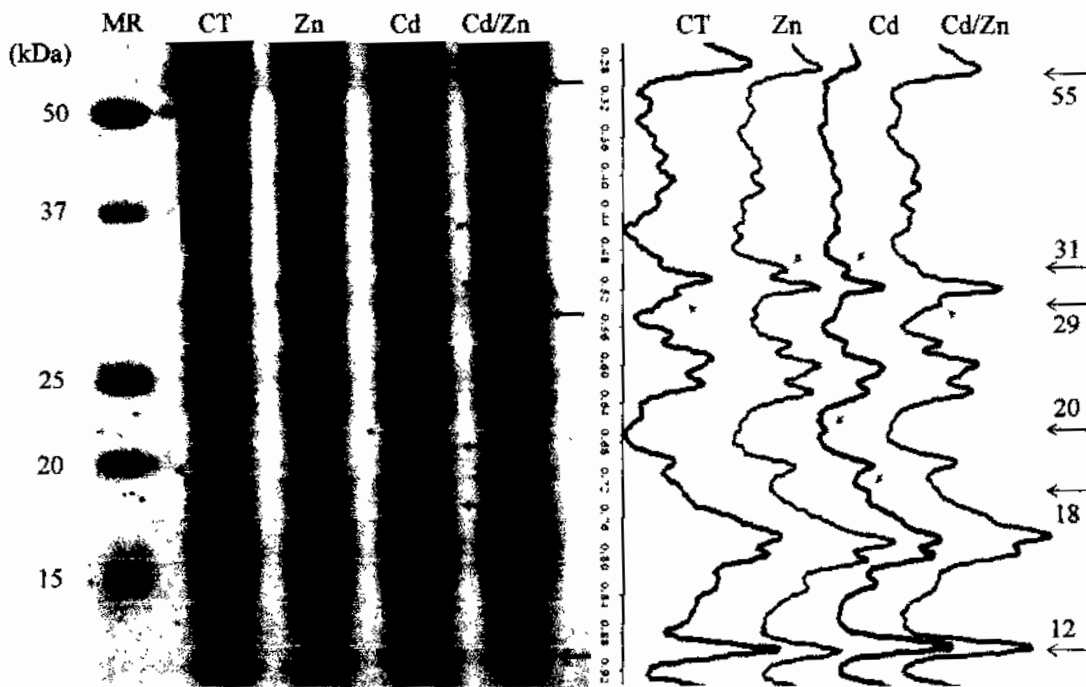


Figure 4.6 Electrophoresis on SDS polyacrylamide gel (12% w/v) of protein extracts from the leaves of *Gynura pseudochina* (L.) DC. treated with deionised water (control), and separately treated with zinc, cadmium and a combination of cadmium and zinc (Cd/Zn); (CT = control; Zn = zinc; Cd = cadmium; MR= protein marker). On the right, the colour graph shows the average density of protein bands in each lane with difference R_f , and the numbers are the induced and/or suppressed proteins.

4.6 The speciation of zinc on crude protein extracts

The speciation of zinc on crude protein extracts was studied by XAFS techniques. The XANES spectra of zinc in the samples and the zinc model compounds are shown in figure 4.7. The edge energy of zinc on the crude protein extracts of *G. pseudochina* (L.) DC. were different between the proteins extracted from the zinc treated plants (Protein-Zn) and the proteins extracted from the control plants (Protein-CT). The XANES spectrum of Protein-Zn fitted to the zinc models of Zn-Cysteine and ZnS. The fitting indicated that the coordination environment of zinc in Protein-Zn was similar to Zn-Cysteine and ZnS, therefore, zinc in the Protein-Zn might be the zinc ion (Zn^{2+}) coordinated with sulphur. In addition, the XANES spectra and fitting programs indicated that Protein-CT fitted with the zinc models of Zn-Cellulose, $Zn(NO_3)_2$, $ZnSO_4 \cdot 7H_2O$ and ZnO, in which the zinc coordinates with oxygen. However, the edge energy of ZnO shifts, which causes the differences in geometry.

The extended X-ray absorption fine structure (EXAFS) was studied to investigate the local structure of zinc on the crude protein extracts. The curve fitting of EXAFS oscillation yielded coordination number (N), inter atomic distance (R) and Debye-Waller factor (σ^2) which are shown in Table 4.2. The apparent EXAFS fitting shows that nearest neighboring atom and interatomic distances of zinc in the Protein-Zn was different from the Protein-CT. Therefore, the plants had a mechanism for defending a high zinc concentration. The EXAFS of Protein-Zn showed that the nearest neighboring atom for the first shell, Zn-S coordination shell were 1.45 (N), 2.30 Å (R) and 0.008 (σ^2). Zinc cysteine was a reference material for indication of a sulfur ligand to zinc, the N and R obtained from this experiment were similar to the Zinc-cysteine complexes that were reported by Kelly *et al.* (2002) and Straczek *et al.* (2008). However, the number of S neighboring atoms of the Protein-Zn was 1.45, which was lower than Zn-cysteine of 4.0 (N). That might due to our methodology, which used mercatoethanol in every extraction step, and the chemical might affect the sulfur ligand structure of Protein-Zn and Protein-CT. In addition, the different atomic geometries of zinc forms are four, five and six coordinate complexes by Tetrahedral, Trigonal Bipyramidal, Square Pyramidal and Octahedral, respectively (Patel *et al.*, 2007). Therefore, zinc was bound to cysteine residue by coordination with sulfur (Bracey *et al.*,

1994). In addition, Yu *et al.* (2008) reported the formation of a stable Zn tetrahedral configuration with four sulfur ligands on a protein of KTI11. Therefore, the results indicated that Zn in the Protein-Zn was coordinated with S as Zn-S in the first shell, therefore, the amino acids containing sulfur groups such as cysteine might be in the zinc binding proteins. The EXAFS of Protein-CT showed that the matches for the nearest neighboring atom for zinc in the first shell were oxygen and nitrogen, and the interatomic distances were approximately 2.10 Å. Kelly *et al.* (2002) also reported the coordination environment of zinc in the cell of *Datura innoxia* was best represented as mixed N/O ligands and 5 coordinate systems with average bond length of O/N ranging from 2.00 to 2.12 Å. Gavel *et al.* (2008) reported that zinc had 4 and 5 coordination, and mixed sulfur and nitrogen or oxygen donors. Some reports have shown that histidine can act as a tridentate ligand via its carboxylate, amine and imadazole function, and/or nicotianamine, these have alternating carboxylate and amino groups for metal complexes (Callahan *et al.*, 2006). Schmidt *et al.* (2007) showed that superoxide dismutase was a heavy metal resistance. Therefore, zinc on the Protein-CT might be represented as mixed N/O ligands obtaining from various carboxylate and amino groups. In addition, the EXAFS of zinc models in this experiment were similar to the zinc reference materials that were reported by Parsons *et al.* (2002), Numako and Nakai (1999) and Mosel *et al.* (2001).

In addition, XANES of sulfur K-edge was investigated to obtain the possible geometry structure of sulfur on Protein-Zn. The normalized XANES spectra of S K-edge in the Protein-Zn and the reference materials are shown in figure 4.8. The edge energy of sulfur on Protein-Zn and Zn-cysteine were in the same position of 2.47 keV, which indicated a relation between Protein-Zn and Zn-cysteine in coordination environment and chemical geometry. The S K-edge spectrum of Zn-cysteine had double peaks due to the chemical form of sulfur on the cysteine that occurs in two possible forms of C-S and S-S (Prange *et al.*, 2002). The spectrum of Zn-cysteine might indicate the stability of sulfur as S-S bridges oxidation form (Dauphin *et al.*, 2003; Prange *et al.*, 2003). Therefore, the chemical form of sulfur in Protein-Zn might be the disulfide state of oxidation form (S-S bridges) of cysteine. In addition, the decreasing number of sulfur ligands on the protein-Zn of *G. pseudochina* (L.) DC. might result from the disulfide bonds being cleaved by mercaptoethanol.

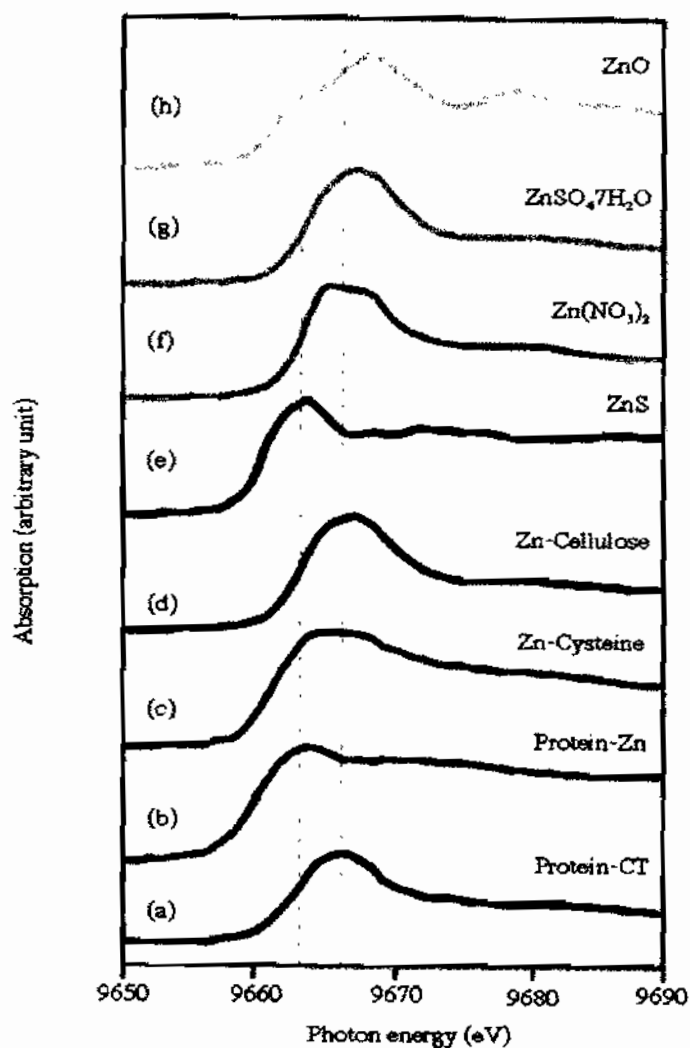


Figure 4.7 Zn K-edge XANES spectra of the protein extracted from plants treated with zinc ($1,000 \text{ mg l}^{-1}$, pH 5.5), and deionized water, and the Zn K-edge of zinc reference materials. (a) protein of control (Protein-CT), (b) protein of zinc (Protein-Zn), (c) Zn-cysteine, (d) Zn-cellulose, (e) ZnS, (f) Zn (NO_3)₂, (g) ZnSO₄·7H₂O, and (h) ZnO.

Table 4.2 EXAFS fitting of the samples and reference compounds showing the bond, coordination number (N), atomic radius R (\AA), and Debye-Waller factor (σ^2) values.

Sample	Bond	First Shell			Reference
		N	$R(\text{\AA})$	σ^2	
Protein-Zn	Zn-S	1.45	2.30	0.008	This experiment
Protein-CT	Zn-O	3.10	2.10	0.048	
	Zn-N	3.45	2.15	0.038	
Zn-Cysteine	Zn-S	4.08	2.25	0.053	This experiment
Zn-Cellulose	Zn-O	6.15	2.08	0.038	
ZnS	Zn-S	4.00	2.33	0.032	
ZnSO ₄ 7H ₂ O	Zn-O	5.00	2.05	0.029	
ZnO	Zn-O	4.03	1.99	0.024	
Zn(NO ₃) ₂	Zn-O	6.26	2.09	0.048	
Protein of Kti11 from <i>S.cerevisiae</i> S288C	Zn-S	4.000	2.310	-	Yu <i>et al.</i> , 2008
Zn-Cysteine	Zn-S	4	2.339	0.0028	Kelly <i>et al.</i> , 2002
Zn-Cysteine	Zn-S	4.5	2.35	0.007	Straczek <i>et al.</i> , 2008
Zn-Cellulose	Zn-O	6.0	2.07	0.006	
Zn(II)Sulfide	Zn-S	4	2.35	0.0026	Parsons <i>et al.</i> , 2002
Zn(NO ₃) ₂	Zn-O	6	2.090	0.079	Numako and Nakai,
ZnS	Zn-S	4	2.334	0.036	1999
ZnO	Zn-O	4	1.98	-	Mosel <i>et al.</i> , 2001

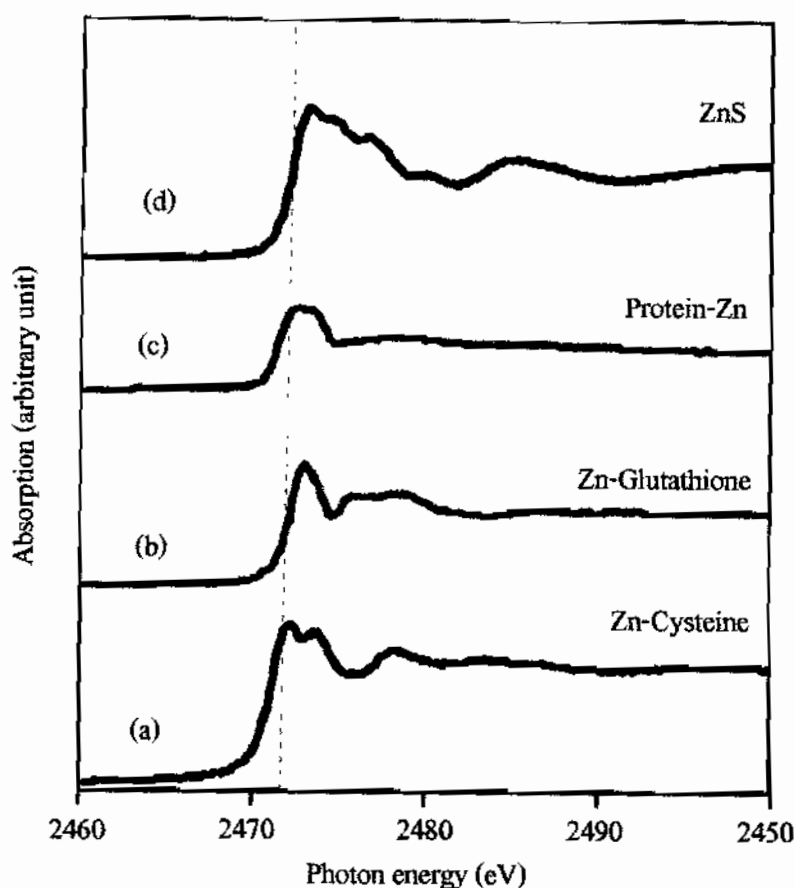


Figure 4.8 Sulfur K-edge XANES spectra of protein extracted from the plants treated with zinc ($1,000 \text{ mg l}^{-1}$, pH 5.5), (a) Zn-cysteine, (b) Zn-Glutathione, (c) the crude protein extract (Protein-Zn), and (d) ZnS.

4.7 Effect of zinc on the secondary structure of protein

FTIR spectroscopy is often used to elucidate the secondary structure of proteins (Souza *et al.*, 2008). The FTIR spectra and derivative FTIR spectra of the crude proteins extracted from the plants' leaves treated with $1,000 \text{ mg l}^{-1}$ of zinc (Zn) and untreated (control, CT) in the region of $3,900\text{-}700 \text{ cm}^{-1}$ and $1,750\text{-}950 \text{ cm}^{-1}$ are shown in figure 4.9. The spectra showed, that the positions of amide I ($1,750\text{-}1,600 \text{ cm}^{-1}$), amide II ($1,600\text{-}1,400 \text{ cm}^{-1}$) and sulfur spectrum ($1,100\text{-}950 \text{ cm}^{-1}$) exhibited no shifting upon zinc ion complex formation. Therefore, the integral interesting areas of the FTIR spectrum were produced in the same absorbance scales (Figures 4.9-4.10). The interpretation of

the results showed that zinc complex formation significantly increased the intensity of the amide I and amide II (Figure 4.10) due to direct zinc protein binding via peptide C=O and C-N ($p < 0.01$). The spectra change also suggested chemical interactions between the zinc ions and the amide groups by inducing polypeptide. Nahar and Tajmair-Riahi (1995) analyzed the protein conformational variation metal ion, and they reported an increase in intensity of FTIR at amide I and amide II, with some metals and binding was through the polypeptide group. On the other hand, zinc could decrease the values of amide I and amide II, and the primary binding was glycerol and amide site (Barone *et al.*, 2007). Our results showed that the intensity of FTIR spectra of sulfur position was decreased due to alteration of function group S=O after zinc accumulation. In addition, the curve fitting of FTIR spectra of crude proteins extracted from leaves of control and zinc treated plants based on the self-deconvolution and secondary derivative spectra (Figure 4.11 and Table 4.3) indicated a major increase in the β -sheet structure (43.85 %) of the crude protein in the presence of zinc. They showed a larger perturbation of the protein's secondary structure, which was induced by zinc ions. Goldgur *et al.* (2007) reported that the protein secondary structure of ASR1 for tomato treated with zinc gained more α -helixes and β -sheets. Consequently, these results confirmed that *G. pseudochina* (L.) DC. has a mechanism for detoxification of zinc by inducing zinc binding proteins and changing of protein secondary structure.

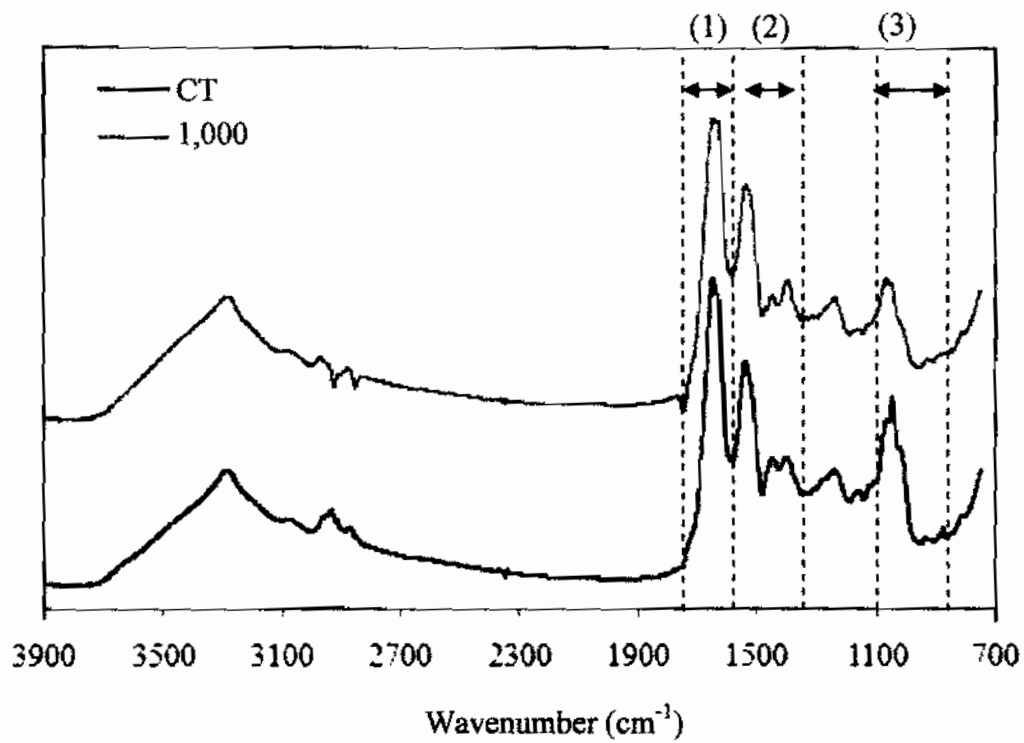


Figure 4.9 FTIR spectra of the crude proteins extracted from the leaves of zinc treated plants ($1,000 \text{ mg l}^{-1}$ of zinc) and the control plant (CT); (1)=amide I, (2)=amide II and (3) sulfur group (S=O).

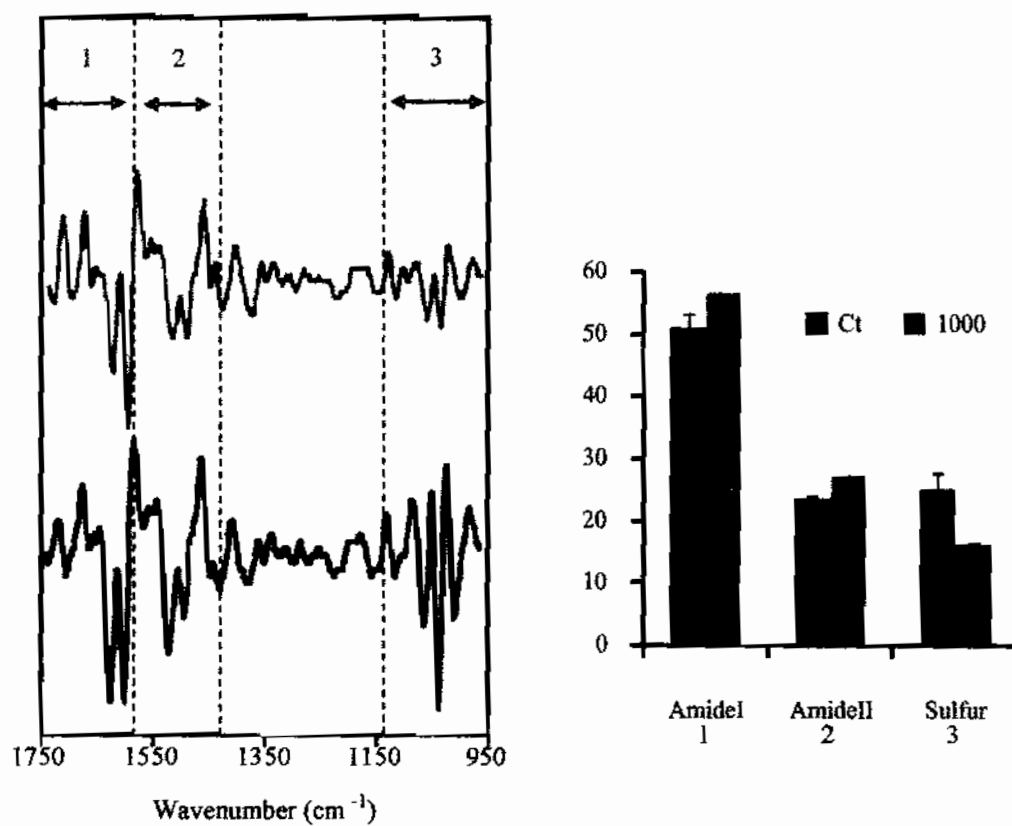


Figure 4.10 Derivatives FTIR spectra and integral areas of the crude proteins extracted from the leaves of zinc treated plants ($1,000 \text{ mg l}^{-1}$ of zinc) and the control plant (CT); (A)= derivative FTIR spectrum and (B)=integral interested areas.

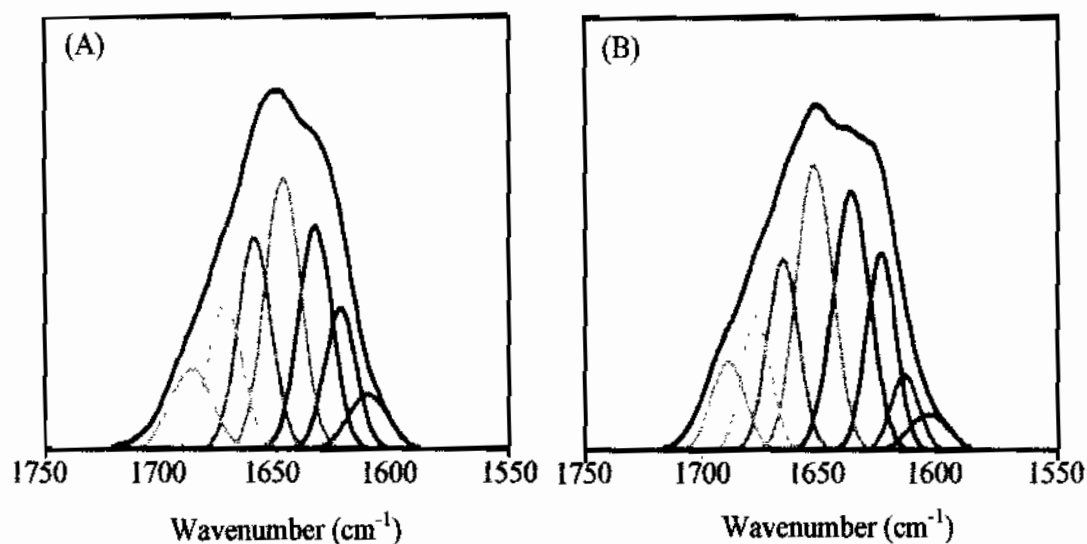


Figure 4.11 Curve-fitted and secondary structure determination of the crude proteins extracted from the leaves of zinc treated plants ($1,000 \text{ mg l}^{-1}$ of zinc) and the control plants (CT); (A) = control and (B)=zinc treatment.

Table 4.3 The relative percentages of the component structure in the crude proteins extracted from the leaves of zinc treated plants ($1,000 \text{ mg l}^{-1}$ of zinc) and the control plants.

% Component structure of protein	Range of wavenumber (cm^{-1})	Treatments	
		Control	Zinc
β -sheet	1615-1640	34.69	43.85
α -helix	1647-1660	41.06	37.69
Turn	1660-1680	12.36	9.04
Antiparallel β -sheet	1681-1692	11.89	9.42

CHAPTER 5

Conclusions and suggestions

5.1 Conclusions

In the tissue culture system, *in vitro* shoots of *G. pseudochina* (L.) DC. with one or two buds were transferred to establishment media and cultured for 28 days (4 weeks). The combination of 2 mg l⁻¹ indole-3-acetic acid (IAA) plus 2 mg l⁻¹ indole-3-butyric acid (IBA) on MS medium gave rise to the healthy plants. *G. pseudochina* (L.) DC. had the ability to tolerate and grow in high concentrations of zinc and/or cadmium. Interaction of cadmium and zinc helped reduce the adverse effect of cadmium on plant growth. The 50% level of phytotoxicity was 500 mg l⁻¹ of zinc, 60 mg l⁻¹ of cadmium and 50+32.50 mg l⁻¹ of cadmium plus zinc. *G. pseudochina* (L.) DC. showed the greatest translocation factor of zinc with high concentration, whereas cadmium was found under concentrations of the 50% phytotoxicity level. On the other hand, the combined treatment of cadmium and zinc decreased the translocation factor when compared with treatment by either cadmium or zinc alone.

G. pseudochina (L.) DC. induced changes in protein patterns for detoxification metals. Proteins with molecular weight of 12 kDa responded to zinc stress, 18 and 20 kDa responded to cadmium stress, 29 and 31 kDa responded to cadmium and zinc combination stress and 55 kDa responded to all metal stress treatments.

The curve fitting of EXAFS oscillation indicated that the chemical form of protein extracts from the leaves of control plants (Protein-CT) were different from the protein extracts from zinc treated plants (Protein-Zn). The first shell coordination of Protein-Zn was Zn-S with 1.45 (*N*) and 2.30 Å (*R*). In addition, sulfur K-edge XANES spectra of Protein-Zn corresponded to the spectra of Zn-cysteine. Therefore, cysteine, an amino acid, in the crude protein extracts might be in a group of zinc binding proteins, and it was a mechanism of zinc detoxification by *G. pseudochina* (L.) DC. In addition, toxic levels of zinc caused changes in the secondary structure of proteins by increasing the β-sheet structure and decreasing the α-helix, trans and antiparallel β-sheet structure.

5.2 Suggestions

5.2.1 The protein expression on SDS-PAGE of *G. pseudochina* (L.) DC. indicated that these protein might be protein binding metals, such as phytochelatins (PCs) and metallothioneins (MTs). However, these proteins should be studied further for classification of specific proteins by the high method of protein purification.

5.2.2 The distribution and speciation of metals on specific protein from the SDS-PAGE was studied by μ -XRF imagine in this experiment. However, we could not obtain results due to loss of bound metals during the protein extraction process. Therefore, the methodology of protein preparation should be improved and studied further.

5.2.3 The EXAFS of Protein-Zn indicated that the smaller number of sulfur in the first shell might be due to cleavage by mercaptoethanol, a reducing agent. Therefore, the effect of mercaptoethanol on the chemical form of zinc should be studied to understand the real chemical form of zinc on the crude protein.

5.2.4 This research has not investigated the chemical from of cadmium because of the detection limits of BL-8, SLRI, Thailand and BL 4A, PF, Japan. Therefore, the chemical form of cadmium on the protein should be continually studied at other synchrotron stations, to explain the mechanism of cadmium detoxification by *G. pseudochina* (L.) DC.

REFERENCES

References

- Ahsan, N., Lee, S.-H., Lee, D.-G., Lee, H., Lee, S.W., Bahk, J.D. and Lee, B.-H. (2007) Physiological and protein profiles alternation of germinating rice seedlings exposed to acute cadmium toxicity. *Comptes Rendus Biologies*, 330 (10), 735-746.
- Amersham. (1999) *Protein Purification Handbook*. Sweden, Amersham Pharmacia Biotech AB.
- An, Z.-Z., Huang, Z.-C., Lei, M., Liao, X.-Y., Zheng, Y.-M. and Chen, T.-B. (2006) Zinc tolerance and accumulation in *Pteris vittata* L. and its potential for phytoremediation of Zn- and As-contaminated soil. *Chemosphere*, 62 (5), 796-802.
- Antiochia, R., Campanella, L., Ghezzi, P. and Movassaghi, K. (2007) The use of vetiver for remediation of heavy metal soil contamination. *Analytical and Bioanalytical Chemistry*, 388 (4), 947-956.
- Arnetoli, M., Vooijs, R., Gonnelli, C., Gabbrielli, R., Verkleij, J.A.C. and Schat, H. (2008) High-level Zn and Cd tolerance in *Silene paradoxa* L. from a moderately Cd- and Zn-contaminated copper mine tailing. *Environmental Pollution*, 156 (2), 380-386.
- ATSDR [2009] *Toxicological profile for cadmium*. [Online]. Available from: <http://www.atsdr.cdc.gov/ToxProfiles/TP.asp?id=48&tid=15> [Accessed 4 th March 2011].
- Barone, J.R., Danganan, K.L. and Schmidt, W.F. (2007) Protein-transition metal ion networks. *Journal of Applied Polymer Science*, 106 (3), 1518-1525.
- Barrutia, O., Epelde, L., García-Plazaola, J.I., Garbisu, C. and Becerril, J.M. (2009) Phytoextraction potential of two *Rumex acetosa* L. accessions collected from metalliferous and non-metalliferous sites: Effect of fertilization. *Chemosphere*, 74 (2), 259-264.
- Becker, M.J., Caldwell, G.A. and Zachgo, E.A. (1996) *Biotechnology a laboratory course*. 2nd edition. New York, Academic Press.
- Benavides, M., Gallego, S.M. and Tomaro, M.L. (2005) Cadmium toxicity in plants. *Brazilian Journal of Plant Physiology*, 17 (1), 21-34.
- Bollag, D.M., Rozycki, M.D. and Edelstein, S.J. (1996) *Protein Methods*. 2 nd edition. United state of America, Wiley-Liss.
- Bracey, M.H., Christiansen, J., Tovar, P., Cramer, S.P. and Bartlett, S.G. (1994) Spinach Carbonic Anhydrase: Investigation of the Zinc-Binding Ligands by Site-Directed Mutagenesis, Elemental Analysis, and EXAFS. *Biochemistry*, 33 (44), 13126-13131.

- Bradford, M.M. (1976) A rapid and sensitive method for the quantitation of microgram quantities of protein utilizing the principle of protein-dye binding. *Analytical Biochemistry*, 12, 248-254.
- Broadley, M.R., White, P.J., Hammond, J.P., Zelko, I. and Lux, A. (2007) Zinc in plants. *New Phytologist*, 173 (4), 677-702.
- Bunluesin, S., Pokethitiyook, P., Lanza, G., Tyson, J., Kruatrachue, M., Xing, B. and Upatham, S. (2007) Influences of Cadmium and Zinc Interaction and Humic Acid on Metal Accumulation in *Ceratophyllum Demersum*. *Water, Air, & Soil Pollution*, 180 (1), 225-235.
- Buxbaum, E. (2007) *Fundamental of protein structure and function*. New York, Springer Science+Business Media Inc.
- Calabrese, E.J. and Blain, R.B. (2009) Hormesis and plant biology. *Environmental Pollution*, 157 (1), 42-48.
- Callahan, D., Baker, A., Kolev, S. and Wedd, A. (2006) Metal ion ligands in hyperaccumulating plants. *Journal of Biological Inorganic Chemistry*, 11 (1), 2-12.
- Cataldo, D.A., Garland, T.R. and Wildung, R.E. (1983) Cadmium Uptake Kinetics in Intact Soybean Plants. *Plant Physiology*, 73 (3), 844-848.
- Chakravarty, B. and Srivastava, S. (1997) Effect of cadmium and zinc interaction on metal uptake and regeneration of tolerant plants in linseed. *Agriculture, Ecosystems & Environment*, 61 (1), 45-50.
- Clemens, S., Kim, E.J., Neumann, D. and Schroeder, J.I. (1999) Tolerance to toxic metals by a gene family of phytochelatin synthases from plants and yeast. *The EMBO Journal*, 18 (12), 3325-3333.
- Cobbett, C. and Goldsbrough, P. (2002) PHYTOCHELATINS AND METALLOTHIONEINS: Roles in Heavy Metal Detoxification and Homeostasis. *Annual Review of Plant Biology*, 53 (1), 159-182.
- Cuenca, S., Amo-Marco, J.B. and Parra, R. (1999) Micropropagation from inflorescence stems of the Spanish endemic plant *Centaurea paui* Loscos ex Willk. (Compositae). *Plant Cell Reports*, 18 (7), 674-679.
- Daniels, W.M.U., Hendricks, J., Salie, R. and van Rensburg, S.J. (2004) A Mechanism for Zinc Toxicity in Neuroblastoma Cells. *Metabolic Brain Disease*, 19 (1), 79-88.

- Dauphin, Y., Cuif, J.-P., Doucet, J., Salomé, M., Susini, J. and Terry Willams, C. (2003) In situ chemical speciation of sulfur in calcitic biominerals and the simple prism concept. *Journal of Structural Biology*, 142 (2), 272-280.
- David, R.L. (2006) *CRC Handbook of Chemistry and Physics*. Boca Raton, Florida, CRC Press.
- De la Rosa, G., Peralta-Videa, J.R., Montes, M., Parsons, J.G., Cano-Aguilera, I. and Gardea-Torresdey, J.L. (2004) Cadmium uptake and translocation in tumbleweed (*Salsola kali*), a potential Cd-hyperaccumulator desert plant species: ICP/OES and XAS studies. *Chemosphere*, 55 (9), 1159-1168.
- Demirevska, K., Simova-Stoilova, L., Vassileva, V. and Feller, U. (2008) Rubisco and some chaperone protein responses to water stress and rewatering at early seedling growth of drought sensitive and tolerant wheat varieties. *Plant Growth Regulation*, 56 (2), 97-106.
- Escarre, J., Lefebvre, C., Gruber, W., Leblanc, M., Lepart, J., Riviere, Y. and Delay, B. (2000) Zinc and cadmium hyperaccumulation by *Thlaspi caerulescens* from metalliferous and nonmetalliferous sites in the Mediterranean area: implications for phytoremediation. *New Phytologist*, 145 (3), 429-437.
- Fosmire, G.J. (1990) Zinc toxicity. *American Journal of Clinical Nutrition*, 51 (2), 225-227.
- Fraser, K.A., Long, H.A., Candlin, R. and Harding, M.M. (1965) The structures of bishistidinonickel(II), -cobalt(II), and -cadmium(II). *Chemical Communications (London)*, (15), 344-345.
- Gallagher, W. [2011] *FTIR Analysis of Protein Structure*. [Online]. Available from: http://www.chem.uwec.edu/Chem455_S05/.../FTIR_of_proteins.pdf [Accessed 4th March 2011].
- Gao, Y., Chen, C., Zhang, P., Chai, Z., He, W. and Huang, Y. (2003) Detection of metalloproteins in human liver cytosol by synchrotron radiation X-ray fluorescence after sodium dodecyl sulphate polyacrylamide gel electrophoresis. *Analytica Chimica Acta*, 485 (1), 131-137.
- Gardea-Torresdey, J.L., Peralta-Videa, J.R., de la Rosa, G. and Parsons, J.G. (2005) Phytoremediation of heavy metals and study of the metal coordination by X-ray absorption spectroscopy. *Coordination Chemistry Reviews*, 249 (17-18), 1797-1810.

- Gavel, O.Y., Bursakov, S.A., Rocco, G.D., Trinclo, J., Pickering, I.J., George, G.N., Calvete, J.J., Shnyrov, V.L., Brondino, C.D., Pereira, A.S., Lampreia, J., Tavares, P., Moura, J.J.G. and Moura, I. (2008) A new type of metal-binding site in cobalt- and zinc-containing adenylate kinases isolated from sulfate-reducers *Desulfovibrio gigas* and *Desulfovibrio desulfuricans* ATCC 27774. *Journal of Inorganic Biochemistry*, 102 (5-6), 1380-1395.
- Gibthai [2011] *SDS-PAGE*. [Online]. Available from: http://www.gibthai.com/services/technical_detail.php?ID=21&page=5 [Accessed 4 th March 2011].
- Goldgur, Y., Rom, S., Ghirlando, R., Shkolnik, D., Shadrin, N., Konrad, Z. and Bar-Zvi, D. (2007) Desiccation and Zinc Binding Induce Transition of Tomato Abscisic Acid Stress Ripening 1, a Water Stress- and Salt Stress-Regulated Plant-Specific Protein, from Unfolded to Folded State. *Plant Physiology*, 143 (2), 617-628.
- Gwóźdz, E., Przymusiński, R., Rucińska, R. and Deckert, J. (1997) Plant cell responses to heavy metals: molecular and physiological aspects. *Acta Physiologiae Plantarum*, 19 (4), 459-465.
- Hall, J.L. (2002) Cellular mechanisms for heavy metal detoxification and tolerance. *Journal of Experimental Botany*, 53 (366), 1-11.
- Hart, J.J., Welch, R.M., Norvell, W.A. and Kochian, L.V. (2002) Transport interactions between cadmium and zinc in roots of bread and durum wheat seedlings. *Physiologia Plantarum*, 116 (1), 73-78.
- Hayden, D.B., Baker, N.R., Percival, M.P. and Beckwith, P.B. (1986) Modification of the Photosystem II light-harvesting chlorophyll a/b protein complex in maize during chill-induced photoinhibition. *Biochimica et Biophysica Acta (BBA) - Bioenergetics*, 851 (1), 86-92.
- Heiss, S., Wachter, A., Bogs, J., Cobbett, C. and Rausch, T. (2003) Phytochelatin synthase (PCs) protein is induced in *Brassica juncea* leaves after prolonged Cd exposure *Journal of Experimental Botany*, 54, 1833-1839.
- Hoagland, D.R. and Arnon, D.I. (1950) *The water culture method for growing plants without soil*. Berkley: University of California.
- Holleman, A.F., Wiberg, E. and Wiberg, N. (1985) *Lehrbuch der Anorganischen Chemie*. German, Walter de Gruyter.

- Kabata-Pendias, A. and Pendias, H. (1992) *Trace Element in Soils and Plant*. Florida, CRC Press Inc.
- Karley, A.J., Leigh, R.A. and Sanders, D. (2000) Where do all the ions go? The cellular basis of differential ion accumulation in leaf cells. *Trends in Plant Science*, 5 (11), 465-470.
- Kelly, R.A., Andrews, J.C. and DeWitt, J.G. (2002) An X-ray absorption spectroscopic investigation of the nature of the zinc complex accumulated in *Datura innoxia* plant tissue culture. *Microchemical Journal*, 71 (2-3), 231-245.
- Kobayashi, R. and Yoshimura, E. (2006) Differences in the binding modes of phytochelatin to cadmium (II) and Zinc (II) ions. *Biological Trace Element Research*, 114 (1), 313-318
- Kramer, U., Cotter-Howells, J.D., Charnock, J.M., Baker, A.J.M. and Smith, J.A.C. (1996) Free histidine as a metal chelator in plants that accumulate nickel. *Nature*, 379 (6566), 635-638.
- Kruger, C., Berkowitz, O., Stephan, U.W. and Hell, R. (2002) A Metal-binding Member of the Late Embryogenesis Abundant Protein Family Transports Iron in the Phloem of *Ricinus communis* L. *THE JOURNAL OF BIOLOGICAL CHEMISTRY*, 277 (28), 25062-25069.
- Laursen, K., Adamsen, C.E., Laursen, J., Olsen, K. and Moller, J.K.S. (2008) Quantification of zinc-porphyrin in dry-cured ham products by spectroscopic methods: Comparison of absorption, fluorescence and X-ray fluorescence spectroscopy. *Meat Science*, 78 (3), 336-341.
- McGrath, S.P. and Zhao, F.-J. (2003) Phytoextraction of metals and metalloids from contaminated soils. *Current Opinion in Biotechnology*, 14 (3), 277-282.
- Memon, A.R., Aktoprakligul, D., Aylin Zdemur and Verti, A. (2001) Heavy Metal Accumulation and Detoxification Mechanisms in Plants. *Turkish Journal of Botany*, 25 (3), 111-121.
- Miller, R.O. (1998) Nitric-Perchloric acid wet digestion in an open vessel. in: Kalra, Y. P. (eds.) *In Reference Methods for Plant Analysis*. Florida, CRC Press.
- Minorsky, P.V. and Colledge, M. (2005) On the Inside Jasmonic Acid and the Establishment of *Arbuscular Mycorrhizae*. *Plant Physiology*, 139, 1097-1098
- Mosel, G., Hübert, T., Nofz, M., Brenneis, R., Köcher, P. and Kley, G. (2001) Zn-K EXAFS investigations on ZnS/ZnO containing vitrified ashes from municipal incinerator facilities. *Journal of Materials Science*, 36 (20), 5017-5025.

- Murashige, T. and Skoog, F. (1962) A revised medium for rapid growth and bioassays with tobacco tissue cultures. *Physiology Plant*, 15, 473-497.
- Nahar, S. and Tajmir-Riahi, H.A. (1995) Do metal ions alter the protein secondary structure of a light-harvesting complex of thylakoid membranes? *Journal of Inorganic Biochemistry*, 58 (3), 223-234.
- Nakbanpote, W., Panitlertumpai, N., Sukadeetad, K., Meesungneoe, O. and Noisanguan, W. (2010) Advances in Phytoremediation Research: A Case Study of *Gynura pseudochina* (L.) DC. in: Fürstner, I. (eds.) *Advanced Knowledge Application in Practice*. India, Sciyo Press.
- Natoli, C.R., Benfatto, M., Della Longa, S. and Hatada, K. (2003) X-ray absorption spectroscopy: state-of-the-art analysis. *Journal of Synchrotron Radiation*, 10 (1), 26-42.
- Nishizono, H., Kubota, K., Suzuki, S. and Ishii, F. (1989) Accumulation of Heavy Metals in Cell Walls of *Polygonum cuspidatum* Roots from Metalliferous Habitats. *Plant and cell Physiology*, 30 (4), 595-598.
- Nordberg, G.F., Kjellstrom, T. and M., N. (1985) Kinetics and metabolism. in: Friberg, L., Elinder, C. G., Kjellstrom, T. and Nordberg, G. F. (eds.) *Cadmium and Health: A toxicological and epidemiological appraisal*. Boca Raton, CRC Press.
- Numako, C. and Nakai, I. (1999) XAFS analysis of coprecipitation of zinc by sulfide ions in an acidic solution. *Spectrochimica Acta Part B: Atomic Spectroscopy*, 54 (1), 133-141.
- Panitlertumpai, N., Nakbanpote, W., Thiravetyan, P. and Surarungchai, W. (2003) The exploration of zinc-hyperaccumulative plants from mining area of Tak province in Thailand: in - (eds.). *29 th Congress on Science and Technology of Thailand*, 20-22 October, Khon Kean, Khon Kaen University, Thailand.
- Parsons, J.G., Hejazi, M., Tiemann, K.J., Henning, J. and Gardea-Torresdey, J.L. (2002) An XAS study of the binding of copper(II), zinc(II), chromium(III) and chromium(VI) to hops biomass. *Microchemical Journal*, 71 (2-3), 211-219.
- Patel, K., Kumar, A. and Durani, S. (2007) Analysis of the structural consensus of the zinc coordination centers of metalloprotein structures. *Biochimica et Biophysica Acta*, 1774 (10), 1247-1253.
- Peer, W.A., Baxter, I.R., Richards, E.L., Freeman, J.L. and Murphy, A.S. (2005) Phytoremediation and hyperaccumulator plants. *Topics in Current Genetics*, 14, 299-340.

- Penner-Hahn, J.E. (2005) Characterization of "spectroscopically quiet" metals in biology. *Coordination Chemistry Reviews*, 249 (1-2), 161-177.
- Phaenark, C., Pokethitiyook, P., Kruatrachue, M. and Ngernsansaruay, C. (2009) Cd and Zn accumulation in plants from the Padaeng zinc mine area. *International Journal of Phytoremediation*, 11 (5), 479 - 495.
- Prange, A., Dahl, C., Truper, H.G., Behnke, M., Hahn, J., Modrow, H. and Hormes, J. (2002) Investigation of S-H bonds in biologically important compounds by sulfur K-edge X-ray absorption spectroscopy. *The European Physical Journal D*, 20 (3), 589-596.
- Prange, A., Birzele, B., Kramer, J., Modrow, H., Chauvistre, R., Hormes, J. and Kohler, P. (2003) Characterization of Sulfur Speciation in Low Molecular Weight Subunits of Glutenin after Reoxidation with Potassium Iodate and Potassium Bromate at Different pH Values Using X-ray Absorption Near-Edge Structure (XANES) Spectroscopy. *Journal of Agricultural and Food Chemistry*, 51 (25), 7431-7438.
- Prasad, M.N.V. (1995) Cadmium toxicity and tolerance in vascular plants. *Environmental and Experimental Botany*, 35 (4), 525-545.
- Raskin, I., Smith, R.D. and Salt, D.E. (1997) Phytoremediation of metals: using plants to remove pollutants from the environment. *Current Opinion in Biotechnology*, 8 (2), 221-226.
- Rausser, W.E. (1990) Phytochelatins. *Annual Review of Plant Biochemistry*, 59 (1), 61-86.
- Rehm, H. (2006) *Protein Biochemistry and Proteomics*. California, Academic Press.
- Riesmeier, J.W., Flugge, U.I., Schulz, B., Heineke, D., Heldt, H.W., Willmitzer, L. and Frommer, W.B. (1993) Antisense repression of the chloroplast triose phosphate translocator affects carbon partitioning in transgenic potato plants. *Proceedings of the National Academy of Sciences USA*, 90 (13), 6160-6164.
- Salt, D.E., Smith, R.D. and Raskin, I. (1998) PHYTOREMEDIATION. *Annual Review of Plant Physiology and Plant Molecular Biology*, 49 (1), 643-668.
- Salt, D.E., Prince, R.C., Pickering, I.J. and Raskin, I. (1995) Mechanisms of Cadmium Mobility and Accumulation in Indian Mustard. *Plant Physiology*, 109 (4), 1427-1433.
- Sangdee, A., Sirithorn, P. and Thummabenjapone, P. (2000) Virus and Viroid Causal Agent(s) of Bunchy Top and Severe Necrosis of Tomato. *Khon Kaen Agricultural Journal*, 31(3), 161-170.
- Santa-Marla, G.E. and Cogliatti, D.H. (1998) The regulation of zinc uptake in wheat plants. *Plant Science*, 137 (1), 1-12.

- Schmidt, A., Schmidt, A., Haferburg, G. and Kothe, E. (2007) Superoxide dismutases of heavy metal resistant streptomycetes. *Journal of Basic Microbiology*, 47 (1), 56-62.
- Si, D., Yang, L., Yan, H. and Wang, Q. (2009) Bioaccumulation and transformation of cadmium by *Phaeodactylum tricornutum*. *Science in China Series B: Chemistry*, 52 (12), 2373-2380.
- Sobkowiak, R. and Deckert, J. (2006) Proteins induced by cadmium in soybean cells. *Journal of Plant Physiology*, 163 (11), 1203-1206.
- Souza, L., Devi, P., M.P, D.S. and Naik, C.G. (2008) Use of Fourier Transform Infrared (FTIR) Spectroscopy to Study Cadmium-Induced Changes in *Padina Tetrastromatica* (Hauck). *Analytical Chemistry Insights*, 2008, 135.
- Sridhar, B.B.M., Diehl, S.V., Han, F.X., Monts, D.L. and Su, Y. (2005) Anatomical changes due to uptake and accumulation of Zn and Cd in Indian mustard (*Brassica juncea*). *Environmental and Experimental Botany*, 54 (2), 131-141.
- Straczek, A., Sarret, G., Manceau, A., Hinsinger, P., Geoffroy, N. and Jaillard, B. (2008) Zinc distribution and speciation in roots of various genotypes of tobacco exposed to Zn. *Environmental and Experimental Botany*, 63 (1-3), 80-90.
- Thomine, S., Wang, R., Ward, J.M., Crawford, N.M. and Schroeder, J.I. (2000) Cadmium and iron transport by members of a plant metal transporter family in *Arabidopsis* with homology to *Nramp* genes. *PNAS*, 97 (9), 4991-4996.
- van Keulen, H., Wei, R. and Cutright, T.J. (2008) Arsenate-induced expression of a class III chitinase in the dwarf sunflower *Helianthus annuus*. *Environmental and Experimental Botany*, 63 (1-3), 281-288.
- Verbi, F.M., Arruda, S.C.C., Rodriguez, A.P.M., Prez, C.A. and Arruda, M.A.Z. (2005) Metal-binding proteins scanning and determination by combining gel electrophoresis, synchrotron radiation X-ray fluorescence and atomic spectrometry. *Journal of Biochemical and Biophysical Methods*, 62 (2), 97-109.
- Vogel-Mikus, K., Simic, J., Pelicon, P., Budnar, M., Kump, P., Necemer, M., Mesjasz-Przybylowicz, J., Przybylowicz, W.J. and Regvar, M. (2008) Comparison of essential and non-essential element distribution in leaves of the Cd/Zn hyperaccumulator *Thlaspi praecox* as revealed by micro-PIXE. *Plant, Cell and Environment*, 31 (10), 1484-1496.

- Weseloh, G., Kühbacher, M., Bertelsmann, H., Özaslan, M., Kyriakopoulos, A. and Knöchel, A. (2004) Analysis of metal-containing proteins by gel electrophoresis and synchrotron radiation X-ray fluorescence. *Journal of Radioanalytical and Nuclear Chemistry*, 259 (3), 473-477.
- Wikipedia [2011] *Sodium lauryl sulfate*. [Online]. Available from: http://en.wikipedia.org/wiki/Sodium_lauryl_sulfate [Accessed 4 th March 2011].
- Yadav, S.K., Juwarkar, A.A., Kumar, G.P., Thawale, P.R., Singh, S.K. and Chakrabarti, T. (2009) Bioaccumulation and phyto-translocation of arsenic, chromium and zinc by *Jatropha curcas* L.: Impact of dairy sludge and biofertilizer. *Bioresource Technology*, 100 (20), 4616-4622.
- Yang, X., Feng, Y., He, Z. and Stoffella, P.J. (2005) Molecular mechanisms of heavy metal hyperaccumulation and phytoremediation. *Journal of Trace Elements in Medicine and Biology*, 18 (4), 339-353.
- Yoshida, N., Ishii, K., Okuno, T. and Tanaka, K. (2006) Purification and Characterization of Cadmium-Binding Protein from Unicellular Alga *Chlorella sorokinian*. *Current Microbiology*, 52 (6), 460-463.
- Young, R.A. (1991) Toxicity summary for cadmium: in *the U.S. Department of Energy (DOE)* (eds.). *The Risk Assessment Information System*, University of Tennessee. Contract No. DE-AC05-84OR21400.
- Yu, M., Yang, F., Chu, W., Wang, Y., Zhao, H., Gao, B., Zhao, W., Sun, J., Wu, F., Zhang, X., Shi, Y. and Wu, Z. (2008) 3D local structure around Zn in Kti11p as a representative Zn-(Cys)₄ motif as obtained by MXAN. *Biochemical and Biophysical Research Communications*, 374 (1), 28-32.

APPENDIXES

Appendix A
Plant growth

Table A-1 Percent dry weight of *Gynura pseudochina* (L.) DC. exposed to difference concentrations of zinc for 2 weeks.

Concentrations (mg l ⁻¹)	% biomass
0	100.00 ± 0.00 ^a
100	108.59 ± 8.96 ^a
250	127.16 ± 7.15 ^c
500	125.45 ± 9.08 ^{bc}
750	111.10 ± 10.69 ^{ab}
1,000	100.68 ± 2.64 ^a

Table A-2 Percent dry weight of *Gynura pseudochina* (L.) DC. exposed to different concentrations of cadmium for 2 weeks.

Concentrations (mg l ⁻¹)	% biomass
0	100.00 ± 0.00 ^a
5	103.69 ± 29.27 ^a
20	64.89 ± 10.06 ^b
50	58.61 ± 5.76 ^b
100	61.78 ± 6.92 ^b
150	51.79 ± 7.39 ^b

Table A-3 Percent dry weight of *Gynura pseudochina* (L.) DC. exposed to difference concentrations of cadmium and zinc combination for 2 weeks.

Concentrations (mg l ⁻¹)	% biomass
0	100.00 ± 0.00 ^{ab}
50+0	58.61 ± 5.76 ^b
50+100	111.99 ± 32.23 ^a
50+250	123.86 ± 23.85 ^a
50+500	128.94 ± 20.25 ^a
50+750	122.87 ± 6.93 ^a
50+1,000	111.99 ± 32.23 ^a

Table A-4 Percent survival of *Gynura pseudochina* (L.) DC. exposed to difference concentrations of zinc and cadmium alone and the combination of cadmium and zinc for 2 weeks.

Zinc		Cadmium		Cadmium plus zinc	
Conc.	%Survival	Conc.	%Survival	Conc.	%Survival
0	0	0	0	50+0	38
100	0	5	0	50+100	63
250	0	20	25	50+250	75
500	50	50	38	50+500	100
750	63	100	100	50+750	100
1,000	100	150	100	50+1,000	100

Appendix B
Metals accumulation in plants

Table B-1 Concentration of metals in leaves of plants (mg kg^{-1} dry weight)
(Ruskin and Ensley, 2000)

Element	Low	Normal	High
Ca	800	3000-30000	60000
Mg	400	1000-6000	10000
K	1000	5000-20000	50000
Na	400	1000-4000	10000 ^a
P	300	800-3000	5000
Fe	10	60-600	2500 ^b
Mn	5	20-400	2000
Zn	5	20-400	2000
Cd	0.03	0.1-3	20
Pb	0.01	0.1-5	100
Ni	0.2	1-10	100
Co	0.01	0.03-2	20
Cr	0.05	0.2-5	50
Cu	1	5-25	100
Se	0.01	0.01-1	10

^a Sodium levels in some maritime and salt-marsh plants can reach $60,000 \text{ mg kg}^{-1}$

^b Iron levels in a few species can be up to $35,000 \text{ mg kg}^{-1}$

Table B-2 Zinc and cadmium accumulation (averages \pm SD; n=5) in *Gynura pseudochina* (L.) DC. exposed to difference concentrations of zinc and cadmium and translocation factors (n=5).

Treatment	Concentrations (mg l ⁻¹)	Metal content in plants (mg g ⁻¹)		Translocation Factor (TF)
		Root	Shoot	
Zn	0	0.605 \pm 0.179	0.388 \pm 0.127	-
	100	1.708 \pm 0.297	1.059 \pm 0.306	0.613 \pm 0.098 ^a
	250	2.632 \pm 0.291	1.691 \pm 0.161	0.644 \pm 0.023 ^a
	500	5.076 \pm 0.494	3.437 \pm 0.341	0.679 \pm 0.055 ^{ab}
	750	6.240 \pm 0.886	4.960 \pm 0.783	0.795 \pm 0.049 ^{bc}
	1,000	7.293 \pm 0.597	6.614 \pm 0.995	0.903 \pm 0.068 ^c
Cd	0	-	-	-
	5	0.042 \pm 0.004	0.063 \pm 0.009	1.515 \pm 0.108 ^a
	20	0.141 \pm 0.014	0.170 \pm 0.019	1.213 \pm 0.146 ^b
	50	0.286 \pm 0.051	0.266 \pm 0.063	0.949 \pm 0.238 ^{bc}
	100	0.711 \pm 0.081	0.584 \pm 0.121	0.823 \pm 0.152 ^{cd}
	150	0.911 \pm 0.265	0.534 \pm 0.138	0.596 \pm 0.117 ^d

Table B-3 Zinc and cadmium accumulation (averages \pm SD; n=5) in *Gynura pseudochina* (L.) DC. exposed to difference concentrations of cadmium and zinc combination and translocation factors (n=5).

Treatment	Concentrations (mg l ⁻¹)	Metal content in plants (mg g ⁻¹)		Translocation Factor (TF)
		Root	Shoot	
Zn	50/100	1.706 \pm 0.254	0.950 \pm 0.174	0.558 \pm 0.067 ^a
	50/250	2.255 \pm 0.296	1.137 \pm 0.186	0.511 \pm 0.101 ^a
	50/500	3.009 \pm 0.492	1.623 \pm 0.316	0.560 \pm 0.194 ^a
	50/750	4.571 \pm 1.114	2.630 \pm 0.473	0.588 \pm 0.096 ^a
	50/1,000	5.675 \pm 1.209	3.579 \pm 1.057	0.619 \pm 0.098 ^a
Cd	50/100	0.447 \pm 0.040	0.257 \pm 0.053	0.572 \pm 0.086 ^a
	50/250	0.433 \pm 0.050	0.264 \pm 0.047	0.613 \pm 0.114 ^a
	50/500	0.333 \pm 0.052	0.215 \pm 0.036	0.660 \pm 0.154 ^a
	50/750	0.394 \pm 0.089	0.249 \pm 0.056	0.648 \pm 0.141 ^a
	50/1,000	0.426 \pm 0.090	0.263 \pm 0.036	0.637 \pm 0.125 ^a

Appendix C
SPSS

Table C-1 Percent dry weight of *Gynura pseudochina* (L.) DC. exposed to difference concentrations of zinc.

	SS	df	MS	F	p
Between Groups	2996.762	5	599.352	10.779	0.000
Within Groups	1056.442	19	55.602		
Total	4053.204	24			

Table C-2 Percent dry weight of *Gynura pseudochina* (L.) DC. exposed to difference concentrations of cadmium.

	SS	df	MS	F	p
Between Groups	11192.284	5	2238.457	10.965	0.000
Within Groups	4287.150	21	204.150		
Total	15479.434	26			

Table C-3 Percent dry weight of *Gynura pseudochina* (L.) DC. exposed to difference concentrations of cadmium and zinc combination.

	SS	df	MS	F	p
Between Groups	14190.427	6	2365.071	5.296	0.002
Within Groups	9825.013	22	446.592		
Total	24015.440	28			

Table C-4 Translocation factor of *Gynura pseudochina* (L.) DC. exposed to difference concentrations of zinc.

	SS	df	MS	F	p
Between Groups	0.213	4	0.053	14.191	0.000
Within Groups	0.053	14	0.004		
Total	0.265	18			

Table C-5 Translocation factor of *Gynura pseudochina* (L.) DC. exposed to difference concentrations of cadmium.

	SS	df	MS	F	p
Between Groups	2.344	4	0.586	22.677	0.000
Within Groups	0.491	19	0.026		
Total	2.835	23			

Table C-6 Translocation factor of *Gynura pseudochina* (L.) DC. exposed to difference concentrations of cadmium and zinc combination for zinc.

	SS	df	MS	F	p
Between Groups	0.039	4	0.010	0.670	0.618
Within Groups	0.406	28	0.015		
Total	0.445	32			

Table C-7 Translocation factor of *Gynura pseudochina* (L.) DC. exposed to difference concentrations of cadmium and zinc combination for cadmium.

	SS	df	MS	F	p
Between Groups	0.034	4	0.008	0.528	0.716
Within Groups	0.448	28	0.016		
Total	0.482	32			

Table C-8 Comparing a percent dry weight of *Gynura pseudochina* (L.) DC. exposed to difference concentrations of zinc.

Conc.	Conc.	CT	100	250	500	750	1000
Mean	100.000	100.000	108.589	127.162	125.449	111.101	100.679
CT	100.000	-	0.094	0.000*	0.000*	0.036	0.890
100	108.589	-	-	0.003*	0.003*	0.609	0.121
250	127.162	-	-	-	0.930	0.008*	0.000*
500	125.449	-	-	-	-	0.009*	0.000*
750	111.101	-	-	-	-	-	0.047

P<0.01;

Conc. = Concentration

Table C-9 Comparing a percent dry weight of *Gynura pseudochina* (L.) DC. exposed to difference concentrations of cadmium.

	Conc.	CT	5	20	50	100	150
Conc.	Mean	100.000	103.687	64.890	58.612	61.782	51.785
CT	100.000	-	0.412	0.003*	0.000*	0.002*	0.000*
5	103.687	-	-	0.000*	0.000*	0.000*	0.000*
20	64.890	-	-	-	0.276	0.718	0.079
50	58.612	-	-	-	-	0.443	0.481
100	61.782	-	-	-	-	-	0.144

P<0.01;

Conc. = Concentration

Table C-10 Comparing a percent dry weight of *Gynura pseudochina* (L.) DC. exposed to difference concentrations of cadmium and zinc combination.

	Conc.	CT	50/0	50/100	50/250	50/500	50/750	50/1000
Conc.	Mean	100.0000	58.612	111.987	123.856	128.935	122.870	111.987
CT	100.000	-	0.008*	0.402	0.105	0.022	0.119	0.402
50/0	58.612	-	-	0.001*	0.000*	0.000*	0.000*	0.001*
50/100	111.987	-	-	-	0.407	0.118	0.446	1.000
50/250	123.856	-	-	-	-	0.439	0.945	0.407
50/500	128.935	-	-	-	-	-	0.400	0.118
50/750	122.870	-	-	-	-	-	-	0.446

P<0.01;

Conc. = Concentration

Table C-11 Comparing translocation factor of *Gynura pseudochina* (L.) DC. exposed to difference concentrations of zinc.

Conc.	Conc.	100	250	500	750	1000
100	Mean	0.644	0.679	0.795	0.903	0.613
250	0.644	-	0.535	0.319	0.005*	0.000*
500	0.679	-	-	0.713	0.014	0.000*
750	0.795	-	-	-	0.017	0.000*
	0.903	-	-	-	-	0.030

P<0.01;

Conc. = Concentration

Table C-12 Comparing a percent dry weight of *Gynura pseudochina* (L.) DC. exposed to difference concentrations of cadmium.

Conc.	Conc.	5	20	50	100	150
5	Mean	1.515	1.213	0.949	0.823	0.596
20		-	0.015	0.000*	0.000*	0.000*
50		-	-	0.029	0.003*	0.000*
100		-	-	-	0.269	0.013
		-	-	-	-	0.099

P<0.01;

Conc. = Concentration

Table C-13 Comparing a translocation factor of *Gynura pseudochina* (L.) DC. exposed to difference concentrations of cadmium and zinc combination for zinc.

Conc.	Conc.	50/100	50/250	50/500	50/750	50/1000
	Mean	0.558	0.511	0.560	0.588	0.619
50/100	0.558	-	0.522	0.972	0.659	0.388
50/250	0.511	-	-	0.501	0.294	0.149
50/500	0.560	-	-	-	0.685	0.406
50/750	0.588	-	-	-	-	0.652

P<0.01;

Conc. = Concentration

Table C-14 Comparing a Translocation factor of *Gynura pseudochina* (L.) DC. exposed to difference concentrations of cadmium and zinc combination for cadmium.

Conc.	Conc.	50/100	50/250	50/500	50/750	50/1000
	Mean	0.572	0.613	0.660	0.648	0.637
50/100	0.572	-	0.639	0.245	0.309	0.455
50/250	0.613	-	-	0.517	0.614	0.771
50/500	0.660	-	-	-	0.878	0.725
50/750	0.648	-	-	-	-	0.836

P<0.01;

Conc. = Concentration

APPENDIX D
SDS-PAGE

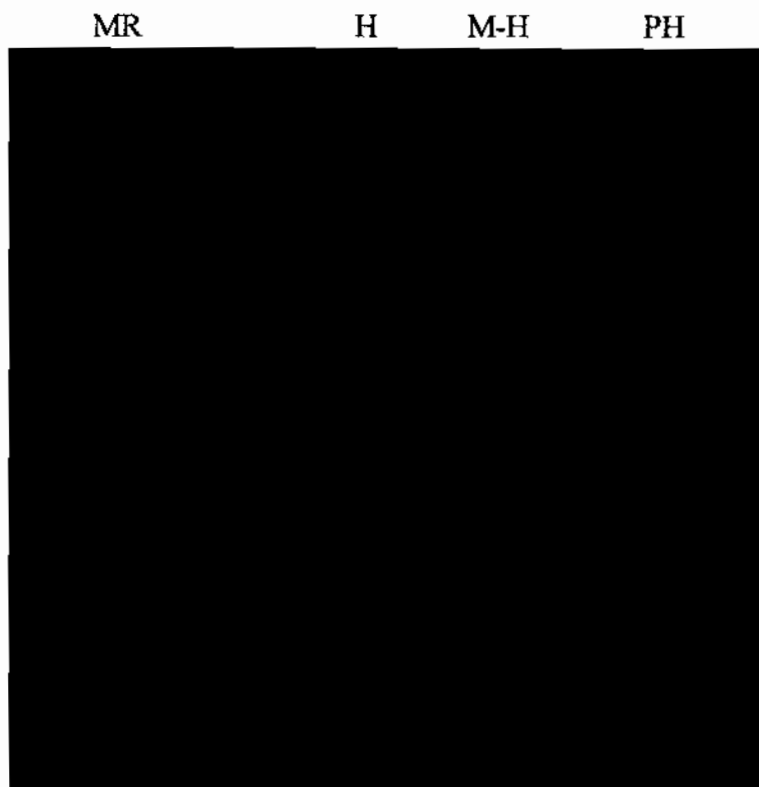


Figure D-1 Compared the efficiency of extraction buffers during HEPES buffer (H), modified HEPES buffer (M-H) and phenol buffer (PH) by separating on SDS polyacrylamide gel (12% w/v) of 1 μ g of soluble proteins from leaves of *G. pseudochina* (L.) DC.; MR= protein marker.

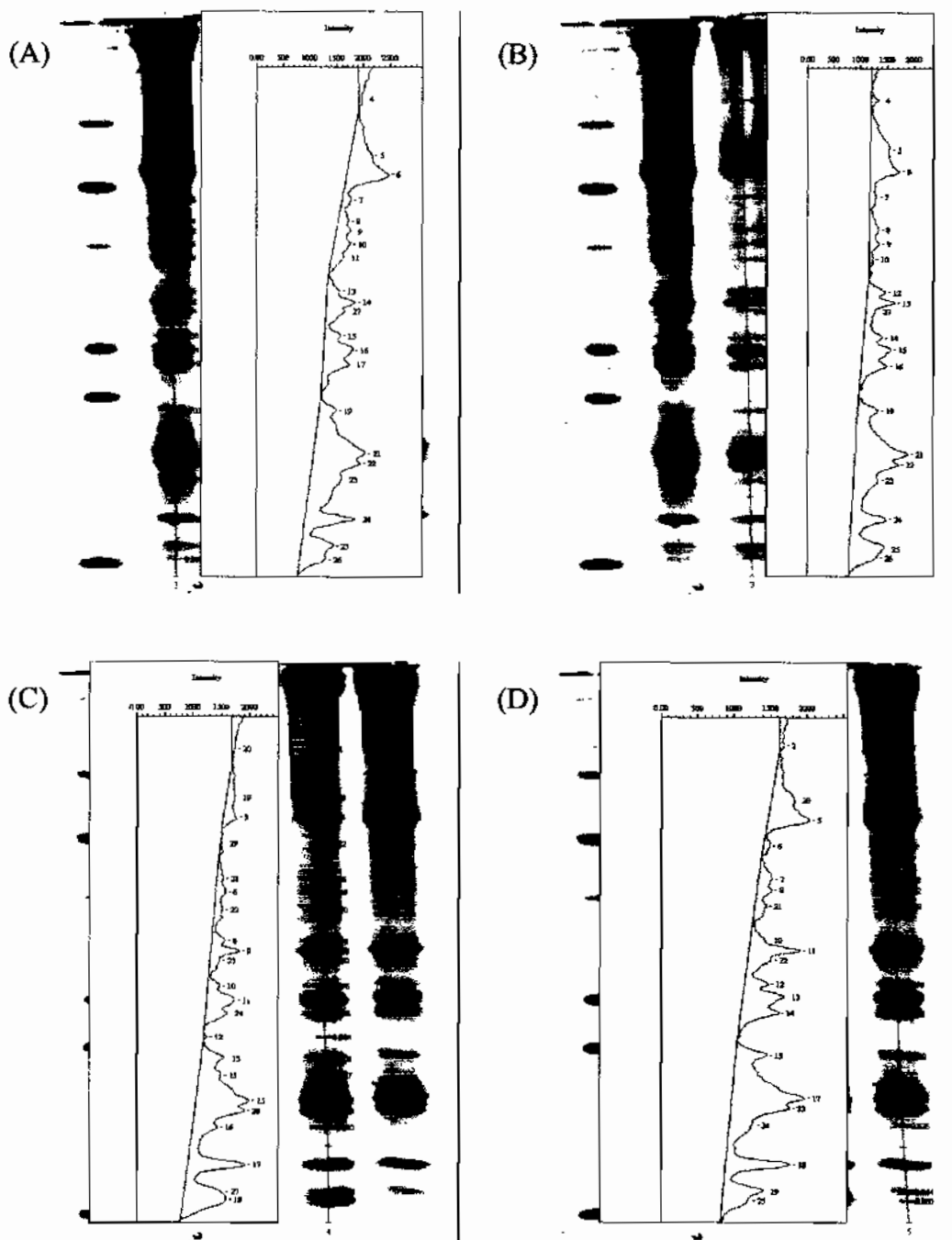


Figure D-2 Intensity of band on SDS-PAGE was determined by Quantity One version 4 (Bio-Rad) for identification the expression protein; (A) band protein of leaves control, (B) band protein of leaves treated zinc with 1,000 mg l⁻¹, (C) band protein of leaves treated cadmium with 150 mg l⁻¹ and (D) band protein of leaves treated cadmium and zinc combination with 50+1,000 mg l⁻¹.

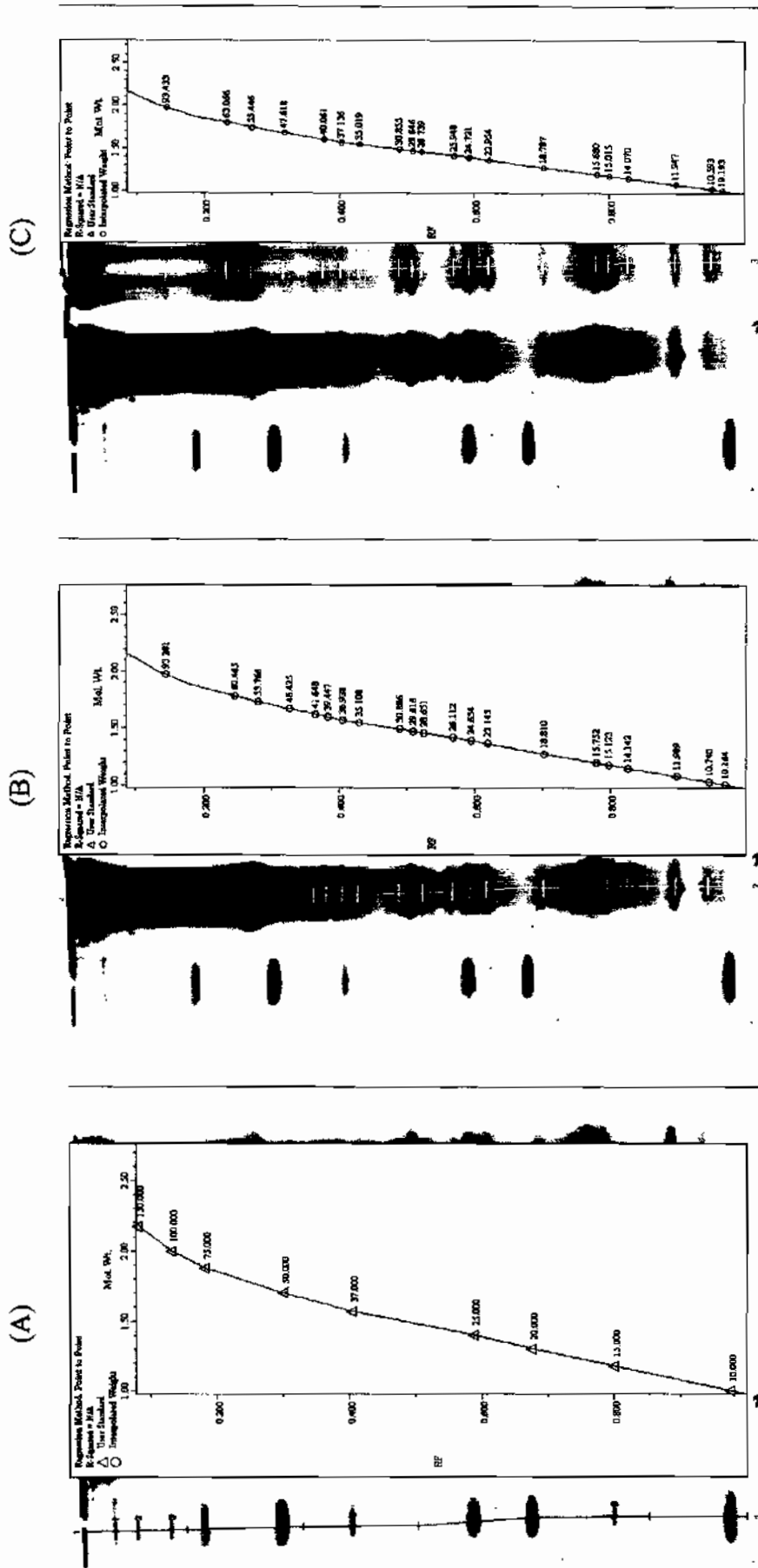


Figure D-3 Identification molecular weight of protein expressions were determined by Quantity One version 4 (Bio-Rad); (A) Standard curve, (B) molecular weight of protein expressions for control and (C) molecular weight of protein expressions for zinc.

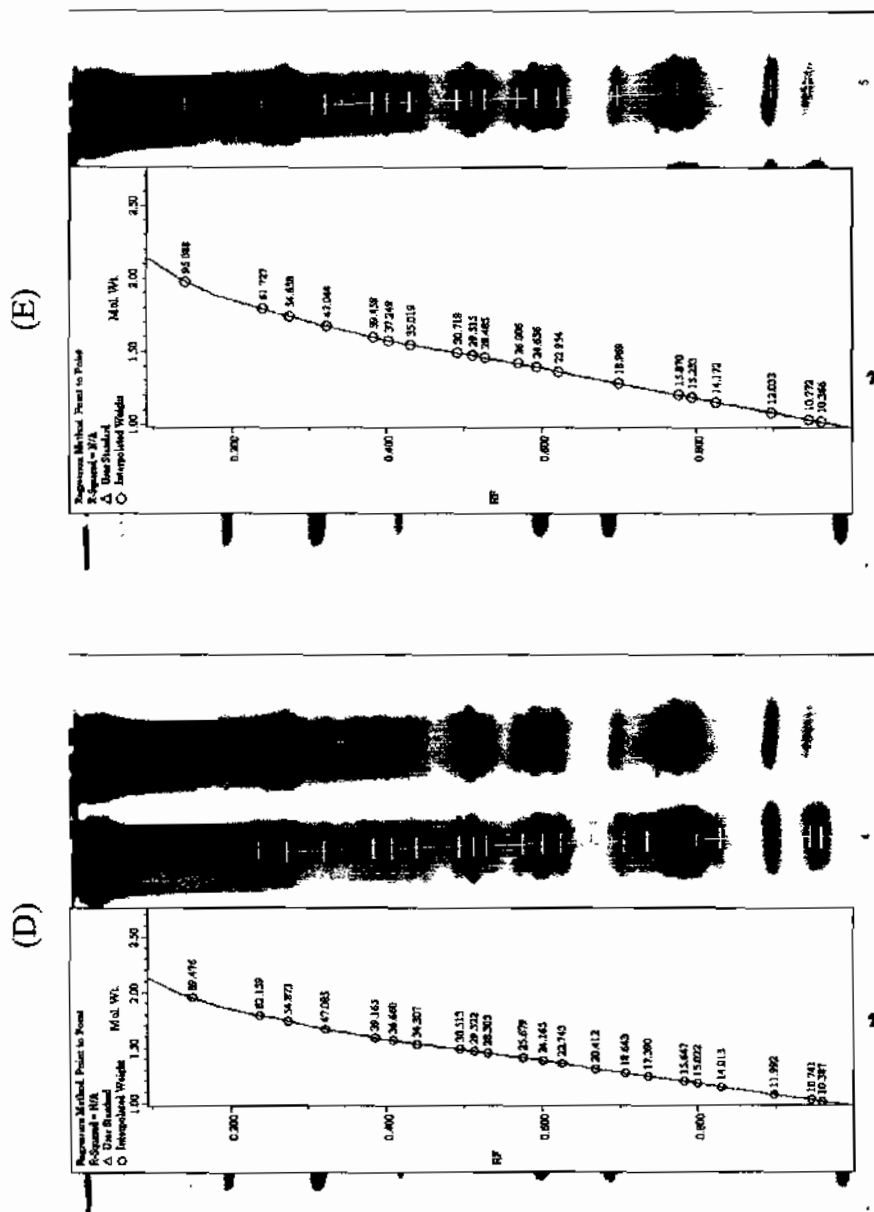
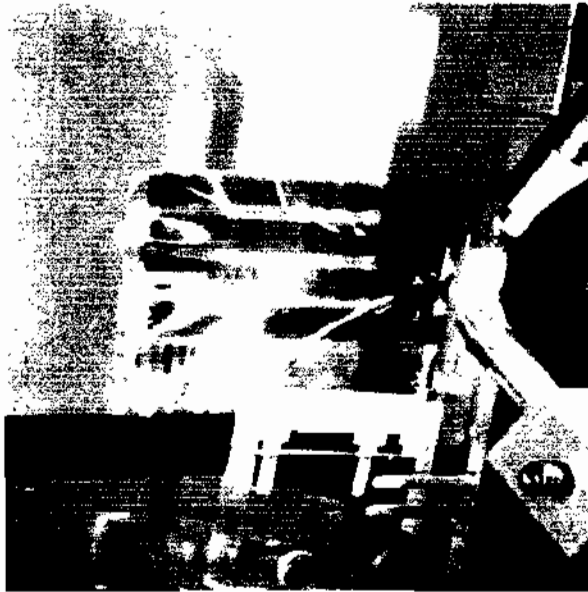
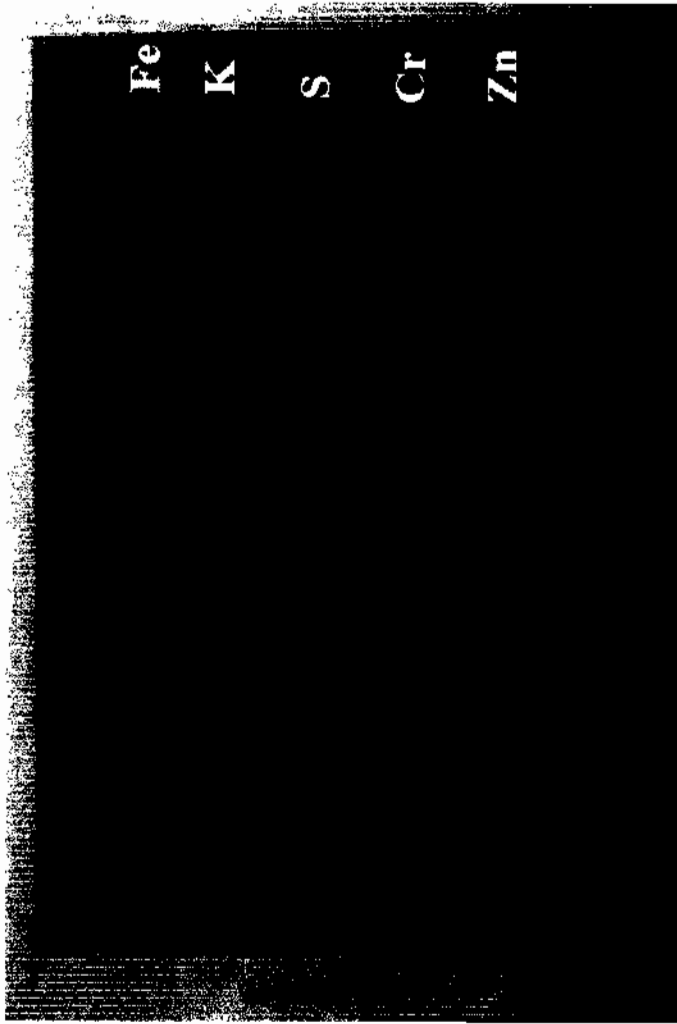


Figure D-4 Identification molecular weight of protein expressions were determined by Quantity One version 4 (Bio-Rad); (D) molecular weight of protein expressions for cadmium and (E) molecular weight of protein expressions for cadmium and zinc combination.



(A)



(B)

Figure D-5 μ -XRF spectra of SDS-PAGE gel; (A) experiment condition in room temperature and (B) Relative content of metals in protein bands.

APPENDIX E
X-ray absorption spectroscopy

1.1 Curve fitting of protein control

B.G. Method	Victoreen $1(DX^4+CX^3+const)$
k Weight	3
R Range	1.197-2.056
Fitting Range	1.90-11.55
dR Limit	0.005
Fitting Method	Back k-space
R-value (%)	0.262

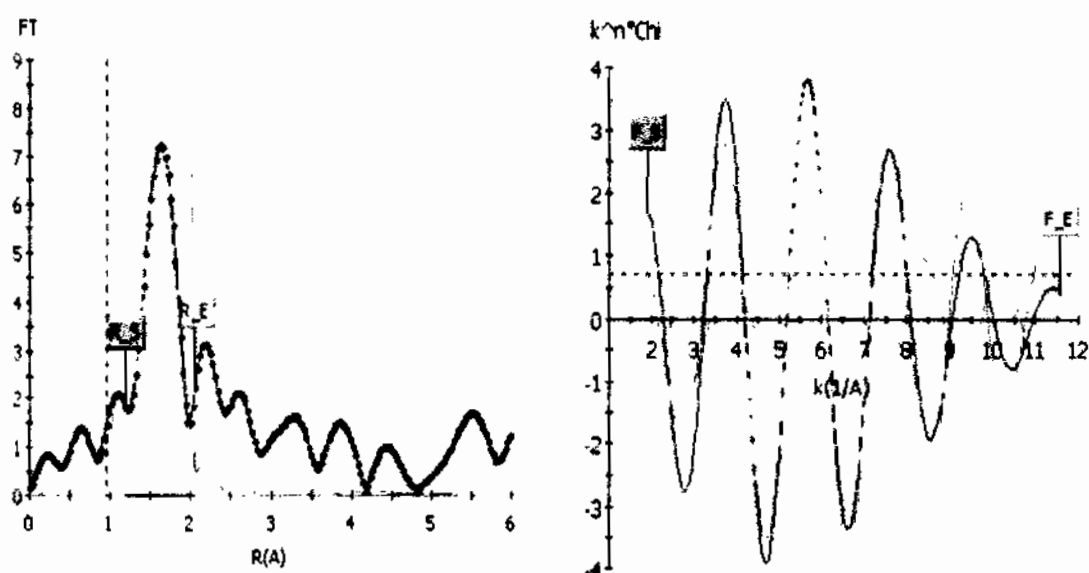


Figure E-1 Radial-distribution-function (leaf) Inverse-FOURIER-Transform (right) for protein control

Table E-1 EXAFS fitting of the model compounds showing the bond, coordination number (N), atomic radius $R(\text{Å})$, and the Debye-Waller factor is represented by σ^2 for protein control.

Sample	Bond	N	$R(\text{Å})$	σ^2
Protein-CT	Zn-O	3.095	2.103	0.048
	Zn-N	3.452	2.152	0.038
	Zn-S	1.589	2.203	0.052

1.2 Curve fitting of protein zinc

B.G. Method	Victoreen 1($DX^4+CX^3+const$)
k Weight	3
R Range	1.381-2.700
Fitting Range	2.150-10.200
dR Limit	0.005
Fitting Method	Back k-space
R-value (%)	0.008

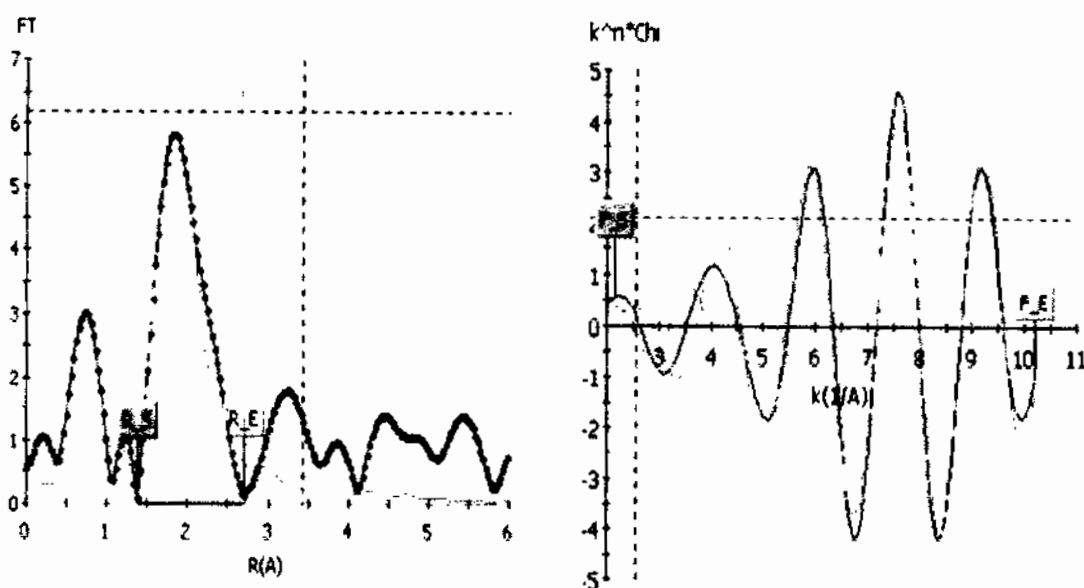


Figure E-2 Radial-distribution-function (left) Inverse-FOURIER-Transform (right) for protein zinc

Table E-2 EXAFS fitting of the model compounds showing the bond, coordination number (N), atomic radius $R(\text{Å})$, and the Debye–Waller factor is represented by σ^2 for protein zinc.

Sample	Bond	N	$R(\text{Å})$	σ^2
Protein-Zn	Zn-S	1.449	2.304	0.008

1.3 Curve fitting of zinc cysteine model

B.G. Method	Victoreen 1($DX^4+CX^3+const$)
k Weight	3
R Range	1.258-2.209
Fitting Range	1.650-11.150
dR Limit	0.005
Fitting Method	Back k-space
R-value (%)	0.262

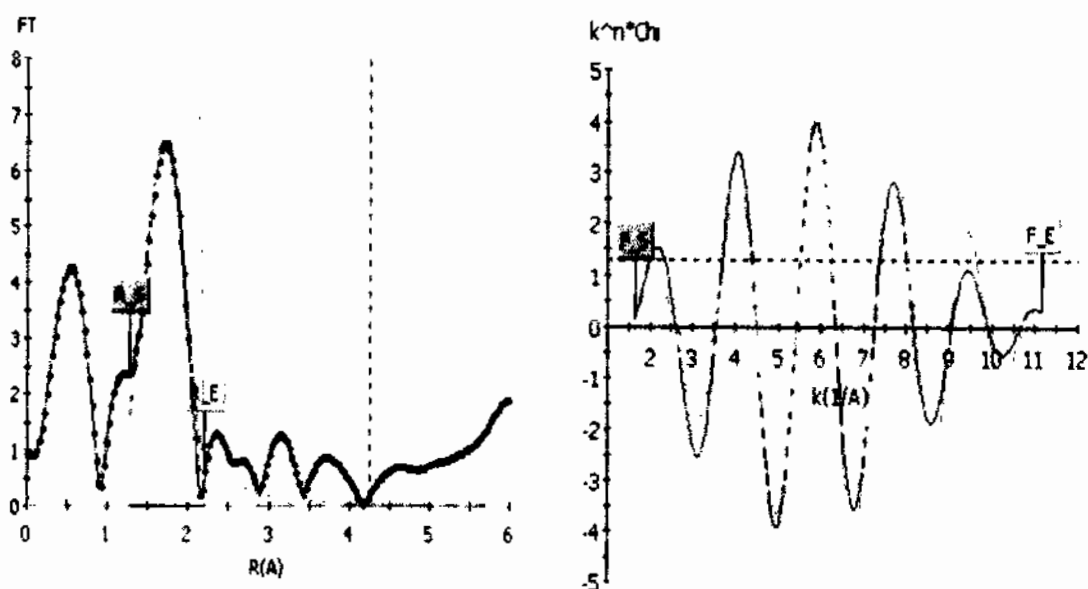


Figure E-3 Radial-distribution-function (left) Inverse-FOURIER-Transform (right) for zinc cysteine model

Table E-3 EXAFS fitting of the model compounds showing the bond, coordination number (N), atomic radius $R(\text{Å})$, and the Debye–Waller factor is represented by σ^2 for zinc cysteine model.

Sample	Bond	N	$R(\text{Å})$	σ^2
Zn-cysteine	Zn-S	4.078	2.245	0.053

1.4 Curve fitting of zinc cellulose model

B.G. Method	Victoreen 1($DX^4+CX^3+const$)
k Weight	3
R Range	0.890-2.025
Fitting Range	2.000-12.600
dR Limit	0.005
Fitting Method	Back k-space
R-value (%)	0.114

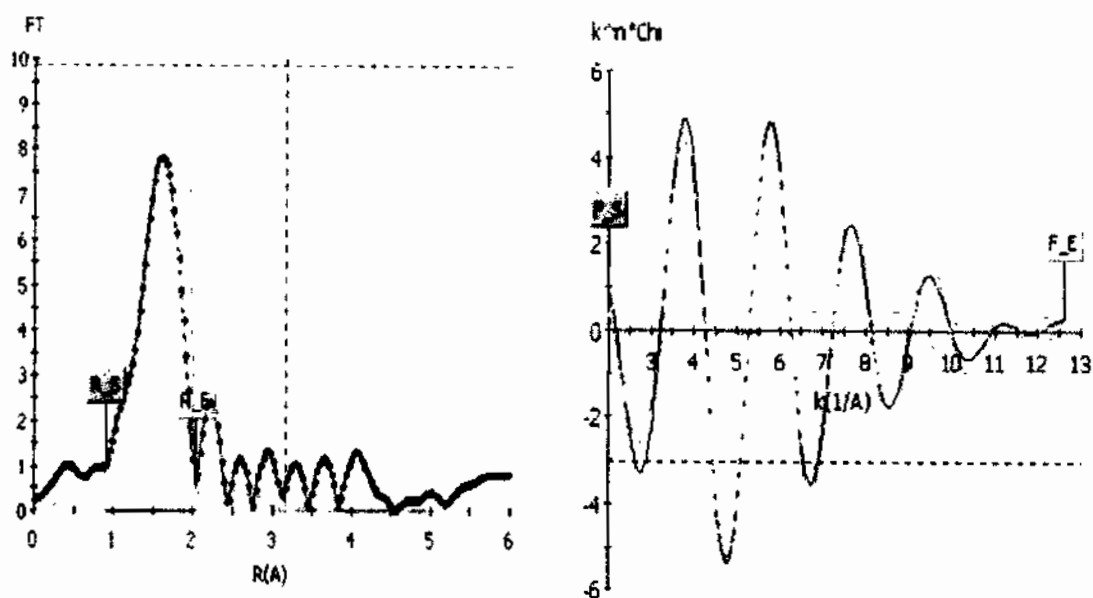


Figure E-4 Radial-distribution-function (left) Inverse-FOURIER-Transform (right) for zinc cellulose model

Table E-4 EXAFS fitting of the model compounds showing the bond, coordination number (N), atomic radius $R(\text{Å})$, and the Debye–Waller factor is represented by σ^2 for zinc cellulose model.

Sample	Bond	N	$R(\text{Å})$	σ^2
Zn-cellulose	Zn-O	6.151	2.077	0.038

1.5 Curve fitting of zinc oxide model

B.G. Method	Victoreen 1(DX ⁴ +CX ³ +const)
k Weight	3
R Range	1.074-1.963
Fitting Range	1.000-10.350
dR Limit	0.005
Fitting Method	Back k-space
R-value (%)	0.336

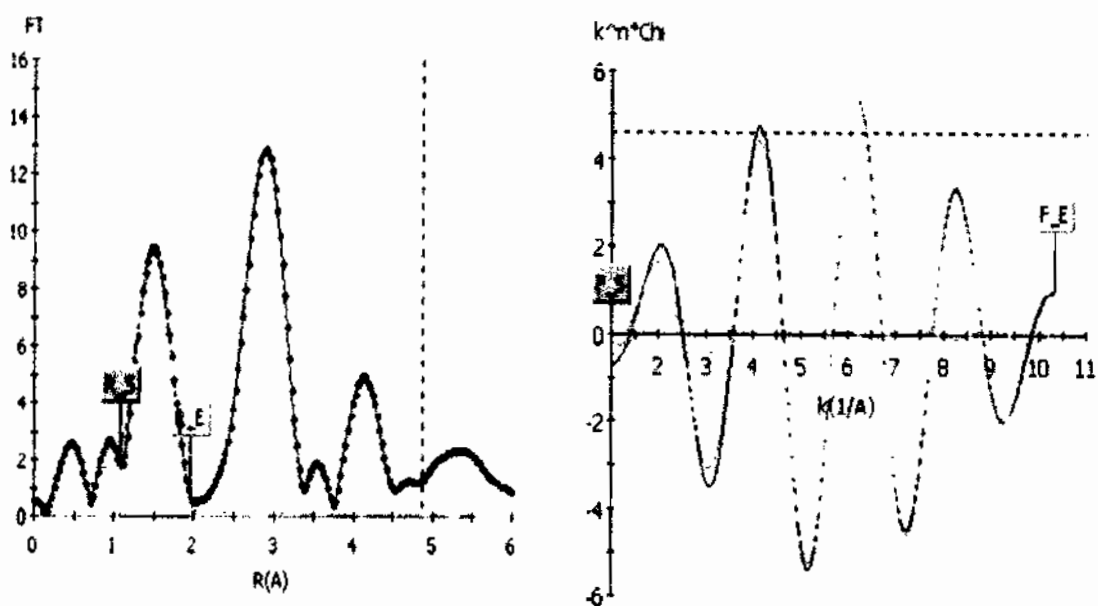


Figure E-5 Radial-distribution-function (left) Inverse-FOURIER-Transform (right) for zinc oxide model

Table E-5 EXAFS fitting of the model compounds showing the bond, coordination number (N), atomic radius $R(\text{Å})$, and the Debye–Waller factor is represented by σ^2 for zinc oxide model.

Sample	Bond	N	$R(\text{Å})$	σ^2
ZnO	Zn-O	4.028	1.989	0.024

1.6 Curve fitting of zinc sulfide model

B.G. Method	Victoreen 1($DX^4+CX^3+const$)
k Weight	3
R Range	1.258-2.301
Fitting Range	2.600-13.350
dR Limit	0.005
Fitting Method	Back k-space
R-value (%)	0.023

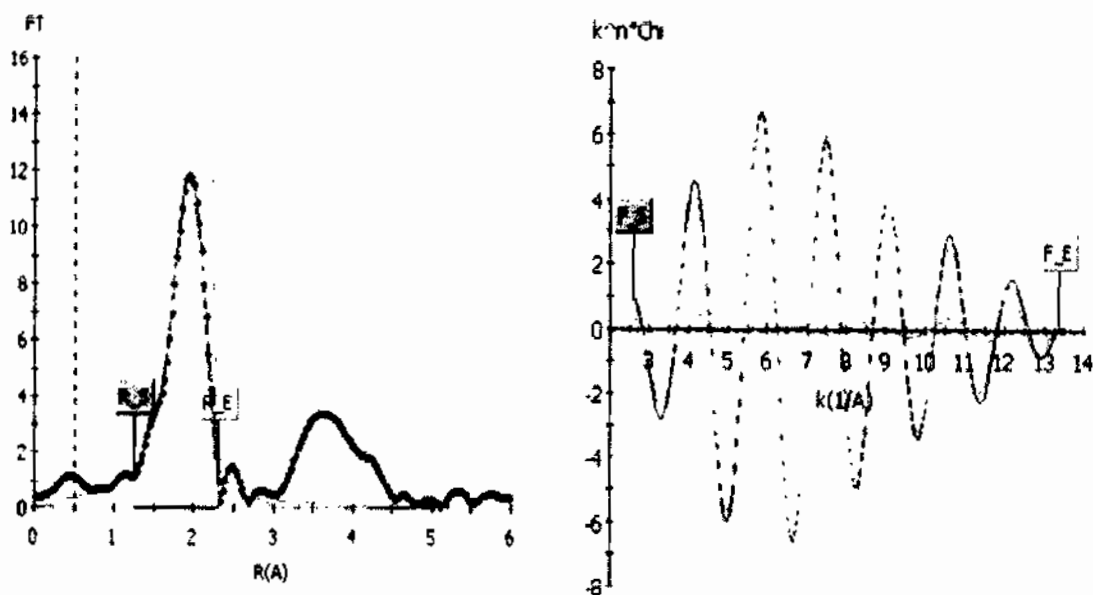


Figure E-6 Radial-distribution-function (left) Inverse-FOURIER-Transform (right) for zinc sulfide model

Table E-6 EXAFS fitting of the model compounds showing the bond, coordination number (N), atomic radius $R(\text{Å})$, and the Debye–Waller factor is represented by σ^2 for zinc sulfide model.

Sample	Bond	N	$R(\text{Å})$	σ^2
ZnS	Zn-S	4.002	2.325	0.032

1.7 Curve fitting of zinc sulfate model

B.G. Method	Victoreen 1($DX^4+CX^3+const$)
k Weight	3
R Range	0.675-1.994
Fitting Range	1.950-13.050
dR Limit	0.005
Fitting Method	Back k-space
R-value (%)	0.037

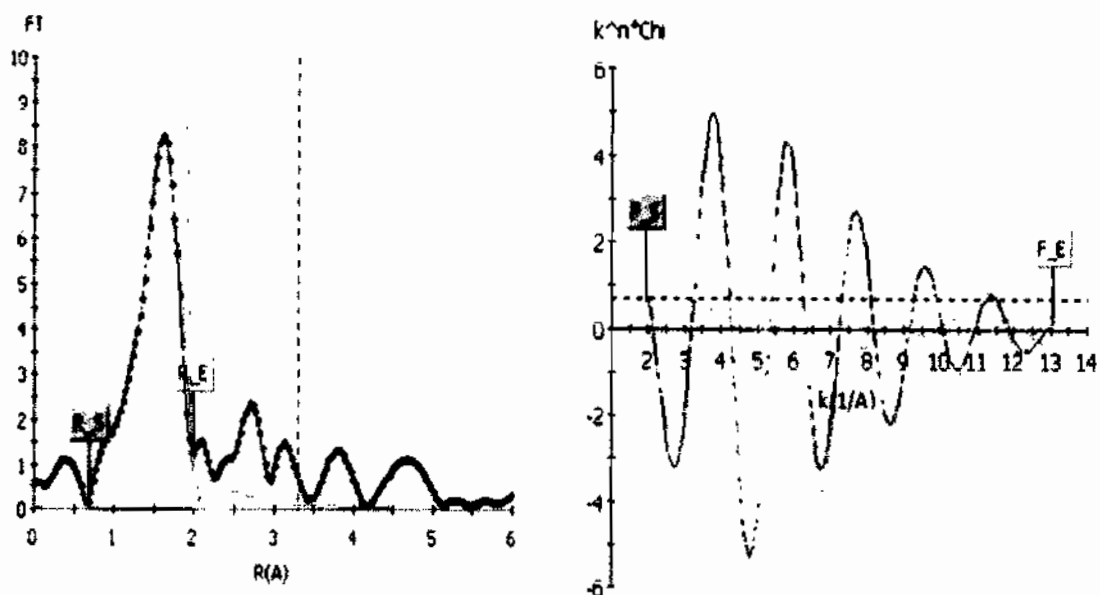


Figure E-7 Radial-distribution-function (left) Inverse-FOURIER-Transform (right) for zinc sulfate model

Table E-7 EXAFS fitting of the model compounds showing the bond, coordination number (N), atomic radius $R(\text{Å})$, and the Debye-Waller factor is represented by σ^2 for zinc sulfate model.

Sample	Bond	N	$R(\text{Å})$	σ^2
ZnSO ₄	Zn-O	4.997	2.054	0.029

1.8 Curve fitting of zinc nitrate model

B.G. Method	Vicoreen 1(DX ⁴ +CX ³ +const)
k Weight	3
R Range	0.920-2.148
Fitting Range	2.000-12.000
dR Limit	0.005
Fitting Method	Back k-space
R-value (%)	0.153

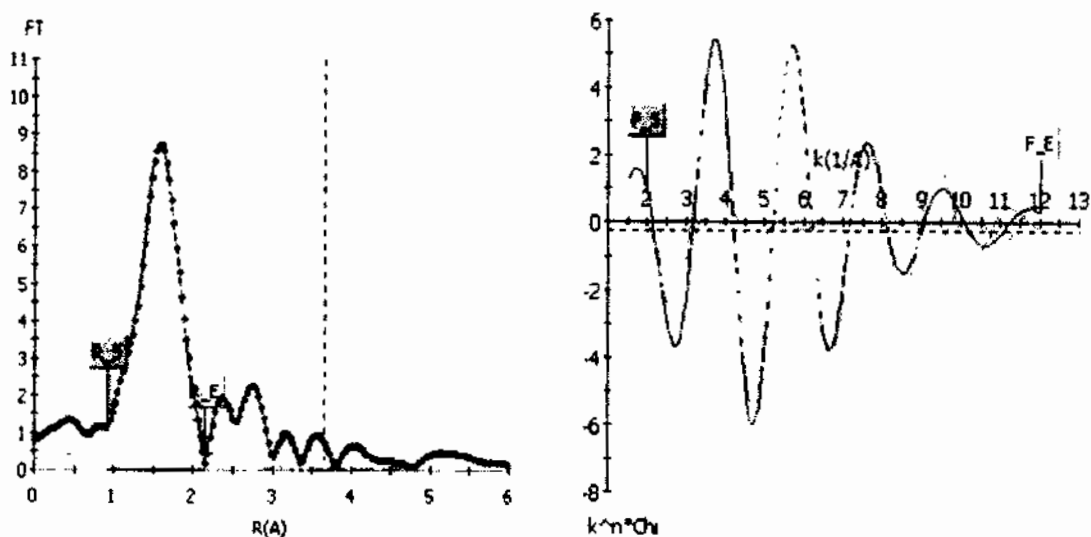


Figure E-8 Radial-distribution-function (left) Inverse-FOURIER-Transform (right) for zinc nitrate model

Table E-8 EXAFS fitting of the model compounds showing the bond, coordination number (N), atomic radius $R(\text{Å})$, and the Debye-Waller factor is represented by σ^2 for zinc nitrate model.

Sample	Bond	N	$R(\text{Å})$	σ^2
Zn(NO ₃) ₂	Zn-O	6.260	2.087	0.048

BIOGRAPHY

Biography

Name: Mr.Natthawoot Panitlertumpai

Date of Birth: 7th August 1984
Nakhon Ratchasima province, Thailand

Education Background

- 2007-2011 The degree of Master of Science (Biology).
Mahasarakham University, Thailand.
- 2003-2007 Bachelor of Engineer (Chemical engineering).
King Mongkut's University of Technology Thonburi, Thailand.

Contract address 109/1, Prapa Road, Mueng District,
Nakhon Ratchasima province, 30000, Thailand
Phone : +66837412118 E-mail : p_natthawoot@yahoo.com

Scholarship

- 2003-2011 Junior Science Talent Project (JSTP)
National Science and Technology Development Agency (NSTDA).

Academic Publications

- Nakbanpote, W., **Panitlertumpai, N.**, Sukadeetad, K., Meesungneoe, O. and Noisanguan, W. (2010) Advances in Phytoremediation Research: A Case Study of *Gynura pseudochina* (L.) DC. in: Fürstner, I. (eds.) *Advanced Knowledge Application in Practice*. India, Sciyo Press.
- **Panitlertumpai, N.**, Sukadeetad, K., Nakbanpote, W., Sangdee, A., Izumi, N. and Hokura, A. (2009) The potential of zinc accumulation in *Gynura pseudochina* (L.) DC.: study in a tissue culture system, *Proceeding of International Conference on Green and Sustainable Innovation (ICGSI) 2009, December 2 – 4, 2009, Chiang Rai, pp. 886-893*. (Oral presentation).